

# Variance and extreme events in population ecology

by

Sean C. Anderson

M.Sc., Dalhousie University, 2010

B.Sc. (Hons.), Dalhousie University, 2006

Thesis Submitted in Partial Fulfillment  
of the Requirements for the Degree of

Doctor of Philosophy

in the

Department of Biological Sciences

Faculty of Science

© Sean C. Anderson 2015

SIMON FRASER UNIVERSITY

Spring 2015

All rights reserved.

However, in accordance with the *Copyright Act of Canada*, this work may be reproduced without authorization under the conditions for “Fair Dealing.” Therefore, limited reproduction of this work for the purposes of private study, research, criticism, review and news reporting is likely to be in accordance with the law, particularly if cited appropriately.

## APPROVAL

**Name:** Sean C. Anderson  
**Degree:** Doctor of Philosophy  
**Title of Thesis:** Variance and extreme events in population ecology

**Examining Committee:** Dr. Christopher J. Kennedy, Professor  
Chair

---

Dr. Nicholas K. Dulvy, Senior Supervisor  
Professor

---

Dr. Andrew B. Cooper, Co-Supervisor  
Associate Professor, School of Resource and Environmental  
Management

---

Dr. Jonathan W. Moore, Supervisor  
Assistant Professor

---

Dr. Trevor A. Branch, Supervisor  
Assistant Professor, School of Aquatic and Fishery Sci-  
ences, University of Washington

---

Dr. Arne Ø. Mooers, Internal Examiner  
Professor

---

Dr. Leah R. Gerber, External Examiner  
Professor, School of Life Sciences,  
Arizona State University

**Date Approved:** March 4, 2015

## Partial Copyright Licence



The author, whose copyright is declared on the title page of this work, has granted to Simon Fraser University the non-exclusive, royalty-free right to include a digital copy of this thesis, project or extended essay[s] and associated supplemental files ("Work") (title[s] below) in Summit, the Institutional Research Repository at SFU. SFU may also make copies of the Work for purposes of a scholarly or research nature; for users of the SFU Library; or in response to a request from another library, or educational institution, on SFU's own behalf or for one of its users. Distribution may be in any form.

The author has further agreed that SFU may keep more than one copy of the Work for purposes of back-up and security; and that SFU may, without changing the content, translate, if technically possible, the Work to any medium or format for the purpose of preserving the Work and facilitating the exercise of SFU's rights under this licence.

It is understood that copying, publication, or public performance of the Work for commercial purposes shall not be allowed without the author's written permission.

While granting the above uses to SFU, the author retains copyright ownership and moral rights in the Work, and may deal with the copyright in the Work in any way consistent with the terms of this licence, including the right to change the Work for subsequent purposes, including editing and publishing the Work in whole or in part, and licensing the content to other parties as the author may desire.

The author represents and warrants that he/she has the right to grant the rights contained in this licence and that the Work does not, to the best of the author's knowledge, infringe upon anyone's copyright. The author has obtained written copyright permission, where required, for the use of any third-party copyrighted material contained in the Work. The author represents and warrants that the Work is his/her own original work and that he/she has not previously assigned or relinquished the rights conferred in this licence.

Simon Fraser University Library  
Burnaby, British Columbia, Canada

revised Fall 2013

# Abstract

Assessing, managing, and communicating variance and risk is fundamental to effective ecological decision making. One promising approach is to borrow concepts from financial portfolio management. Ecological populations behave like portfolios in many ways—we can treat the abundance of populations, such as salmon in streams, as financial stock value, and groups of populations, such as salmon within a river catchment, as portfolios. If a group of populations react differently to an environmental event then the probability of sudden decline may be lowered, similar to a diversified financial portfolio. This risk reduction has been referred to as the portfolio effect. In this thesis I consider three applications of portfolio concepts to ecology. I begin by evaluating ways of estimating portfolio effects and applying these metrics to moth, reef fish, and salmon metapopulations from around the world. I show an inherent bias to a commonly used method, develop a new method based on Taylor’s power law of mean–variance scaling, and outline recommendations for estimating portfolio effects. Next, I use a portfolio approach to inform conservation priorities for salmon populations under a changing climate. I show that preserving a diversity of thermal tolerances minimizes risk and ensures persistence given long-term environmental change. However, this reduction in variability can come at the expense of long-term persistence if climate change increasingly restricts available habitat, forcing ecological managers to balance society’s desire for short-term stability and long-term viability. Finally, I take the concept of black swans (extreme and unexpected events) from the financial literature and ask what the evidence is for these events across hundreds of bird, mammal, insect, and fish abundance time series. I find strong evidence for the infrequent (3–5%) occurrence of ecological black swans. Black swans are predominantly (87%) downward events and tend to be associated with extreme climate, natural enemies (predators and parasites), or the combined effects of multiple factors, with little relationship to life history. My thesis demonstrates the importance of conserving ecological properties that may contribute to portfolio effects, such as thermal-tolerance diversity and habitat heterogeneity, and developing conservation strategies that are robust to unexpected extreme events.

**Keywords:** biocomplexity; catastrophes; diversity–stability; modern portfolio theory; response diversity; synchrony

# Acknowledgments

I am first thankful to Nick Dulvy and Andy Cooper for their helpful guidance and for giving me the freedom and encouragement to work on a broad set of topics beyond my thesis. Thanks to Jon Moore for insightful discussions about my work and for his contributions to Chapter 3 of this thesis, together with those of Michelle McClure's. I am grateful to Trevor Branch and the School of Fisheries and Aquatic Sciences for hosting me in Seattle in 2011–12. I also thank Trevor for the ideas that sparked Chapter 4, and for his quick and enthusiastic feedback. Thanks to Leah Gerber and Arne Mooers for acting as external and internal examiners of this thesis and to Chris Kennedy for chairing my thesis defence. I am grateful for funding from NSERC, Fulbright Canada, a Garfield Weston Foundation / BC Packers Ltd. Graduate Fellowship in Marine Sciences, SFU, Nick Dulvy, and Andy Cooper.

I have been fortunate to be surrounded by wonderful groups of grad students and postdocs both during my time in the Earth to Oceans group and at the University of Washington. Thanks to all of you for enriching my past four years. In particular, thanks to Noel Swain, Rowan and Laurel Trebilco, Jordy Thomson, Chris Mull, Michelle Nelson—my time at Wall St. was a blast. Mike Beakes and Corey Phillis, you kept me sane. Justin Yeakel, thanks for geeking out with me about the quantitative part of quantitative ecology. Cole Monnahan, Melissa Muradian, and Peter Kuriyama, thanks for being my home away from home.

Thanks to the members of the NESCent working group on extinction risk for helping me think on 100 million year time scales—especially Seth Finnegan and Paul Harnik. Our main project has now outlived my thesis. I am very appreciative of Heike Lotze for setting me up so well on my scientific path and for continuing to do so. Thanks to my co-developers of ss3sim for exploring the depths of stock assessment with me.

Finally, I'm deeply thankful to my family for supporting me through all these years of education. To Gran, you have instilled in me the value of education and shown a keen interest in my work. To my parents, you've always given me the freedom and encouragement to work on whatever interests me. Mom and Dad, look how far I've come since you taught me how to write my first research paper and the joys of Reverse Polish Notation calculators 25 years ago! And to Sacha, thank you for your unwavering support—you have made the years I've spent working on this thesis immeasurably better.

# Contents

Approval	ii
Partial Copyright License	iii
Abstract	iv
Acknowledgments	vi
Contents	vii
List of Tables	x
List of Figures	xi
<b>1 Introduction</b>	<b>1</b>
1.1 Ecological portfolios as a metaphor . . . . .	2
1.2 The portfolio-effect metric . . . . .	3
1.3 Ecological portfolio management . . . . .	4
1.4 Extreme risk . . . . .	6
1.5 Contributions . . . . .	8
<b>2 Quantifying metapopulation portfolio effects</b>	<b>9</b>
2.1 Abstract . . . . .	9
2.2 Introduction . . . . .	10
2.3 Materials and methods . . . . .	13
2.3.1 Defining the metapopulation portfolio . . . . .	13
2.3.2 Theoretical evaluation of portfolio effects . . . . .	14

2.3.3	Empirical evaluation of portfolio effects . . . . .	15
2.3.4	Alternative ways of extrapolating the mean-variance PE . . . . .	16
2.3.5	Accounting for non-stationary time-series . . . . .	17
2.3.6	The ecofolio R package . . . . .	17
2.4	Results . . . . .	17
2.4.1	Theoretical evaluation of portfolio effects . . . . .	17
2.4.2	Empirical evaluation of portfolio effects . . . . .	18
2.4.3	Diagnosing the ecological properties of empirical portfolio effects . . .	19
2.5	Discussion . . . . .	23
2.5.1	The influence of mean-variance scaling . . . . .	23
2.5.2	Mechanisms driving metapopulation portfolio effects . . . . .	25
2.5.3	Limitations of phenomenological portfolio effects . . . . .	25
2.5.4	Practical recommendations for quantifying ecological portfolio effects	26
2.6	Acknowledgements . . . . .	29
2.7	Supporting materials . . . . .	30
2.7.1	R package to estimate metapopulation portfolio effects . . . . .	30
2.7.2	Data sources for the empirical portfolio effect analysis . . . . .	30
2.7.3	Diagnosing the ecological properties of empirical portfolio effects . . .	32
2.7.4	Supporting Tables and Figures . . . . .	33
<b>3</b>	<b>Metapopulation portfolio conservation</b>	<b>50</b>
3.1	Abstract . . . . .	50
3.2	Introduction . . . . .	51
3.3	Methods . . . . .	54
3.3.1	Defining the ecological portfolio . . . . .	54
3.3.2	Salmon metapopulation dynamics . . . . .	56
3.3.3	Fishing . . . . .	57
3.3.4	Environmental dynamics . . . . .	59
3.3.5	Conservation scenarios . . . . .	60
3.4	Results . . . . .	62
3.4.1	Spatial conservation scenarios . . . . .	62
3.4.2	Unknown thermal tolerances . . . . .	64
3.4.3	Declining habitat availability . . . . .	66
3.5	Discussion . . . . .	66



3.5.1	Implications for salmon conservation . . . . .	66
3.5.2	Broad ecological implications and conservation priorities . . . . .	70
3.6	Acknowledgements . . . . .	72
3.7	Supporting materials . . . . .	73
3.7.1	Supporting Tables and Figures . . . . .	74
<b>4</b>	<b>Ecological black swans</b>	<b>87</b>
4.1	Abstract . . . . .	87
4.2	Introduction . . . . .	88
4.3	Methods . . . . .	89
4.3.1	Time-series data . . . . .	89
4.3.2	Population models . . . . .	90
4.3.3	Covariates of population dynamic black swans . . . . .	92
4.4	Results . . . . .	93
4.5	Discussion . . . . .	96
4.6	Acknowledgements . . . . .	101
4.7	Supporting materials . . . . .	102
4.7.1	Data selection . . . . .	102
4.7.2	Details on the heavy-tailed Gompertz probability model . . . . .	104
4.7.3	Alternative priors . . . . .	105
4.7.4	Alternative population models . . . . .	105
4.7.5	Simulation testing the model . . . . .	108
4.7.6	Modelling covariates of heavy-tailed dynamics . . . . .	110
4.7.7	Additional acknowledgements . . . . .	112
<b>5</b>	<b>General discussion</b>	<b>131</b>
5.1	Challenges . . . . .	132
5.2	Outlook . . . . .	133
	<b>Bibliography</b>	<b>136</b>

# List of Tables

2.1	Metapopulations used in the empirical PE analyses. . . . .	34
2.2	Moth sites used from the Rothamsted Insect Survey database. . . . .	35
2.3	Reef locations used from the AIMS LTMP Great Barrier Reef database. . . . .	36
3.1	Input parameters to the salmon metapopulation simulation with default values.	74
4.1	Example population dynamic black swans from the Global Population Dynamics Database and a description of their causes. . . . .	98
4.3	Summary statistics for the filtered Global Population Dynamics Database time series arranged by taxonomic class. . . . .	114
4.4	All populations with $\Pr(\nu < 10) > 0.5$ in the base heavy-tailed Gompertz population dynamics model. . . . .	115
5.1	Attributes of financial and ecological data and their implications for ecological portfolios. . . . .	134

# List of Figures

1.1	Desirable traits of ecological metaphors, metrics, and management approaches.	2
1.2	An introduction to modern portfolio theory mean-variance optimization. . . .	5
1.3	Trends in variance and risk terminology in ecological literature. . . . .	7
2.1	Estimating the two PEs from empirical data. . . . .	12
2.2	The ecological factors driving the PE in theoretical systems. . . . .	18
2.3	PEs across 51 metapopulations. . . . .	20
2.4	The sensitivity of PE metrics across two detrending methods and three mean-variance model fits. . . . .	21
2.5	Empirical ecological PEs overlaid in theoretical PE parameter space. . . . .	22
2.6	Decision tree showing options for quantifying ecological portfolios. . . . .	27
2.7	Subpopulation time series . . . . .	37
2.8	Map of included metapopulation . . . . .	38
2.9	Calculation of the mean-variance PE using Taylor's power law. . . . .	39
2.10	Taylor's power law z values across metapopulations. . . . .	40
2.11	Intra- vs. inter-subpopulation mean-variance scaling relationship (Taylor's power law z-value). . . . .	41
2.12	PEs with the mean-variance PEs estimated from a quadratic model. . . . .	42
2.13	PEs with the mean-variance PEs estimated from a linear-quadratic averaged model. . . . .	43
2.14	PEs from linear detrended time series. . . . .	44
2.15	PEs from loess detrended time series . . . . .	45
2.16	Empirical ecological PEs overlaid in theoretical PE parameter space. . . . .	46
2.17	Predicted vs. observed mean-variance and average-CV PEs. . . . .	47

2.18	Relationship between the drivers of the PE in empirical systems for moths (red), reef fishes (purple), and salmon (blue). . . . .	48
2.19	The PE used as an index of ecosystem change. . . . .	49
3.1	Flow chart of the salmon-metapopulation simulation. . . . .	55
3.2	Different ways of prioritizing thermal-tolerance conservation. . . . .	58
3.3	The components of an example metapopulation simulation. . . . .	61
3.4	The importance of preserving thermal-tolerance diversity through spatial conservation strategies. . . . .	63
3.5	The importance of preserving as many populations as possible when we do not know how thermal-tolerance is distributed. . . . .	65
3.6	Risk-return trade-off in the case where habitat is lost over time through stream flow reduction. . . . .	67
3.7	An example straying matrix. . . . .	75
3.8	The impact of increasing or decreasing various parameter values on metapopulation return abundance. . . . .	76
3.9	A comparison of the log(returns) between populations. . . . .	77
3.10	Conserving <b>one half</b> of response diversity (spatial conservation strategy) with <b>short-term</b> environmental fluctuations. . . . .	78
3.11	Conserving a <b>full range</b> of response diversity (spatial conservation strategy) with <b>long-term</b> environmental change. . . . .	79
3.12	Conserving <b>one half</b> of response diversity (spatial conservation strategy) with <b>long-term</b> environmental change. . . . .	80
3.13	<b>Two populations</b> conserved with random response diversity and <b>short-term</b> environmental fluctuations. . . . .	81
3.14	<b>Sixteen populations</b> conserved with random response diversity and <b>short-term</b> environmental fluctuations. . . . .	82
3.15	<b>Two populations</b> conserved with random response diversity and <b>long-term</b> environmental change. . . . .	83
3.16	<b>Sixteen populations</b> conserved with random response diversity and <b>long-term</b> environmental change. . . . .	84
3.17	<b>Two populations</b> conserved with random response diversity and <b>long-term declining stream flow</b> . . . . .	85

3.18	<b>Sixteen populations conserved with random response diversity and long-term declining stream flow.</b> . . . . .	86
4.1	An illustration of fitting population dynamic models that allow for heavy tails, represented by the Student-t degrees of freedom parameter $\nu$ . . . . .	91
4.2	Estimates of population dynamics heavy-tailedness for 606 populations of birds, mammals, insects, and fishes. . . . .	94
4.3	Posterior probability distributions from beta regression multilevel models. . .	95
4.4	Potential covariates of heavy-tailed population dynamics. . . . .	97
4.5	All filtered time series used in our analysis. . . . .	121
4.6	Probability density of the Bayesian priors for the Gompertz models. . . . .	122
4.7	Estimates of $\nu$ from alternative models plotted against the base Gompertz model estimates of $\nu$ . . . . .	123
4.8	Estimates of $\nu$ from Gompertz models with alternative priors on $\nu$ . . . . .	124
4.9	Testing the ability to estimate $\nu$ and the scale parameter of the process deviations for a given number of samples drawn from a distribution with a given true $\nu$ value. . . . .	125
4.10	Simulation testing the Gompertz estimation model when the process deviation draws were chosen so that $\nu$ could be estimated close to the true value outside the full population model (“effective $\nu$ ” within a CV of 0.2 of specified $\nu$ ). . . .	126

# Chapter 1

## Introduction

In the coming century we face a loss of biodiversity on the order of 100–10,000 times greater than average rates in the fossil record (Millennium Ecosystem Assessment 2005)—a rate as fast if not faster than any of the five past mass extinctions (Barnosky et al. 2011; Harnik et al. 2012). Compounding this problem for conservation managers is uncertainty in future climate conditions (Heller and Zavaleta 2009) and the unknown responses of species and communities to those conditions (Lavergne et al. 2010). Therefore, several urgent questions need to be addressed: Exactly how big a problem is the loss of biodiversity for the stability of ecological systems? How can conservation biologists communicate the insurance benefit of biodiversity to the public and policy makers? And, how can we apply limited conservation funds to manage biodiversity and limit risk in the face of increasing environmental uncertainty?

Nearly a decade ago, Figge (2004) and Koellner and Schmitz (2006) laid the foundation for why concepts from financial portfolio theory are ideally suited to addressing these questions. Financial portfolio theory seems applicable to ecological systems for at least four reasons. First, like financial systems, ecological systems are structured hierarchically (Odum 1959; Holling 2001). Groups of populations form metapopulations and groups of species form communities; groups of financial assets form investment funds, which in turn form portfolios. Additionally, ecological and financial managers have similar goals. Ecological resource managers might wish to minimize the probability of population decline while maintaining an acceptable level of hunting or fishing; financial portfolio managers minimize the probability of large economic losses for an acceptable level of expected financial returns (May et al. 2008). Another reason why portfolio theory is ideally suited for ecology is that substantial resources have gone into developing mathematical theory for optimizing financial investments (e.g. Markowitz 1952; Rachev

et al. 2008). There is therefore a rich body of theory and experience to draw from. Finally, the portfolio metaphor is an engaging and accessible way for ecologists to think about variance and biological diversity and convey the importance of this (often abstract) literature.

A number of recent studies have used financial portfolios as a metaphor, metric, or management approach (Fig. 1.1) to estimate and communicate the stabilizing benefit of diversity and prioritize its conservation. I review many of these applications below and throughout my thesis. Portfolio theory promises to move conservation biology beyond the familiar concepts of the quantity, variety, and distribution of species (Mace 2005) and into a new dimension that emphasizes elements of variance, covariance, stability, synchrony, and extremeness (Loreau 2010; Thompson et al. 2013).

Concept	Desirable traits
<b>Metaphor</b>	Accurate (not misleading) Widely and quickly comprehensible Facilitates new solutions
↓	
<b>Metric</b>	Truthful (measures what it purports to) Precise Unbiased Easily measurable Easily interpretable
↓	
<b>Management approach</b>	Operationable (produces actionable decisions) Works with clearly defined goals Conveys tradeoffs clearly Based on defensible assumptions Accurate (produces intended consequences)

Figure 1.1: Desirable traits of ecological metaphors, metrics, and management approaches (decision-making tools).

## 1.1 Ecological portfolios as a metaphor

Metaphors are powerful tools for communicating and shaping scientific ideas (Brown 2003) and are particularly useful in developing and communicating concepts in the field of conservation biology (Larson 2011). The portfolio concept has long been used as a metaphor to emphasize the need to not put all your eggs in one basket. This metaphor has come into particular prominence in recent decades. For example, the IUCN Criterion B2a recognizes the risks associated

with a species existing in few locations ([IUCN] The World Conservation Union 2001). As another example, ecologists have suggested the need to bet-hedge by developing a portfolio of approaches when tackling conservation issues (e.g. Ehrlich and Pringle 2008). Ecologists have also used the metaphor to refer to diverse ecosystems and communities as portfolios of species (Figge 2004).

## 1.2 The portfolio-effect metric

We can apply the portfolio metaphor to obtain the portfolio-effect metric, which asks what the precise benefit is of a unit increase in diversity. The portfolio effect is derived from an economic question: How much better off are we by investing in a diversified portfolio instead of investing everything in a single asset (Markowitz 1952)? In conservation biology, we can consider the current ecological system the diversified portfolio and a theoretical homogeneous (or monoculture) system the single asset (Anderson et al. 2013). For example, we could ask how much more stable is a metapopulation of salmon from different streams, rivers, or watersheds (the portfolio) compared to a theoretical homogeneous stream population (the single asset) (Schindler et al. 2010; Carlson and Satterthwaite 2011). So, to accurately measure a portfolio effect we need to predict the variability of a theoretical homogeneous system—a system that lacks the element of biodiversity we are interested in.

Early work focused on theoretical aspects of the portfolio effect for greatly simplified systems—identifying when we would expect a stabilizing portfolio effect and what factors would enhance it (Doak et al. 1998; Tilman et al. 1998; Lehman and Tilman 2000). Over time, theoretical studies developed indices that relaxed assumptions about the systems they describe (e.g. Loreau 2010; Thibaut and Connolly 2013; Gross et al. 2013). A recent trend has been to apply these indices to empirical data, albeit primarily to salmon (e.g. Greene et al. 2010; Schindler et al. 2010; Carlson and Satterthwaite 2011; Gross et al. 2013; Anderson et al. 2013; Mellin et al. 2014).

This recent empirical work has mostly concentrated on applying simple portfolio-effect metrics that make strong assumptions rarely met in empirical systems (Thibaut and Connolly 2013). Violation of these assumptions, for example, the assumption that the temporal standard deviation scales directly with the mean, or that populations are approximately equal in size, can distort our perception of the portfolio effect and hence the perceived benefit of diversity to ecological stability. I tackle this issue in Chapter 2, where I consider a simple portfolio-effect metric that has been used to infer the stabilizing effects of population diversity in salmon



metapopulations. I extend the theoretical work of Doak et al. (1998) and Tilman et al. (1998) to develop an additional empirical portfolio effect that accounts for the population abundance mean-variance relationship and unequal population sizes. I show how these metrics theoretically differ and how they differ in practice when applied to metapopulations from around the world. I conclude by making practical recommendations for ecologists when choosing how to measure ecological portfolio effects.

### 1.3 Ecological portfolio management

In addition to measuring the portfolio-effect metric, we can use financial portfolio theory to inform decisions about conservation management. Markowitz's seminal contribution to financial portfolio theory was a focus on portfolio selection through what is now referred to as modern portfolio theory—the idea that out of all possible portfolios there exists a subset that maximize returns for a level of risk (or minimize risk for a level of return) (Markowitz 1952) (Fig. 1.2). In conservation biology, the goals of conservation practitioners often parallel those of financial managers, even though they are rarely expressed as such (Figge 2004). I see ecological portfolio management happening in one of three ways: choosing existing management structures that promote diversified portfolios, using portfolio theory to optimize ecological resource extraction, or using portfolio theory to optimize an ecological system itself.

First, we can identify resource management structures that promote diverse portfolios. For example, fishers can engage in catch-pooling cooperatives where fishers share the profits from their catches according to predefined rules. Sethi et al. (2012) showed that this portfolio-like scheme reduces risk for red king crab fishers in the Bering Sea by up to 40%. Other fisheries management tools, such as community-based management, individual transferable quotas, and licensing systems that allow for fishing a diversity of species, can create diversified catch portfolios for fishers and buffer fishers against the risk of poor profits (Hilborn et al. 2001; Kasperski and Holland 2013). Alternatively, we can consider the properties of a diversified portfolio, such as representation, resilience, and redundancy, and look for management strategies that promote these properties in ecological systems (Haak and Williams 2012)

Second, we can use portfolio theory directly to optimally allocate harvesting efforts. This suggestion is not new—some of the earliest references to ecological portfolios suggest portfolio theory as a management tool (Baldursson and Magnússon 1997; Costanza et al. 2000) and interest in the topic expanded in subsequent years (e.g. Edwards 2004; Sanchirico et al.

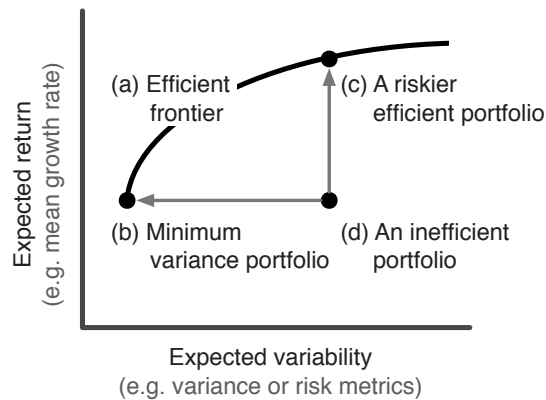


Figure 1.2: An introduction to modern portfolio theory mean-variance optimization. In finance, portfolios are formed by choosing how much to invest in various assets. Modern portfolio theory focuses on identifying the set of portfolios that optimizes the trade-off between expected return (mean) and expected variance or risk. (a) This set of portfolios is referred to as the efficient frontier. (b) The minimum variance portfolio achieves the lowest expected risk; the remaining risk is said to be undiversifiable. (c) A riskier, but still efficient portfolio. (d) An example inefficient portfolio, which has a lower expected return than (c) and greater expected risk than (b). Adapted from Hoekstra (2012).

2008; Halpern et al. 2011; Moloney et al. 2011). In conservation biology, portfolio optimization can be applied spatially. For example, Halpern et al. (2011) used portfolio theory to illustrate the tradeoff between fishing profits and spatial unevenness of marine resource value. Portfolio theory has also been used to optimize decisions about whether to clearcut or retain standing trees (Hyytiainen and Penttinen 2008; Hildebrandt and Knoke 2011). As a third example, Moloney et al. (2011) used portfolio theory to optimize the choice of grazing animals on Australia's rangelands. With few exceptions, however, the application of portfolio theory for harvesting decisions has been limited to fishery and forestry examples.

Finally, we can use ecological portfolio management to allocate conservation efforts to manage risk for an ecological system as a whole. For example, portfolio optimization can be used to spatially allocate conservation activity for wetlands to maximize ecosystem services at a given level of risk under the uncertainty of climate change (Ando and Hannah 2011; Ando and Mallory 2012). In forestry, portfolio theory has been used to select the optimal weighting of seed sources for regenerating forests under a variety of climate change scenarios (Crowe and Parker 2008). I focus on this last issue for Chapter 3, where I use portfolio theory to assess the risk–return trade-off for salmon metapopulation productivity and persistence given choices

about what habitat to conserve under climate change and stream-flow reduction scenarios.

## 1.4 Extreme risk

Early work in financial portfolio optimization focussed on mean-variance portfolio optimization (Markowitz 1952). But even by the late 1950s, Markowitz (1959) was suggesting we consider *risk* instead of variance. Whereas variance puts equal weight on upward and downward events, *risk* specifically refers to both the probability of an undesired event happening and the magnitude of loss associated with that event (Morgan and Henrion 1990; Reckhow 1994). It is increasingly common in the financial literature to assume that that rate of change of financial asset value follows a distribution that is heavier-tailed than the normal distribution (Rachev et al. 2008). First, there is ample evidence that financial returns are heavy tailed. Second, the consequences to portfolio optimization of assuming normal-tailed returns when they are heavy tailed can have dramatic consequences for risk forecasts and hence portfolio investment decisions (Rachev et al. 2008). For example, normal tailed returns would not allow for the stock market crash of 2008, but we know that events this extreme are not only possible, they have happened with surprising frequency in the last 100 years (Sornette 2009).

Taleb (2007) wrote about the concept of heavy-tailed events in detail. He coined the term ‘black swan’ to refer to rare events with large impact that are typically rationalized in retrospect. For ornithologists, the discovery of a single black-coloured swan was sufficient to disprove the hypothesis that all swans are white. Many of the major events that have shaped human history could be considered black swans. For example, with hindsight, World War I and II, the great depression, and the spread of the Internet could be considered black swans (Taleb 2007). In recent years, the fields of finance and sociology have moved towards systematically measuring these heavy-tailed events (e.g. Sornette 2009; Janczura and Weron 2012; Johnson et al. 2013).

Ecology has likewise seen a move towards focusing on risk and extremeness (e.g. Gerber and Hilborn 2001; Jentsch et al. 2007; Thompson et al. 2013, Fig. 1.3). Recent work in ecology has noted the frequency and influence of population dynamic catastrophes (Gerber and Hilborn 2001; Ward et al. 2007), ecological surprises (Lindenmayer et al. 2010; Doak et al. 2008), counterintuitive responses of populations to management (Pine III et al. 2009), and even explored how the specific concept of black swans could apply to ecology and evolution (Nuñez and Logares 2012). Discussion of the importance of catastrophic events has a long history in the ecological literature. As early as 1898, Bumpus (1899) observed that a severe winter storm off

Providence, Rhode Island killed a disproportionate number of very small and large sparrows (and this thesis uncovers a number of other catastrophic events from the 1800s). In the 1990s, both Sugihara and May (1990) (using fractals) and Mangel and Tier (1994) (using population catastrophes) highlighted extreme events as perhaps the most important force behind how long species persist in nature.

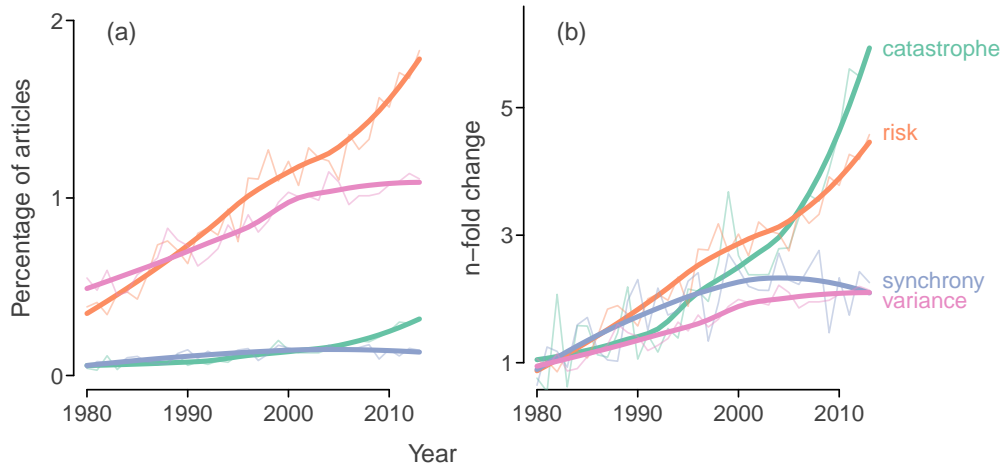


Figure 1.3: Trends in the ecological literature of four categories of terms from 1980 to 2013. I extracted the number of articles in the Web of Science Sci-Expanded database that used various groups of terms in the title of English articles from the subject fields of ‘Biodiversity & Conservation’, ‘Environmental Sciences & Ecology’, or ‘Marine & Freshwater Biology’. The term groups were: ‘extreme or catastrophe’, ‘risk’ ‘synchrony or asynchrony or covariance or synchronous or asynchronous or synchronization or synchronize’, and ‘variance or variability’. (a) Percentage of articles from these subject fields with the terms in the title. (b) Change in percentage of articles using the groups of terms since the mean percentage in 1980–1985. For example, we see approximately a five-fold increase in the number of ecological articles with the term ‘risk’ in the title since the early 1980s. The thick lines are loess smoothers fit to the underlying raw data.

In Chapter 4, I explore the concept of black swans in population dynamics by asking how often and how severely process deviations—the multiplicative stochastic jumps in abundance from time step to time step—are more heavy tailed than the commonly assumed normal distribution. I develop and simulation test a black-swan detection method based on a heavy-tailed Gompertz population model and apply it to hundreds of populations of mammals, birds, insects, and fishes. I find strong evidence for black swan dynamics, although they are rare and unrelated to life-history characteristics. Importantly, the black swan events are almost always

downwards events, which given previous work on the importance of catastrophes to population persistence times, has important implications for estimates of extinction risk that typically rely on normal-tailed population dynamics. Together, my thesis expands our understanding of ecological portfolios and in doing so contributes to our understanding of variance and covariance (Chapter 2), managing for variance and covariance (Chapter 3), and extreme events (Chapter 4) in ecological systems.

## 1.5 Contributions

This introduction and Chapter 5 (General discussion) are written in the first-person singular. Chapters 2–4 are written in the first-person plural since they are derived from published manuscripts (Chapter 2 and 3) or from a manuscript that was written for submission to a journal with co-authors (Chapter 4). Portions of Chapters 1 and 5 are derived from a draft manuscript co-authored with Nick Dulvy and Andy Cooper. This draft manuscript has also benefited from previous discussions with Jon Moore and Trevor Branch. For Chapters 2, 3, and 4, I wrote the code, analyzed the data, and wrote the first drafts of the text. The idea for Chapter 2 grew out of discussions between Nick Dulvy, Andy Cooper, and myself. Jon Moore and Michelle McClure contributed their ideas for a manuscript, which I merged with my own ideas to carry out Chapter 3. Trevor Branch first suggested I consider ecological black swans, the topic of Chapter 4. Chapters 2, 3, and 4 benefited from discussions, editing, and comments from the co-authors listed at the beginning of each chapter.

## Chapter 2

# Ecological prophets: Quantifying metapopulation portfolio effects<sup>1</sup>

### 2.1 Abstract

1. A financial portfolio metaphor is often used to describe how population diversity can increase temporal stability of a group of populations. The portfolio effect (PE) refers to the stabilizing effect from a population acting as a group or “portfolio” of diverse subpopulations instead of a single homogeneous population or “asset”. A widely used measure of the PE (the average-CV PE) implicitly assumes that the slope ( $z$ ) of a log-log plot of mean temporal abundance and variance (Taylor’s power law) equals two.
2. Existing theory suggests an additional unexplored empirical PE that accounts for  $z$ , the mean-variance PE. We use a theoretical and empirical approach to explore the strength and drivers of the PE for metapopulations when we account for Taylor’s power law compared to when we do not. Our empirical comparison uses data from 51 metapopulations and 1070 subpopulations across salmon, moths, and reef fishes.
3. Ignoring Taylor’s power law may overestimate the stabilizing effect of population diversity for metapopulations. The disparity between the metrics is greatest at low  $z$  values where the average-CV PE indicates a strong PE. Compared to the mean-variance method,

---

<sup>1</sup>A version of this chapter appears as Anderson, S.C., A.B. Cooper, N.K. Dulvy. 2013. Ecological prophets: Quantifying metapopulation portfolio effects. *Methods in Ecology and Evolution*. 4(10): 971-981. <http://doi.org/10.1111/2041-210X.12093>.

the average-CV PE estimated a stronger PE in 84% of metapopulations by up to seven-fold. The divergence between the methods was strongest for reef fishes ( $1.0 < z < 1.7$ ) followed by moths ( $1.5 < z < 1.9$ ). The PEs were comparable for salmon where  $z \approx 2$ .

4. We outline practical recommendations for estimating ecological PEs based on research questions, study systems, and available data. Since most PEs were stabilizing and diversity can be slow to restore, our meta-analysis of metapopulations suggests the safest management approach is to conserve biological complexity.

## 2.2 Introduction

Biological complexity is increasingly recognized as a critical factor underpinning the stability of ecological systems (e.g. Hilborn et al. 2003; Ives and Carpenter 2007; Schindler et al. 2010). While the diversity-stability relationship for ecosystem properties is generally held to be true, what is not known is the relative increase in benefit from each additional element of biodiversity for stability and persistence (Cardinale et al. 2012). For example, Schindler et al. (2010) found that sockeye salmon populations in Bristol Bay were twice as stable as a homogeneous population and management should focus on retaining biological diversity to ensure a ten-fold reduction in the frequency of fishery closures. The stabilizing benefit of such population diversity is clearly a critical and undervalued component of ecological systems for resource management to conserve, yet there are few ways to quantify its benefit.

The empirical portfolio effect (PE) is a rapidly popularized metric (e.g. Schindler et al. 2010; Carlson and Satterthwaite 2011; IMCC 2011) derived from theory introduced a decade earlier (Doak et al. 1998; Tilman et al. 1998; Tilman 1999) that aims to measure the increase in stability due to subpopulation diversity within a metapopulation (or greater species diversity within a community). For example, we can think of salmon from individual streams as assets (subpopulations) within a portfolio (metapopulation) that comprises the watershed. If subpopulations react differently to environmental variability, then the metapopulation may experience a reduced risk of collapse or decline. Similarly, financial managers choose portfolios of diverse financial assets to reduce their risk of financial losses.

Financial managers estimate the benefit of diversifying a financial portfolio by comparing the variability in returns from investing in a single asset to the variability from investing in a diversified portfolio (Markowitz 1959). In ecology, the empirical PE has been calculated by

comparing the temporal coefficient of variation (CV) of metapopulation abundance (the diversified portfolio; Fig. 2.1a) to the average CV of subpopulation abundances (the single assets; Fig. 2.1b) (Secor et al. 2009; Schindler et al. 2010; Carlson and Satterthwaite 2011). We refer to this approach as the average-CV PE (Fig. 2.1c). But ecological and financial systems differ; it is timely to consider whether we can apply the same approach to ecological systems.

One crucial difference between financial and ecological portfolios is how asset variability scales with investment. For a financial asset, the standard deviation of an investor's returns increases linearly with investment because investing in a financial stock doesn't meaningfully affect the stock's properties. Therefore, as mean financial investment increases, we expect the variance in returns to increase by a power of two. This is not true in ecological systems. As abundance of a subpopulation grows (i.e. as investment in the single asset grows), the standard deviation usually increases nonlinearly according to Taylor's power law: the slope ( $z$ ) of a log-log plot of the variance and mean of subpopulation abundance is typically less than two (Taylor et al. 1980; Taylor and Woivod 1982). This means that larger populations may be less variable than expected if we applied the financial metaphor. The CV is not necessarily a size-independent metric of variability (McArdle et al. 1990).

The theoretical work of Tilman et al. (1998) implies an alternative way to measure the empirical PE that accounts for the mean-variance relationship. Rather than assuming we can represent the variability of the theoretical homogeneous metapopulation (the single asset) by the average subpopulation CV, we can estimate the variance of the homogeneous metapopulation by extrapolating the mean-variance relationship to the observed metapopulation size (Fig. 2.1d). We can then compare this expected homogeneous-population variability to the observed metapopulation variability to get what we call the mean-variance PE. This mean-variance PE asks: If the mean-variance relationship continued to scale as we observed for larger and larger subpopulations, how much more variable would we expect the metapopulation to be if it was identically sized but acted with the same dynamics as any one subpopulation? Therefore, although both the mean-variance PE and the average-CV PE get at the benefit of splitting one large population into many subpopulations, only the mean-variance PE accounts for the observed mean-variance scaling relationship—the average-CV PE assumes that  $z = 2$ . Given this theoretical advantage of the mean-variance PE, what happens when we apply the average-CV PE to empirical data where  $z$  is typically less than two, as recent literature has done (Secor et al. 2009; Schindler et al. 2010; Carlson and Satterthwaite 2011)?



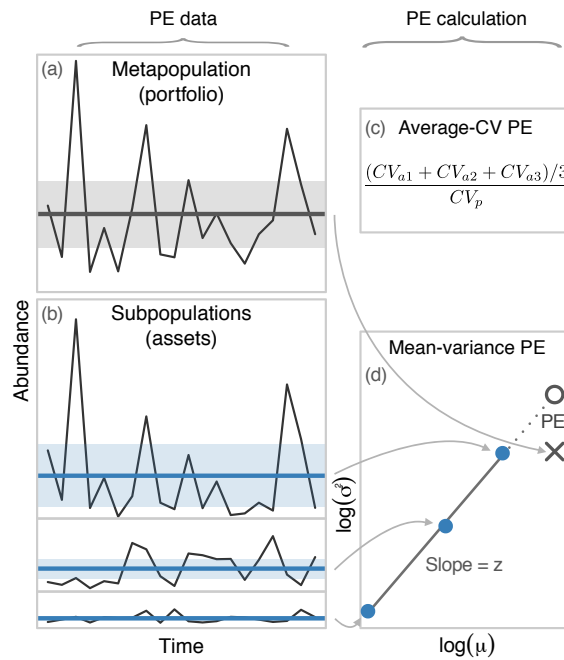


Figure 2.1: Estimating the two PEs from empirical data. (a, b) Example metapopulation (portfolio) and subpopulation (asset) abundance time-series. Horizontal lines represent the time-series' means and the shaded regions represent variability. (c) We calculated the average-CV PE by dividing the average CV of the subpopulations ( $CV_a$ ) by the CV of the metapopulation ( $CV_p$ ). (d) We calculated the mean-variance PE by (1) plotting the mean and variance of each subpopulation on log-log axes, (2) extrapolating the subpopulation mean-variance relationship to the metapopulation mean (open-grey circle), and (3) comparing the predicted (open-grey circle) and observed (grey cross) metapopulation variability. Both methods will estimate the same PE if the slope of the log-log plot ( $z$ ) equals two.

Here, we conducted the first large-scale cross-taxa evaluation of the average-CV PE compared to the mean-variance PE for metapopulations, specifically addressing three main questions: (1) How does the average-CV PE differ compared to the mean-variance PE when applied to theoretical systems with varying  $z$  values? (2) How prevalent and strong is this difference across 51 metapopulations and 1070 subpopulations of salmon, moths, and reef fishes? (3) Despite its stronger theoretical foundations, is the mean-variance PE a reliable empirical metric of how subpopulation diversity benefits stability? We conclude with a guide to measuring metapopulation PEs based on question, study system, and data type.

## 2.3 Materials and methods

### 2.3.1 Defining the metapopulation portfolio

In our finance-ecology metaphor we represent portfolio value as metapopulation abundance and financial-asset value as subpopulation abundance. We define metapopulations as groups of that behave largely independently but are linked by dispersal of individuals among subpopulations (Levins 1969). Although our data represent subpopulations in the spatial-metapopulation sense, the methods in this paper could be applied more broadly. For example, future studies could consider different age classes, different life-history variants, or populations with different thermal-tolerances as subpopulations. Although the PE has also been applied to multiple species within a community (e.g. Doak et al. 1998; Tilman et al. 1998; Karp et al. 2011), and elements of our analysis are applicable to community portfolio effects, the analysis of PEs in communities is complicated by trophic interactions, changes in mean abundance with increasing diversity (the over-yielding effect), and differing mean-variance scaling relationships across species (e.g. Loreau 2010; Thibaut and Connolly 2013).

When discussing the properties of metapopulation portfolios we use three terms (stability, diversity, and homogeneous population), which we define here. We define *stability* in terms of the variability (CV) of population trajectories through time. We define *subpopulation diversity* as the asynchrony (lack of correlation) between the groups defined as subpopulations. Since our metrics are phenomenological, they don't specify the mechanism generating asynchrony, but a central candidate would be diversity of response to environmental fluctuations (e.g. Elmqvist et al. 2003; Loreau and de Mazancourt 2008; Thibaut et al. 2012). We define a *homogeneous population* as a theoretical population the same size as the existing "diverse" population but lacking whatever subpopulation diversity we are measuring. For metapopulations

we can think of this in one of two ways: (1) a population the same size as the metapopulation that behaves like the average subpopulation or (2) a metapopulation with synchronized subpopulation dynamics.

### 2.3.2 Theoretical evaluation of portfolio effects

We defined the PE as the ratio of the CV of a theoretical system composed of a single subpopulation or asset ( $CV_a$ ) to the observed metapopulation or portfolio CV ( $CV_p$ ). A PE of two, for example, would indicate that a metapopulation is two times less variable than if it were comprised of a single homogeneous population. For uncorrelated subpopulations and  $\sigma^2 = c\mu^z$  (where  $\sigma^2$  is the temporal variance,  $\mu$  is the temporal mean, and  $c$  is a constant that doesn't affect the PE and is hereafter ignored for simplicity), both interpretations of the PE define  $CV_p$  for subpopulations  $i = 1$  through  $n$  as

$$CV_p = \frac{\sqrt{\mu_i^z + \mu_{i+1}^z + \dots + \mu_n^z}}{\mu_i + \mu_{i+1} + \dots + \mu_n}. \quad (2.1)$$

The average-CV PE defines  $CV_a$  as

$$CV_a = \frac{\frac{\sqrt{\mu_i^z}}{\mu_i} + \frac{\sqrt{\mu_{i+1}^z}}{\mu_{i+1}} + \dots + \frac{\sqrt{\mu_n^z}}{\mu_n}}{n}, \quad (2.2)$$

whereas the mean-variance PE defines  $CV_a$  as

$$CV_a = \frac{\sqrt{(\mu_i + \mu_{i+1} + \dots + \mu_n)^z}}{\mu_i + \mu_{i+1} + \dots + \mu_n}. \quad (2.3)$$

Equations 2.2 and 2.3 are equal if  $z = 2$ .

To extend the theoretical PE calculations to metapopulations with  $\rho$  correlation between subpopulations, we can calculate the metapopulation or portfolio variance  $\sigma_p^2$  as

$$\sigma_p^2 = \sum_{i=1}^n \sigma_i^2 + \sum_{i=1}^n \sum_{j=1}^n \rho \sqrt{\sigma_i^2 \sigma_j^2}. \quad (2.4)$$

We explored the implications of the two PE definitions across four statistical properties that are ecologically meaningful and have precedence in the PE literature (Tilman 1999; Cottingham et al. 2001; Loreau 2010; Thibaut and Connolly 2013): the correlation between subpopulations, the temporal mean-variance scaling relationship ( $z$ ), the number of subpopulations, and the evenness of subpopulation mean abundance. The expected effect of these properties on stability has been addressed in the literature cited above. Our focus, instead, is to understand the

performance of the average-CV method compared to the mean-variance PE across these four ecological attributes. We show that differences between these PE metrics arise in real-world metapopulations, and for each taxon we diagnose the ecological reasons why the differences arise.

### 2.3.3 Empirical evaluation of portfolio effects

#### Data sources

To test the real-world strength of the average-CV and mean-variance PEs, we collected meta-population time-series data for salmon, moths, and reef fishes (Supporting materials Table 2.1; Figs 2.7, 2.8). We obtained salmon returns from the primary literature, in particular Dorner et al. (2008), and government research documents (Table 2.1). We obtained moth abundance trends from the Rothamsted Insect Survey (Conrad et al. 2004). These data represent univoltine moths captured by light traps. We obtained reef visual census fish counts from the Australian Institute of Marine Science Long-term Monitoring Program (Sweatman et al. 2008). See Tables 2.2 and 2.3 for the subpopulation site locations of the moth and reef fish populations, respectively. Details on our data sources are available in the Supporting Information.

We defined data inclusion criteria to ensure adequate estimation of temporal mean-variance relationships. For salmon and moths we excluded populations with less than four subpopulations or ten years of data and where the largest subpopulation temporal mean was less than three times the size of the smallest temporal mean. To reduce the number of reef fish populations to an approximately comparable number, we used the metapopulations used by Mellin et al. (2010). Their main inclusion criteria were five subpopulations, 15 years of data, and two orders of magnitude difference in subpopulation means.

#### Average-CV PE

We calculated the empirical average-CV PE as the ratio of the mean subpopulation CV to the observed metapopulation CV (Fig. 2.1c). We estimated confidence intervals by bootstrap; we sampled the subpopulations within each metapopulation 500 times, with replacement, and recalculated the PE. We then used the adjusted bootstrap percentile (BCa) 95% confidence intervals (Canty and Ripley 2012).

### Mean-variance PE

To calculate the empirical mean-variance PE, we estimated  $z$  as the slope of a linear regression of the subpopulations' ( $i$ ) interannual  $\log(\sigma^2)$  and  $\log(\mu)$ ,

$$\log(\sigma_i^2) = \beta_0 + z \cdot \log(\mu_i) + \epsilon_i \quad (2.5)$$

where  $\epsilon_i$  represents independent and identically distributed residual error with mean zero and an estimated variance. We used this model to predict the variance given the mean of the meta-population abundance ( $\hat{\sigma}^2$ ; Fig. 2.1d). The  $\hat{\sigma}^2$  reflects the variance we would expect if the portfolio was composed of a homogeneous population. We then calculated the mean-variance PE as the ratio of observed  $\sigma^2$  to predicted  $\hat{\sigma}^2$ . The mean-variance PE is therefore equivalent to the average subpopulation CV adjusted for the observed subpopulation CV mean-variance scaling relationship. We obtained confidence intervals on the mean-variance PE by re-calculating the PE using the 95% confidence intervals on the predicted metapopulation variance.

Our empirical mean-variance PE calculation assumes the inter-subpopulation mean-variance relationship can be used as a proxy for the intra-subpopulation relationship. To test this we estimated the intra-subpopulation mean-variance relationship between the first and second halves of the subpopulation time series for the time-series in which one half was at least two-times greater. We compared these intra-subpopulation  $z$  values with the inter-subpopulation  $z$  values used in our analysis.

#### 2.3.4 Alternative ways of extrapolating the mean-variance PE

*Quadratic extrapolations:* In our main analysis, we estimated Taylor's power law  $z$  values by linear regression of the time-series' log-transformed mean and variance values. In some cases, a quadratic fit may be more appropriate (Routledge and Swartz 1991; Perry and Woiwod 1992). We fit a quadratic model,

$$\log(\sigma_i^2) = \beta_0 + \beta_1 \log(\mu_i) + \beta_2 \log(\mu_i)^2 + \epsilon_i, \quad \beta_2 \geq 0 \quad (2.6)$$

Perry and Woiwod (1992) suggest limiting the lower value of  $\beta_2$  to 0 since a negative  $\beta_2$  would imply that at some value of  $\mu$  the  $\sigma^2$  would decrease with increasing  $\mu$  and eventually become negative. We used the R package `nls` (R Core Team 2013) with the `port` algorithm to fit the quadratic model and bound the lower value of  $\beta_2$  to 0. If  $\beta_2 = 0$  the quadratic model simplifies to the linear model.

*Model averaging:* Whereas the quadratic version of Taylor’s power law can only provide a closer fit to the data than the linear version due to the added coefficient, it does so at the expense of greater model complexity and potentially poorer predictive capacity. We also examined predictions averaged across the linear and quadratic models with the predictions weighted by the Akaike weights of their respective models (Burnham and Anderson 2002). We fit an AICc-model-averaged version of the linear and quadratic Taylor’s power law fits using the R package MuMIn (Bartoń 2012).

### 2.3.5 Accounting for non-stationary time-series

Long-term trends in data can upwardly bias variability metrics such as the CV. We therefore conducted two alternative analyses in which we detrended the data before estimating the PEs. We used the residuals from (1) a fitted linear model and (2) a fitted loess smoother (Loess function; R Core Team 2013) with a smoothing span of 75% of the data. For both the subpopulations and metapopulations we calculated the mean abundance before detrending. We estimated the variance of each subpopulation using the detrended time-series. We estimated the variance of the metapopulations using the detrended version of the original metapopulation abundance time-series. A more thorough analysis of PEs for non-stationary time series might consider the distribution of means, variances, and CVs within each subpopulation, but was beyond the scope of our analysis.

### 2.3.6 The *ecofolio* R package

We provide an R package *ecofolio* to estimate the PEs described in this paper (see the Supporting Information). In addition to the average-CV and mean-variance PEs, our package includes options to fit quadratic mean-variance scaling models, average across mean-variance model predictions, and detrend non-stationary time-series.

## 2.4 Results

### 2.4.1 Theoretical evaluation of portfolio effects

By assuming  $z = 2$ , the average-CV method can misrepresent the effect of changes in subpopulation number, correlation, and evenness on the PE (Fig. 2.2). The average-CV PE universally becomes more stabilizing (higher PE) as subpopulation number increases regardless of  $z$ , whereas when we account for the mean-variance relationship, the PE can become destabilizing

with more subpopulations at small  $z$  values (Fig. 2.2a). The PE becomes less stabilizing as correlation increases regardless of the method, although accounting for the mean-variance relationship shifts the PE uniformly (assuming even subpopulation sizes) across all correlation values (Fig. 2.2b). The average-CV PE can erroneously become more stabilizing as subpopulations become uneven; the mean-variance PE indicates that the PE would become less stabilizing at high  $z$  values or remain relatively constant at low  $z$  values (Fig. 2.2c).

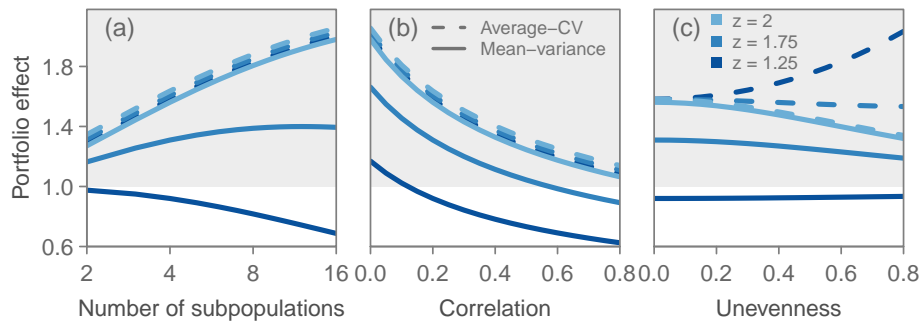


Figure 2.2: The ecological factors driving the PE in theoretical systems. A PE of two, for example, would indicate a two-fold increase in stability for the portfolio compared to what we would expect in a single homogeneous population of the same size. We show the mean-variance PE and average-CV PE for three  $z$  values across (a) number of subpopulations, (b) correlation between subpopulation time-series, and (c) unevenness of mean subpopulation abundance. We generated uneven mean subpopulation abundances by drawing four values at quantiles of 0.2, 0.4, 0.6, and 0.8 from a log-normal distribution with log-mean  $\mu$  ( $\mu = 2$ ) and log-standard deviation of the unevenness value (the x-axis) times  $\mu$ . We fixed correlation at 0.2 and subpopulation number at four in all panels where these parameters weren't varying. The grey-shading indicates stabilizing PEs. Both PE definitions are equal across all scenarios at  $z = 2$ . In panels (a) and (b) the average-CV PE is the same regardless of  $z$ .

#### 2.4.2 Empirical evaluation of portfolio effects

The key assumption that ecological systems have the same mean-variance relationship as financial systems ( $z = 2$ ) does not hold across taxa. Whereas  $z$  was not significantly different from two for 17/20 of the salmon metapopulations, there was infrequent overlap between the 95% CI and two for the moth metapopulations (3/20), and no overlap for reef fish metapopulations (Supporting materials Figs 2.9, 2.10). The inter-subpopulation mean-variance relationship was a reasonably unbiased proxy for the intra-subpopulation mean-variance relationship. The slope of a regression of median intra- and inter-subpopulation  $z$  was 1.04 (95% CI: 0.51–1.57) although there was a high degree of scatter ( $R^2 = 0.25$ ; Supporting materials Fig. 2.11).

In our empirical meta-analysis, the PEs varied strongly between, but also within, taxonomic groups due to the mean-variance scaling (Fig. 2.3). The mean-variance PE ranged from 0.5–2.0 and the average-CV PE from 0.8–6.3. Hence, at best the mean-variance PE suggests the metapopulation portfolio is twice as stable as the homogeneous single asset. In comparison, the average-CV PE suggests the metapopulation portfolio could be up to six times more stable. The  $z$  values varied by taxonomic group, with the highest observed for salmon populations and the lowest for reef fishes. As  $z$  decreased (reading from top to bottom) the average-CV PE indicated increasingly stabilizing PEs compared to the mean-variance PE (Fig. 2.3a). For salmon, where the  $z$  values tended to be near two, the PE metrics were largely in agreement (Fig. 2.3a, b). By contrast, for reef fishes, where the  $z$  values were small (mean = 1.3, range = 1.0–1.7), the meta-analytic average-CV PE indicated a substantially more stabilizing PE (mean = 3.6, 3.2–4.3 95% CI) than the mean-variance PE (mean = 0.9, 0.8–1.0 95% CI) (Fig. 2.3a, d). The dashed-red lines in Fig. 2.3b–d illustrate the mean-variance fit if  $z$  is assumed to equal two as in the average-CV PE. Whereas the mean-variance relationship assumed by the average-CV appears reasonable for salmon (Fig. 2.3b), it deviates strongly from the observed relationship for some moth and reef fish metapopulations (Fig. 2.3c, d).

The mean-variance PE was highly sensitive to the estimation method (Fig. 2.4). In particular, 13/18 reef fish metapopulations switched from destabilizing to stabilizing PEs with quadratic (Supporting materials Fig. 2.12) or quadratic-linear averaged (Supporting materials Fig. 2.13) models. The AICc of the quadratic models was lower in 11/51 metapopulations and at least two units lower in 8/51, indicating increased support despite the added model complexity. Linear detrending generally created a similar mean-variance PE pattern to the original mean-variance PEs (Fig. 2.4, Supporting materials Fig. 2.14). Loess detrending increased the mean-variance PE in 34/51 cases and the average-CV PE in 34/51, lowering it in the others (Fig. 2.4, Supporting materials Fig. 2.15). None of the detrending options or alternative mean-variance extrapolations resulted in a similar pattern for both the mean-variance and average-CV PE.

### 2.4.3 Diagnosing the ecological properties of empirical portfolio effects

Plotting the empirical metapopulations in the theoretical PE parameter space revealed five key findings (Fig. 2.5). (1) By viewing the coloured shading of the panels from left to right, we can see that the average-CV PE responds inversely to  $z$  compared to the mean-variance PE, and this issue is prevalent for the parameter space observed in real ecological systems. (2) The empirical PEs were strongly grouped by taxonomy (see also Supporting materials Fig. 2.16).



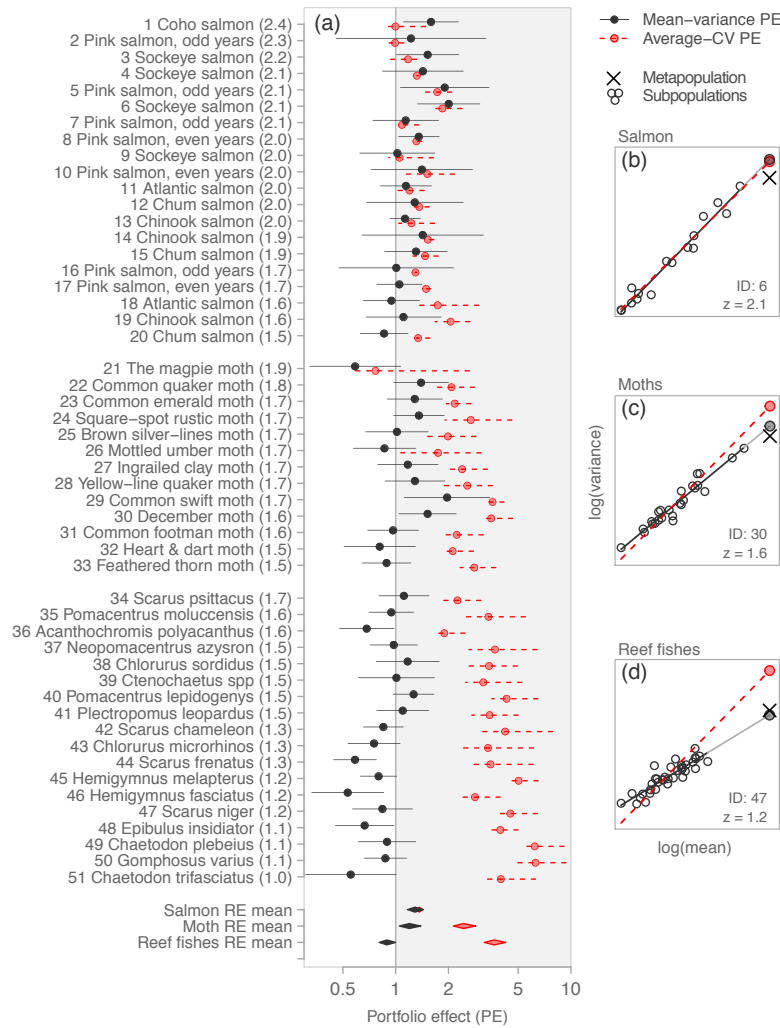


Figure 2.3: PEs across 51 metapopulations. (a) Empirical PEs (circles) and 95% CIs (lines) for the mean-variance method and the average-CV PE method. We ordered metapopulations within taxonomic groups by Taylor’s law  $z$  values (indicated in brackets beside each metapopulation name). Diamonds represent inverse-variance weighted random-effect (RE) meta-analytic means and 95% CIs. Numbers before population names represent population IDs (see Table 2.1). PEs  $> 1$  (grey shading) represent stabilizing effects; note the log-distributed x-axis. (b, c, d) Examples of using Taylor’s power law to calculate the mean-variance PE. The solid black regression line projects the subpopulation mean-variance relationship to the metapopulation mean abundance (shaded grey circle). The  $\times$  denotes the observed metapopulation mean and variance. The ratio of the observed to predicted variance represents the mean-variance PE. The red circle denotes the average-CV PE and the dashed-red line the mean-variance relationship under the assumption that  $z = 2$ , as the average-CV PE assumes.

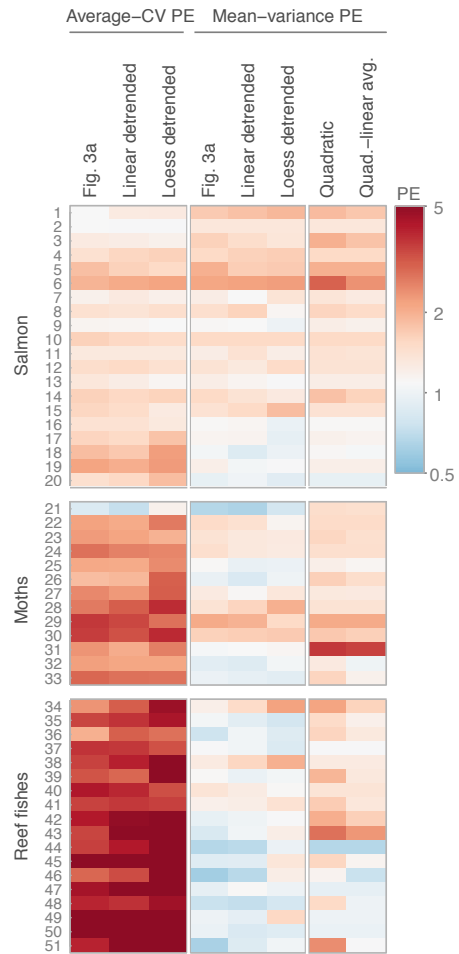


Figure 2.4: The sensitivity of PE metrics across two detrending (linear and loess) methods (columns 2–3 and 5–6) and three mean-variance model fits (columns 4, 7–8). Columns 1 and 4 represent the same PEs as shown in Fig. 2.3, but with colour indicating the strength of stabilizing effect. Red indicates a stabilizing PE, blue indicates a destabilizing PE, and white indicates a neutral PE. The y-axis shows the same metapopulation IDs as Fig. 2.3.

(3) We did not observe metapopulations that were both highly uneven and highly correlated (lower-right panels of Fig. 2.5). (4) The PE surface surrounding the observed metapopulations (the colour shading) was highly sensitive to changes in  $z$  for the mean-variance method when correlation was low (e.g. Fig. 2.5b), but the corresponding surface of the average-CV PE for the same metapopulations was insensitive to changes in  $z$  (e.g. Fig. 2.5k). (5) The average-CV method, however, considerably overestimated the PE compared to the mean-variance PE for uneven metapopulations with small values of  $z$  (Fig. 2.5c versus 2.5l).

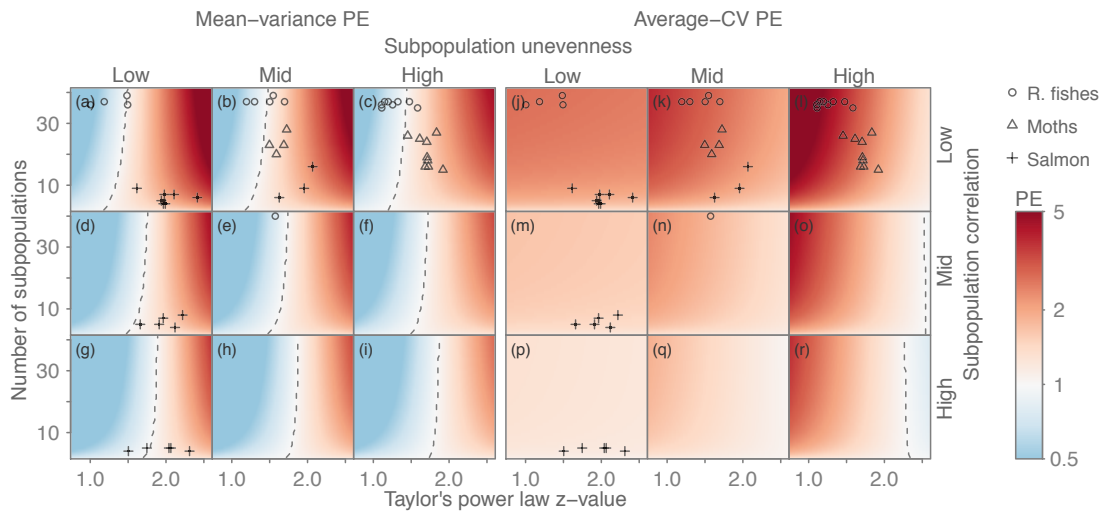


Figure 2.5: Empirical ecological PEs (points) overlaid in theoretical PE parameter space (colour shading). The colour shading indicates the stabilizing-effect of the theoretical mean-variance PEs (a–i) and average-CV PEs (j–r): red indicates a stabilizing effect and blue indicates a destabilizing effect. The dashed lines indicate neutral PEs. Columns from left to right show systems with increasingly uneven subpopulation sizes, and rows from top to bottom show systems with increasingly strong mean correlation between subpopulation (see the Supporting Information).

Predicting the PE using these four properties alone (binned as shown in Fig. 2.5) explained 84% of the variability in the average-CV PE and 53% of the mean-variance PE ( $R^2$  from a regression of log theoretical PE and log empirical PE; Supporting materials Fig. 2.17). The factors driving the PE co-varied; in particular, we observed high correlation of subpopulations associated with high variability (CV) and few subpopulations (Supporting materials Fig. 2.18b, c). High  $z$  values occurred when there were few moderately-to-highly correlated subpopulations (Supporting materials Fig. 2.18e, f).

## 2.5 Discussion

We conclude that the empirical average-CV PE is incompatible with Taylor's power law and, due to the parameter space in which most ecological populations exist, will tend to estimate a stronger benefit of population diversity than the mean-variance PE. In this discussion, we begin by considering the influence of mean-variance scaling on subpopulation and metapopulation stability and the possible mechanisms behind stabilizing portfolio effects. We then review limitations of these phenomenological metrics and discuss the potential of mechanistic models. We conclude by synthesizing our results into practical recommendations for quantifying ecological PEs.

### 2.5.1 The influence of mean-variance scaling

The primary difference between the mean-variance and average-CV PEs is how they depend on  $z$ . The mean-variance PE becomes more stabilizing with increasing  $z$ . The average-CV PE does the opposite (or remains constant) because the theory assumes  $z = 2$  and the measures increasingly diverge as empirical populations deviate from this value. An increased  $z$  value (with all else being equal) means that all subpopulations are more variable (Mellin et al. 2010), but it also increases the benefit of a portfolio structure (Tilman et al. 1998; Tilman 1999; Cottingham et al. 2001). This subtlety highlights a potential source of confusion: the PE is a relative measure comparing two sources of variability. It does not reflect the absolute stability of the portfolio or of the theoretical homogeneous portfolio. The stability of these components could decline while the PE increases. In some scenarios, we can think of the mean-variance PE as a consolation prize for a higher  $z$  value—the subpopulations become less stable and the metapopulation becomes less stable, but the stabilizing effect of diversity increases.

Why is  $z$  usually less than two? Explanations tend to fall into one of three categories. First, the most common explanation is demographic stochasticity. Demographic stochasticity has been implicated via simple stochastic population growth models (e.g. Anderson et al. 1982; Ballantyne IV 2005) and may be a particularly strong driver when density dependence generates chaotic dynamics (Perry 1994). In simplified theoretical systems,  $z$  will tend towards two under conditions that increase population synchrony (such as strong environmental forcing) and tend towards one under conditions that decrease synchrony (such as strong demographic stochasticity) (Loreau 2010). Second, competitive species interactions can affect  $z$  values. (Kilpatrick and Ives 2003). For example, if competition with other species impacts larger populations less

than smaller populations, then  $z$  will be less than two. Third, measurement error in abundance estimates (Perry 1981), and particularly rounding at low abundance (Taylor and Woivod 1982), can create artificially low  $z$  values. However, it remains unclear which of these three explanations, under what conditions, are responsible for observed  $z$  values across real ecological systems. Further,  $z$  can depend on the spatial and temporal scale of analysis (Lepš 1993) and most existing theories do not explain why  $z$  could be greater than two as we observed in 8/51 of our metapopulations and other experimental and observational studies have observed (e.g. Valone and Hoffman 2003).

In financial systems, analysts use the equivalent of the average-CV PE to calculate the benefit of diversifying a financial portfolio. For such systems, the approach makes sense since the standard deviation of investment value should scale directly with investment ( $z = 2$ ). For example, if a financial investor triples investment in an asset, the investor can expect the standard deviation of the returns from that investment to triple. Similarly, the average-CV PE may be an appropriate method if applied to analogous questions about natural resource extraction. For example, we can ask how stable a fisher's catches would be if the fisher targeted a diverse portfolio of stocks instead of a single stock. Here, the analogy is more straightforward: the fisher (the investor) invests time, effort, and resources into fishing a fish stock (the asset) or multiple fish stocks (the portfolio) and catches are returned. Given moderate levels of fishing and ignoring issues related to efficiency, any one fisher will not change the mean-variance properties of the fish stock and hence the average-CV PE will be appropriate.

The PE metrics in this paper compare the observed metapopulation variability to the theoretical variability of a single homogeneous population. This homogeneous-population reference point is the most direct interpretation of the financial portfolio analogy—a financial investor can invest all her money in a single asset (our reference point) or in a diversified portfolio (our comparison). This homogeneous-population reference point is loosely equivalent to the monoculture reference point often used in community PE analyses (e.g. Equation 7 in Thibaut and Connolly 2013). However, other reference points may be more relevant to ecology and easier to test experimentally. For example, researchers might instead choose as a reference point metapopulation variance under a harvesting regime that tends to synchronize subpopulations or metapopulation variance if habitat loss eliminated certain subpopulations.

### 2.5.2 Mechanisms driving metapopulation portfolio effects

Two major mechanisms may generate stabilizing metapopulation PEs. First, diversity of phenotypes across subpopulations can cause subpopulations to react differently to the same environmental forces (response diversity; Elmqvist et al. 2003). Second, since metapopulations can exist over a large area, subpopulations may experience a greater diversity of environmental conditions than an individual population (i.e. Moran effect). In contrast, non-systematic sources of variability such as demographic stochasticity should not generate stabilizing PEs (Loreau and de Mazancourt 2008). Our results suggest a research agenda that seeks to understand the relative contribution of these mechanisms across taxa and geography and the ecological management approaches that can promote stabilizing PEs.

We observed a number of PEs less than one. These PEs indicate the metapopulations would theoretically be less variable as one large homogeneous population than as the product of many small subpopulations. These have been referred to as inverse PEs (Thibaut and Connolly 2013), and documented in other observational studies (DeClerck et al. 2006). One explanation for these inverse PEs could be increased demographic stochasticity at low population densities resulting in an Allee effect (Allee 1931). Further, Minto et al. (2008) demonstrated an increase in the variability of fish offspring survival at low population densities. The same sized metapopulation split into fewer subpopulations might avoid these effects. A second explanation for these apparent inverse PEs could involve hidden diversity. Other elements of diversity, such as size and age structure, can be reduced at low population densities (e.g. Hutchings and Myers 1993). Therefore, inverse PEs could arise if the diversity we are measuring (subpopulation number) increases but the unmeasured diversity within the subpopulations decreases. This hidden diversity may be more relevant to stability.

### 2.5.3 Limitations of phenomenological portfolio effects

Beyond tending to overestimate the benefit of diversity if  $z < 2$ , there are potential consequences to applying the average-CV as an ecosystem index. First, the average-CV PE could fail to prioritize conservation of populations most in need. For example, if we consider two otherwise similar metapopulations, the average-CV PE will always be the same or stronger for metapopulations divided into more subpopulations. However, the mean-variance PE indicates that there is a threshold at which subdivision no longer benefits metapopulation stability (Figs 2.2a, 2.5a–i, Supporting materials Fig. 2.19). Second, used as an ecosystem index through time, the average-CV PE could fail to warn us of critical change or create the false impression

of recovery. For example, if a reef fish metapopulation with a low  $z$  value and moderate evenness (circles in Fig. 2.5k) became more uneven in mean subpopulation size (see Fig. 2.5l) the average-CV PE would become up to about five times more stabilizing. The mean-variance PE informs us, however, that a change in evenness has little influence on the portfolio effect in this parameter space (Fig. 2.5b cf. c).

Despite its stronger theoretical foundations, we emphasize caution when interpreting empirical mean-variance PE values for reasons related to model, biological, and measurement uncertainty. *Model uncertainty*: Is a log-log mean-variance linear model always best supported by the data? We often observed non-linearities in the relationship and studies have suggested numerous other mean-variance models (e.g. quadratic models, Routledge and Swartz 1991; or models with a break-point at low population abundance, Perry and Woivod 1992). *Biological uncertainty*: Even if we knew the mean-variance model precisely, will the same dynamics persist when extrapolating outside the range of observed data? *Measurement uncertainty*: There may be biases in the estimated  $z$  values because of observation error (Perry 1981; Taylor and Woivod 1982), and estimates of  $z$  can depend on how time-series are aggregated (here, what we define as a subpopulation) (Fronczak and Fronczak 2010). Conclusions drawn from any phenomenological mean-variance relationships should be tempered with caveats such as these.

The PE metrics measured in this paper are limited by the observational data to which they are typically applied. Recent mechanistic stability-diversity models that explicitly account for asynchrony of response to environmental conditions exist (e.g. Ives et al. 2003; Loreau and de Mazancourt 2008; Loreau 2010; de Mazancourt et al. 2013) but are still largely unexplored beyond theory. However, mechanistic stability-diversity models have at least two major problems. First, they must assume a functional form to a mechanism and their results may be sensitive to this decision. For example, does the environment affect productivity and does productivity impact population growth rate through a Ricker or logistic growth function? Second, the number of estimated parameters may exceed the power of most ecological data sets (Thibaut and Connolly 2013). Therefore, there remains a need for phenomenological metrics.

#### 2.5.4 Practical recommendations for quantifying ecological portfolio effects

Given the need for phenomenological PE metrics, which metric should you choose? The answer depends on the research question and the scope of the ecological system and data (Fig. 2.6). *Research question*: The PE metrics discussed in this paper ask specifically how much more stable the observed portfolio is than a theoretically homogeneous portfolio. These metrics do

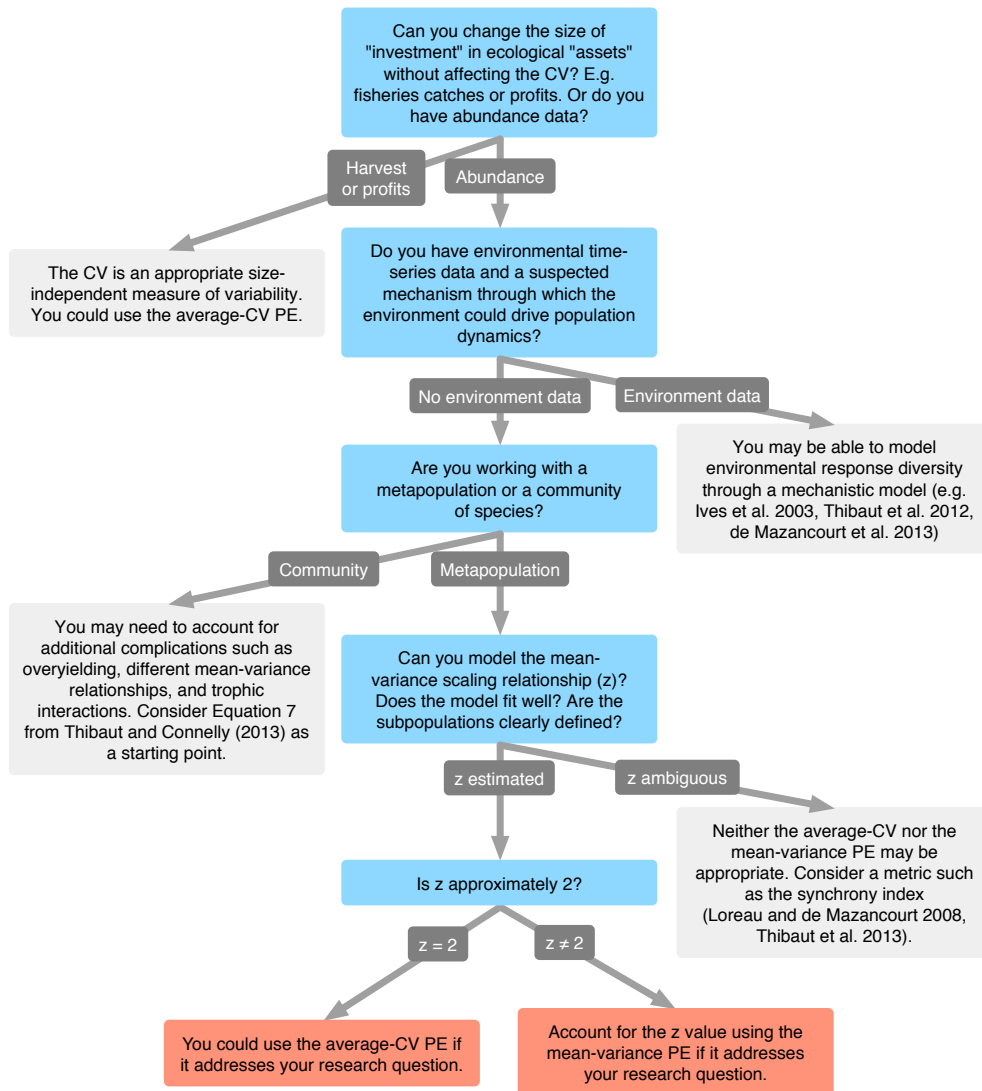


Figure 2.6: Decision tree showing options for quantifying ecological portfolios. Blue boxes in the middle column show questions to ask of the study system and available data. The orange boxes at the bottom represent the methods demonstrated in this paper. The light-grey boxes along the sides show other options to quantify ecological portfolios given different research questions, study systems, and available data.



not address the benefit of increases in portfolio size (e.g. metapopulation size) itself. In financial portfolio terms, these PE metrics address the expected variability of a portfolio without addressing the expected rate of return. *Scope*: The average-CV or mean-variance PEs are relevant to any portfolio-like aggregation in which the stability of the overall portfolio “value” is of interest and the interaction between “assets” is minimal. As demonstrated in this paper, metapopulation abundance or biomass data can fall into this scope. Other examples include fishers harvesting a portfolio of fish stocks or a predator hunting a portfolio of species. These PE metrics are not necessarily appropriate for a community of species where complications such as multiple mean-variance relationships and trophic interactions may require different phenomenological models (Thibaut and Connolly 2013).

Assuming the research question, ecological system, and data are appropriate for the methods shown in this paper, we recommend the following when choosing between the average-CV and mean-variance PEs (Fig. 2.6). First, consider whether the mean-variance scaling relationship can be estimated. Does a power law fit the data well? Are the subpopulations clearly defined? Is there minimal observation error?

- If the answer to any of these questions is no, then mean-variance scaling ( $z$ ) is not well defined and you may need to ask a different question with a different metric. For example, you could quantify the synchrony of the populations using the synchrony index (Loreau and de Mazancourt 2008; Thibaut and Connolly 2013).
- If  $z \approx 2$  then use the average-CV PE, which amounts to the same metric as the mean-variance PE at  $z = 2$  and is simpler to estimate, conceptualize, and communicate.
- If  $z$  is well defined but different than two then account for the mean-variance scaling relationship using the mean-variance PE.

The financial metaphor is an engaging and accessible way to convey the importance of biological diversity to the public and provides a framework to guide stability-diversity research (Figge 2004; Koellner and Schmitz 2006). However, our results indicate the metaphor should be used with caution. By ignoring a fundamental ecological property—the mean-variance scaling relationship—the commonly applied average-CV PE method will tend to overestimate the benefit of subpopulation diversity in real-world systems and may respond in non-intuitive ways to ecosystem change. Conversely, mechanistic stability-diversity models offer the gold-standard of PE metrics but are challenging to apply in practice and so we still need phenomenological PE

metrics. Our results highlight the importance of ground-truthing these metrics and acknowledging their limitations. Based on these results, our paper outlines practical recommendations for estimating ecological PEs for metapopulations and similarly structured ecological systems. Irrespective of the challenges of finding a suitable metric to describe the ecological PE, given the tendency for stabilizing PEs and the challenges of restoring lost population diversity, it is clear we need to find ways of understanding, prioritizing, and conserving the processes that give rise to ecological stability.

## 2.6 Acknowledgements

We thank R.M. Peterman, R. Harrington and P. Verrier (Rothamsted Insect Survey, a UK BBSRC-supported National Capability), and H. Sweatman (Australian Institute of Marine Science Long-term Monitoring Program) for providing data. We thank J.W. Moore, R. Harrington, and H. Sweatman, and four anonymous reviewers for comments that greatly improved this manuscript. We are grateful to M.P. Beakes, T.A. Branch, M. Loreau, C. Monnahan, and S.M. O'Regan for helpful discussions. Funding was provided by NSERC, the Canada Research Chairs Program, Simon Fraser University, and Fulbright Canada.

## 2.7 Supporting materials

### 2.7.1 R package to estimate metapopulation portfolio effects

In an R console, the `ecofolio` package can be installed with,

```
# install.packages("devtools") # if needed
devtools::install_github("seananderson/ecofolio")
```

Current code and install details are available at

<https://github.com/seananderson/ecofolio>

You can load the package, read the vignette, and access the help pages with:

```
library("ecofolio")
vignette("ecofolio")
help(package = "ecofolio")
```

### 2.7.2 Data sources for the empirical portfolio effect analysis

We sought to include as many metapopulation time series from as diverse taxonomic groups as possible. However, due to availability, the included data primarily represent metapopulations in North America (salmon), the United Kingdom (moths), and Australia (reef fishes) (Figure 2.8). We show a summary of the data included in our analysis of empirical ecological systems in Table 2.1 and the time series in Figure 2.7.

#### Salmon

We obtained salmon data from a variety of sources, in particular Dorner et al. (2008). Most of the salmon populations are from the northwest coast of North America, but also: Kola Peninsula, Russia (Jensen et al. 1999), southern New England (Kocik and Sheehan 2006), and Central Valley, California (Carlson and Satterthwaite 2011) (Figure 2.8). All data represent annual estimated returns—fisheries catch plus escapement to the spawning grounds. We divided pink salmon annual estimated returns into odd- and even-year time series due to their strongly distinct runs that do not interbreed (Quinn 2005). To maintain consistency with previous PE analyses involving sockeye salmon (Schindler et al. 2010) and analyses of time series of these data (Dorner et al. 2008), and due to the less distinct separate runs (Quinn 2005), we did not divide the sockeye salmon into separate runs.

Subsets of these salmon data have been used in numerous analyses relating diversity with stability. A particular feature of the salmon literature is a focus on the role of “biocomplexity”—a diversity of life-histories and local adaptations to the environment—in producing stability (Hilborn et al. 2003) and recent papers have focussed on measuring the portfolio effects we investigate in this paper (Schindler et al. 2010; Carlson and Satterthwaite 2011). In studying the mechanisms behind subpopulation asynchrony, and hence portfolio effects, studies of Pacific salmon have generally focussed on drivers that fall into two categories: (1) landscape filtering of the environment so that different subpopulations experience different environmental forces (e.g. local topology affecting stream flow) (e.g. Schindler et al. 2008), and (2) biologically-based response diversity to the environment (e.g. genetically-based variation in thermal tolerances) (e.g. Eliason et al. 2011). These patterns of asynchrony can play out not just at the decadal scale but also over centuries (Rogers et al. 2013).

### **Moths**

We obtained moth abundance time series from the Rothamsted Insect Survey (RIS). L. R. Taylor started the trap network that forms the RIS in the early 1960s; the RIS is now one of the longest-running and largest-scale insect surveys in the world (Conrad et al. 2004). Details on the survey are available in Conrad et al. (2004) and Taylor (1986). The RIS captures moths by light traps (Williams 1948) placed 1–2 m above ground; these traps catch small but reliable samples of moth populations (Williams 1948; Taylor and French 1974; Conrad et al. 2004). Although different species may show different responses to the traps (Muirhead-Thomson 1991; Woiwod and Hanski 1992), we compare across sites within the same species so this should not affect our results.

Our moth data spanned from 1999–2010 for 13 species (Table 2.1) and 28 sites (Table 2.2). We included only moths with single broods per year (univoltine moths) and single annual flight episodes since we were aggregating the data annually to maintain consistency with data from other taxonomic groups that were available. We removed site-species combinations where there were eight or more years with zero moths caught in traps to avoid sites where a given species was exceptionally rare and not likely to be consistently censused. This removed 97 subpopulations leaving 280. Further culling of populations according to the criteria in the Methods section left us with 268 subpopulations. All the species included are common within Great Britain, although some have undergone declines in abundance since the RIS began (Conrad et al. 2004).

Earlier versions of these moth data featured heavily in the work of Taylor and colleagues on the property now known as Taylor's power law (Taylor and Taylor 1977; Taylor et al. 1980; Perry 1981). This early work focussed on behavioural properties that might regulate the stability and variance of moth populations (Taylor et al. 1980). Work has continued with these datasets and studies have shown a number of mechanisms generating stability. For example, authors have shown spatial asynchrony (Gaston 1988), polyphagy (eating different kinds of food) (Redfearn and Pimm 1988), and density dependence to act as stabilizing forces (Hanski and Woiwod 1993).

### Reef fishes

We obtained reef visual census fish counts within the Greater Barrier Reef (GBR) from the Australian Institute of Marine Science's (AIMS) Long-term Monitoring Program (LTMP) (Sweatman et al. 2008). The AIMS survey data used here are from fixed transects at selected sites across 46 reefs from 1994–2010 (Table 2.3). Details of the sampling design are available from Halford and Thompson (1994). Briefly, AIMS surveys reef fish annually within six sectors of the GBR. AIMS identifies inner-, mid-, and outer-shelf positions and three reefs within each shelf position. Within each reef, AIMS chooses three sites of the same habitat and establishes five permanent 50m transects at 6–9m depth 10m apart and parallel to the reef crest. Divers count damselfishes (Pomacentrids) on 1m-wide transects and all other families on 5m-wide transects. AIMS only censuses fish one year or older since recruitment can be highly spatially and temporally variable. AIMS conducts annual standardization exercises to avoid temporal bias in counts within and across divers (Halford and Thompson 1994).

A number of recent studies have used these reef-fish data to investigate stability-diversity relationships, often focusing on functional diversity or reef size and isolation. For example, Thibaut et al. (2012) found strong asynchrony of response to the environment between three functional groups of herbivorous reef fishes, which lead to greater stability. Another benefit to this functional diversity may be increased disease resistance (Raymundo et al. 2009), presumably enhancing stability. Independent of functional roles, Mellin et al. (2010) found that small, isolated reefs have higher population variability and therefore higher probability of local extinction.

### 2.7.3 Diagnosing the ecological properties of empirical portfolio effects

We overlaid the empirical PEs in their respective theoretical parameter space to investigate the ecological properties of real-world metapopulations (subpopulation correlation, mean-variance

scaling, subpopulation number richness, and evenness). Specifically, we matched the empirical linear-regression  $z$  values and the number of subpopulations with their theoretical counterparts.

To present our results graphically in Figure 2.5, we categorized the mean correlation of the empirical subpopulations ( $\bar{\rho}$ ) into bins of  $0 \leq \bar{\rho} < 0.25$ ,  $0.25 \leq \bar{\rho} < 0.5$ , and  $0.50 \leq \bar{\rho} < 0.75$  and matched these with the theoretical PE estimated at the midpoints of these bins (i.e. 0.125, 0.375, and 0.625). We matched the disparity in subpopulation size by: (1) calculating the CV of the log of the subpopulation time series' means,  $CV(\log \mu)$ ; (2) categorizing the empirical metapopulations into bins of  $0 \leq CV(\log \mu) < 0.3$ ,  $0.3 \leq CV(\log \mu) < 0.6$ , and  $0.6 \leq CV(\log \mu) < 0.9$ ; (3) estimating the theoretical PE using evenly-spaced values from a log-normal distribution with a mean of two and standard deviation of the midpoints of these bins (i.e. 0.15, 0.45, and 0.75). Here and in Figure 2.2, we derived these evenly-spaced values as follows. We drew subpopulation ( $i$ ) quantiles  $q_i$  from the evenly-spaced sequence:  $a_1, a_2, \dots, a_n$ , where  $a_1 = 1/(n+1)$  and  $a_n = 1 - (1/(n+1))$ . We then calculated the subpopulation means at each  $q_i$  from a log-normal distribution with log-mean of two and a log-standard deviation of the “unevenness value” times the log-mean.

#### 2.7.4 Supporting Tables and Figures

Table 2.1: Metapopulations used in the empirical PE analyses. ID column numbers correspond to ID numbers in the figures.

ID	Species	Common	Location	Subpopulations	Years	Reference
1	<i>Oncorhynchus kisutch</i>	Coho salmon	Broughton archipelago, BC, Canada	6	16	(Krikošek et al. 2011)
2	<i>Oncorhynchus gorbuscha</i>	Pink salmon, odd years	Puget Sound, WA, United States	4	19	(Dorner et al. 2008)
3	<i>Oncorhynchus nerka</i>	Sockeye salmon	Bristol Bay, AK, United States	8	43	(West and Fair 2006)
4	<i>Oncorhynchus nerka</i>	Sockeye salmon	Kodiak, AK, United States	4	24	(Dorner et al. 2008)
5	<i>Oncorhynchus gorbuscha</i>	Pink salmon, odd years	Broughton archipelago, BC, Canada	7	19	(Krikošek et al. 2011)
6	<i>Oncorhynchus nerka</i>	Sockeye salmon	Fraser River, BC, Canada	16	44	(Dorner et al. 2008)
7	<i>Oncorhynchus gorbuscha</i>	Pink salmon, odd years	Kodiak, AK, United States	5	8	(Dorner et al. 2008)
8	<i>Oncorhynchus gorbuscha</i>	Pink salmon, even years	Chignik, AK, United States	5	16	(Dorner et al. 2008)
9	<i>Oncorhynchus nerka</i>	Sockeye salmon	Upper Cook Inlet, AK, United States	4	29	(Fair et al. 2011)
10	<i>Oncorhynchus gorbuscha</i>	Pink salmon, even years	Broughton archipelago, BC, Canada	7	19	(Krikošek et al. 2011)
11	<i>Salmo salar</i>	Atlantic salmon	Kola Peninsula, Russia	4	15	(Jensen et al. 1999)
12	<i>Oncorhynchus keta</i>	Chum salmon	Puget Sound, WA, United States	7	26	(Dorner et al. 2008)
13	<i>Oncorhynchus tshawytscha</i>	Chinook salmon	Columbia Estuary, OR/WA, United States	9	23	(StreamNet 2011)
14	<i>Oncorhynchus tshawytscha</i>	Chinook salmon	Elochoman River, WA, United States	5	27	(StreamNet 2011)
15	<i>Oncorhynchus keta</i>	Chum salmon	Arctic, Yukon, Kuskokwim, US and Canada	5	18	(Dorner et al. 2008)
16	<i>Oncorhynchus gorbuscha</i>	Pink salmon, odd years	Chignik, AK, United States	5	15	(Dorner et al. 2008)
17	<i>Oncorhynchus gorbuscha</i>	Pink salmon, even years	Kodiak, AK, United States	5	9	(Dorner et al. 2008)
18	<i>Salmo salar</i>	Atlantic salmon	Southern New England, United States	6	39	(Kook and Sheehan 2006)
19	<i>Oncorhynchus tshawytscha</i>	Chinook salmon	Central Valley, California	9	54	(Carlson and Satterthwaite 2011)
20	<i>Oncorhynchus keta</i>	Chum salmon	Alaska Peninsula, AK, United States	4	32	(Dorner et al. 2008)
21	<i>Abroscus grossulariata</i>	The magpie moth	UK	15	12	(Conrad et al. 2004)
22	<i>Orthostea cerasi</i>	Common quaker moth	UK	27	12	(Conrad et al. 2004)
23	<i>Hemiteles aestivaria</i>	Common emerald moth	UK	16	12	(Conrad et al. 2004)
24	<i>Xestia xanthographa</i>	Square-spot rusic moth	UK	28	12	(Conrad et al. 2004)
25	<i>Petrophora chlorosata</i>	Brown silver-lines moth	UK	18	12	(Conrad et al. 2004)
26	<i>Erannis defoliaria</i>	Mottled umber moth	UK	19	12	(Conrad et al. 2004)
27	<i>Diatris meadica</i>	Ingrailed clay moth	UK	24	12	(Conrad et al. 2004)
28	<i>Agrochola (Leptologia) macilenta</i>	Yellow-line quaker moth	UK	23	12	(Conrad et al. 2004)
29	<i>Pharmacis lupulina</i>	Common swift moth	UK	16	12	(Conrad et al. 2004)
30	<i>Poecilocampa populi</i>	December moth	UK	25	12	(Conrad et al. 2004)
31	<i>Eilema lurideola</i>	Common footman moth	UK	20	12	(Conrad et al. 2004)
32	<i>Agrotis exclamatoris</i>	Heart and dart moth	UK	23	12	(Conrad et al. 2004)
33	<i>Colotis pennaria</i>	Feathered thorn moth	UK	26	12	(Conrad et al. 2004)
34	<i>Scarus psittacus</i>	<i>Scarus psittacus</i>	GBR, Australia	37	14	(Sweatman et al. 2008)
35	<i>Pomacentrus moluccensis</i>	<i>Pomacentrus moluccensis</i>	GBR, Australia	35	14	(Sweatman et al. 2008)
36	<i>Acanthochromis polyacanthus</i>	<i>Acanthochromis polyacanthus</i>	GBR, Australia	40	14	(Sweatman et al. 2008)
37	<i>Neopomacentrus azyron</i>	<i>Neopomacentrus azyron</i>	GBR, Australia	39	14	(Sweatman et al. 2008)
38	<i>Chlorurus sordidus</i>	<i>Chlorurus sordidus</i>	GBR, Australia	37	14	(Sweatman et al. 2008)
39	<i>Ctenochaetus spp</i>	<i>Ctenochaetus spp</i>	GBR, Australia	36	14	(Sweatman et al. 2008)
40	<i>Pomacentrus lepidogenys</i>	<i>Pomacentrus lepidogenys</i>	GBR, Australia	39	14	(Sweatman et al. 2008)
41	<i>Plectropomus leopardus</i>	<i>Plectropomus leopardus</i>	GBR, Australia	37	14	(Sweatman et al. 2008)
42	<i>Scarus chameleón</i>	<i>Scarus chameleón</i>	GBR, Australia	37	14	(Sweatman et al. 2008)
43	<i>Chlorurus microrhinos</i>	<i>Chlorurus microrhinos</i>	GBR, Australia	37	14	(Sweatman et al. 2008)
44	<i>Scarus frenatus</i>	<i>Scarus frenatus</i>	GBR, Australia	36	14	(Sweatman et al. 2008)
45	<i>Hemigymmus melapterus</i>	<i>Hemigymmus melapterus</i>	GBR, Australia	37	14	(Sweatman et al. 2008)
46	<i>Hemigymmus fasciatus</i>	<i>Hemigymmus fasciatus</i>	GBR, Australia	37	14	(Sweatman et al. 2008)
47	<i>Scarus niger</i>	<i>Scarus niger</i>	GBR, Australia	37	14	(Sweatman et al. 2008)
48	<i>Epibulus insidiator</i>	<i>Epibulus insidiator</i>	GBR, Australia	37	14	(Sweatman et al. 2008)
49	<i>Chaetodon plebeius</i>	<i>Chaetodon plebeius</i>	GBR, Australia	35	14	(Sweatman et al. 2008)
50	<i>Gomphosus varius</i>	<i>Gomphosus varius</i>	GBR, Australia	36	14	(Sweatman et al. 2008)
51	<i>Chaetodon trifasciatus</i>	<i>Chaetodon trifasciatus</i>	GBR, Australia	36	14	(Sweatman et al. 2008)

Table 2.2: Moth sites used from the Rothamsted Insect Survey database. Sites are ordered from north to south. County refers to the British County. “Number of spp.” refers to the number of moth species remaining that matched our inclusion criteria.

Site name	County	Northing	Easting	Altitude (m)	Number of spp.
Starcross	South Devon	821	2972	9	12
Denny Lodge	South Hampshire	1056	4333	30	10
Bentley Wood	South Wiltshire	1324	4253	130	12
Winkworth	Surrey	1412	4991	130	12
Alice Holt	North Hampshire	1428	4803	122	12
Perry Wood	East Kent	1565	6040	80	13
Wisley II	Surrey	1579	5065	40	10
Westonbirt	West Gloucestershire	1898	3847	46	13
Geescroft I	Hertfordshire	2128	5132	130	12
Allotments	Hertfordshire	2134	5134	130	7
Barnfield	Hertfordshire	2135	5132	130	10
Hereford	Herefordshire	2476	3564	91	10
Cockayne Hatley	Bedfordshire	2494	5253	76	11
Llysdinam	Breconshire	2586	3009	197	11
Tregaron	Cardiganshire	2618	2687	198	10
Broom’s Barn	West Suffolk	2656	5752	73	9
Compton Park	Staffordshire	2988	3889	105	9
Preston Montford II	Shropshire	3143	3433	61	13
Malham Tarn	Mid-west Yorkshire	4672	3894	396	8
Sildon	County Durham	5262	4239	150	9
Forest-in-Teesdale	North-west Yorkshire	5306	3853	381	5
Castle Eden Dene I	County Durham	5394	4428	91	10
Auchincruive II	Ayrshire	6233	2377	52	10
Brodick	Clyde Islands	6380	2014	50	8
Rowardennan	Stirlingshire	6960	2378	15	8
Kindrogan	East Perthshire	7630	3055	259	7
Beinn Eighe I	West Ross & Cromarty	8629	2024	25	9
Cromarty	East Ross & Cromarty	8672	2785	30	10



Table 2.3: Reef locations used from the AIMS LTMP Great Barrier Reef database. Reefs are ordered from north to south. “Number of spp.” refers to the number of fish species remaining that matched our inclusion criteria.

Reef	Latitude (deg south)	Longitude (deg east)	Number of spp.
Carter Reef	14.52	145.58	17
Yonge Reef	14.57	145.62	16
No Name Reef	14.62	145.64	18
Macgillivray Reef	14.64	145.49	18
Lizard Island	14.69	145.46	18
North Direction Reef	14.74	145.51	18
Martin Reef(14123)	14.75	145.37	18
Linnet Reef	14.79	145.35	18
Agincourt Reefs (no 1)	16.04	145.87	17
St Crispin Reef	16.07	145.84	18
Opal (2)	16.20	145.90	18
Low Islands Reef	16.38	145.57	17
Hastings Reef	16.49	146.02	17
Michaelmas Reef	16.55	146.05	18
Green Island Reef	16.77	145.97	18
Fitzroy Island Reef	16.92	145.99	18
Myrmidon Reef	18.25	147.38	18
Dip Reef	18.39	147.45	17
Rib Reef	18.47	146.88	18
John Brewer Reef	18.62	147.08	18
Chicken Reef	18.66	147.72	18
Davies Reef	18.80	147.66	18
Pandora Reef	18.81	146.43	3
Slate Reef	19.66	149.91	18
Hyde Reef	19.73	150.09	18
19131s	19.77	149.38	18
Rebe Reef	19.80	150.16	18
19138s	19.80	149.43	18
Hayman Island Reef	20.05	148.89	4
Langford-bird Reef	20.07	148.87	4
Border Island Reef (no 1)	20.18	149.03	13
East Cay Reef	21.46	152.56	18
Turner Reef	21.70	152.56	18
21529s	21.87	152.18	18
Gannett Cay Reef	21.98	152.47	18
Horseshoe	22.02	152.62	18
Snake (22088)	22.02	152.19	18
Broomfield Reef	23.24	151.94	18
One Tree Reef	23.48	152.09	18
Lady Musgrave Reef	23.88	152.42	18

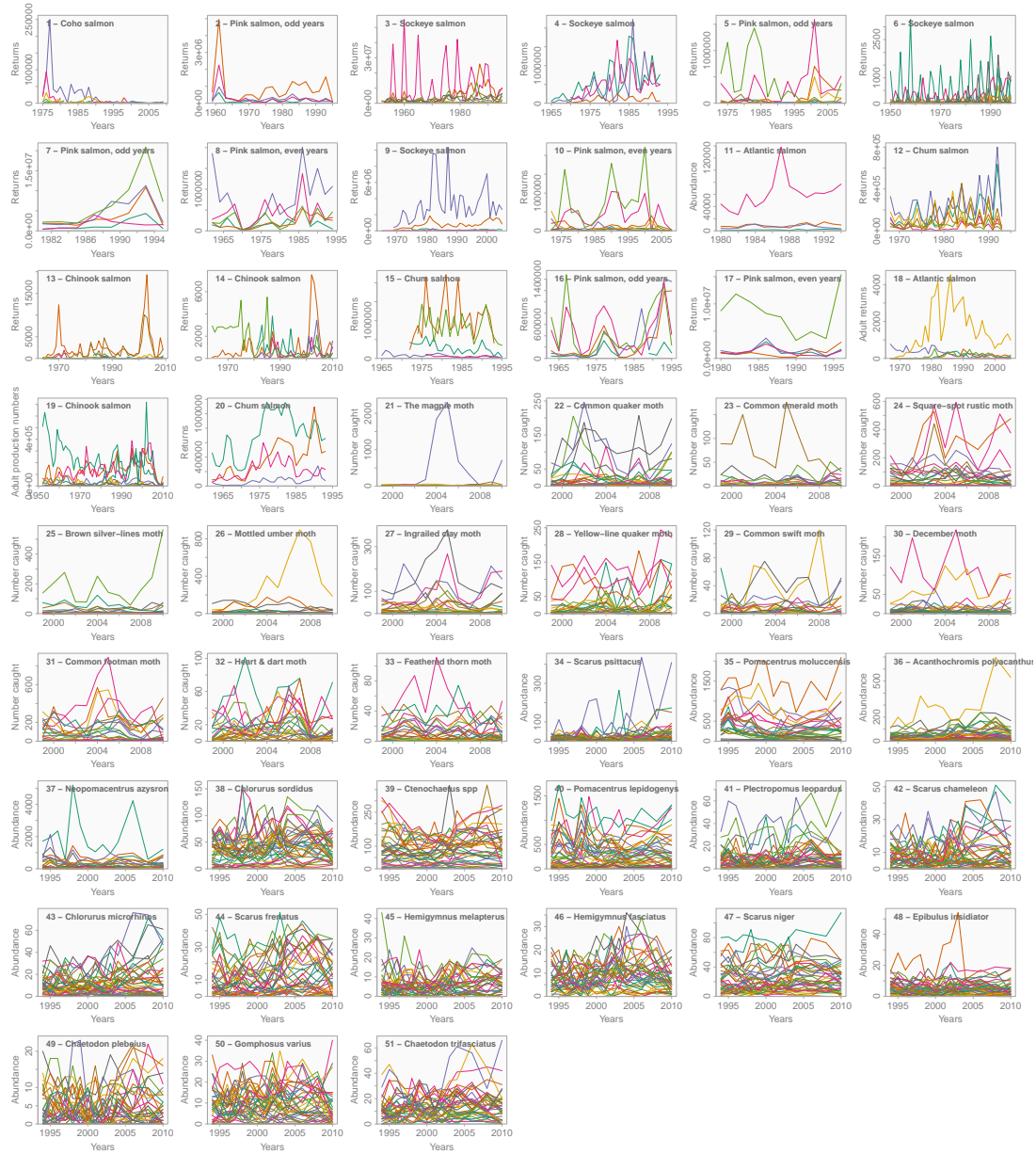


Figure 2.7: Subpopulation time series. Each panel contains one metapopulation. Colours were randomly assigned to distinguish subpopulations. Numbers in top-left corners refer to metapopulation IDs (see Table 2.1).

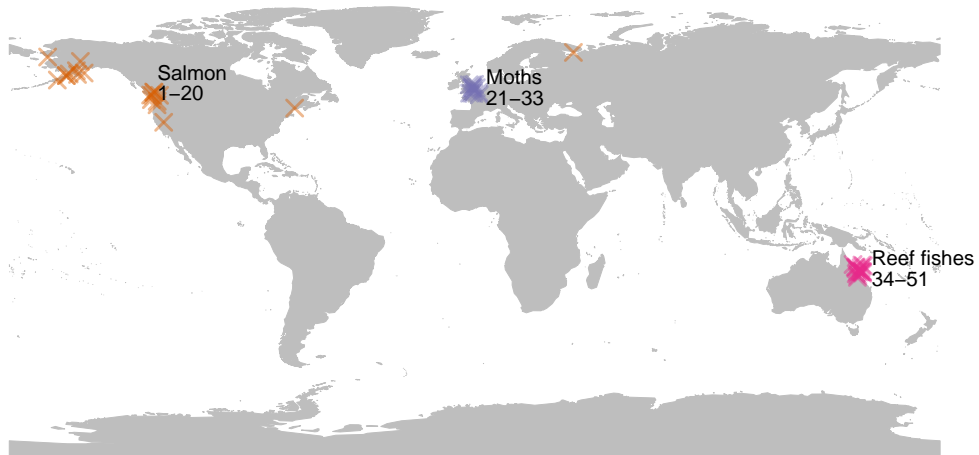


Figure 2.8: Map of included metapopulations. We represented salmon metapopulations with orange symbols, moths with purple, and reef fishes with pink. Numbers refer to metapopulation IDs (Table 2.1). Points are jittered slightly for visual clarity.

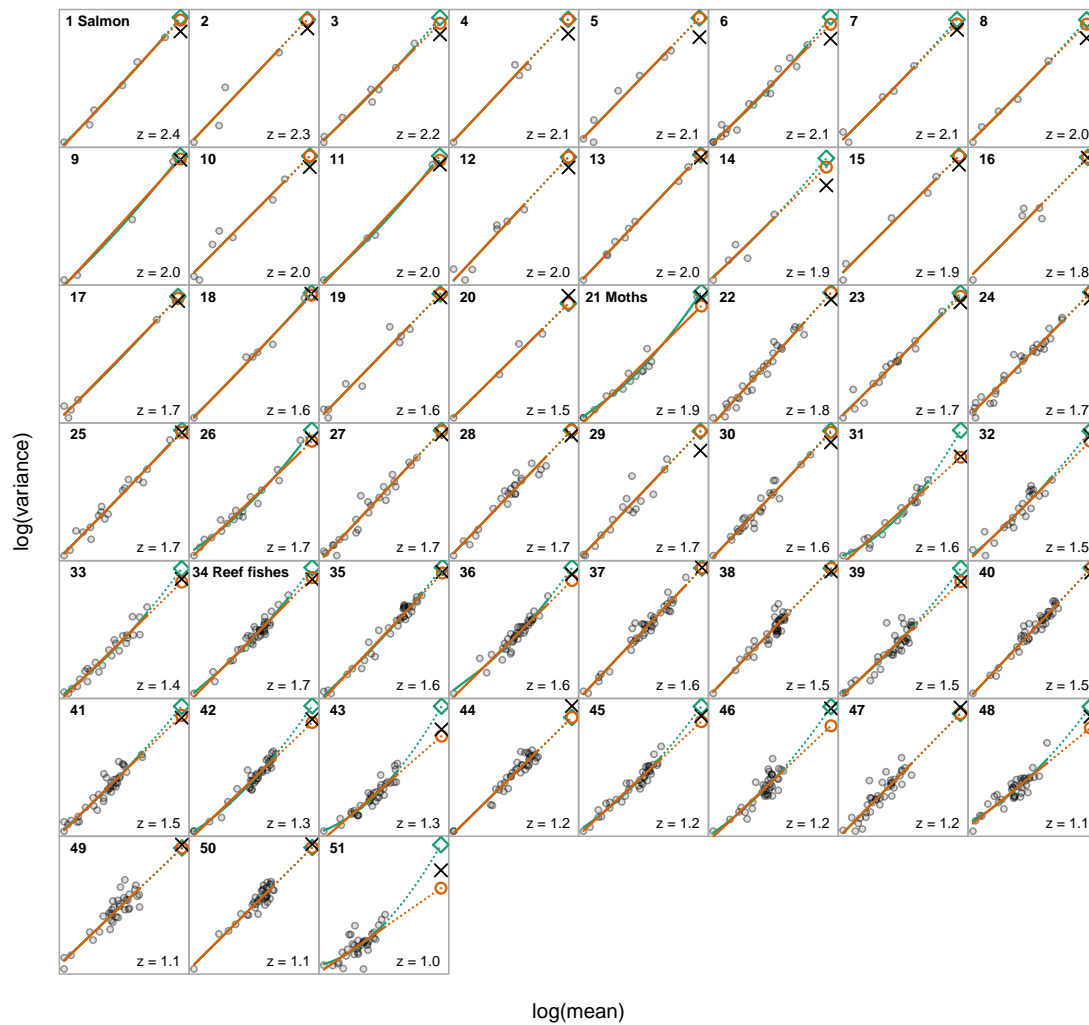


Figure 2.9: Calculation of the mean-variance PE using Taylor’s power law. Each dark-grey circle represents the  $\log(\mu)$  and  $\log(\sigma^2)$  of an individual subpopulation timeseries. The orange lines represent fitted linear regressions. The green lines represent fitted quadratic regressions. Black  $\times$  symbols represent the observed metapopulation or portfolio mean and variance. Dashed lines indicate the extrapolation of the model fit to the observed metapopulation or portfolio mean and variance. Open-orange circles represent the predicted variance under the linear-fit assumption. Open-green diamonds represent the predicted variance under the quadratic-fit assumption. Metapopulations in which the predicted variance is greater than the observed variance represent variance-reducing PEs. We ordered the panels by decreasing Taylor’s power law  $z$ -value (slope of the linear regression) within taxonomic groupings. Numbers in upper left of panels refer to metapopulation IDs (Table 2.1)

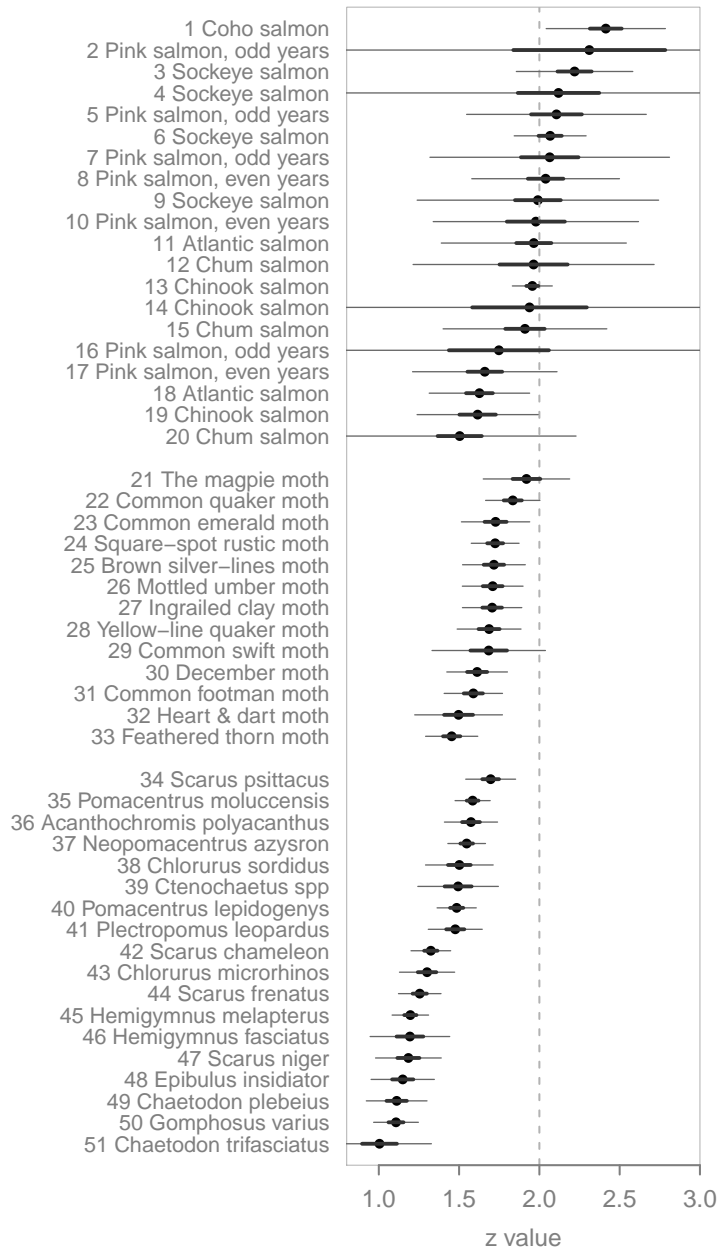


Figure 2.10: Taylor's power law z values across metapopulations. Points represent maximum likelihood estimates, thick line segments represent 50% confidence intervals, and thin line segments represent 95% confidence intervals. The vertical dashed line at  $z = 2$  represents the value assumed by the average-CV PE method.

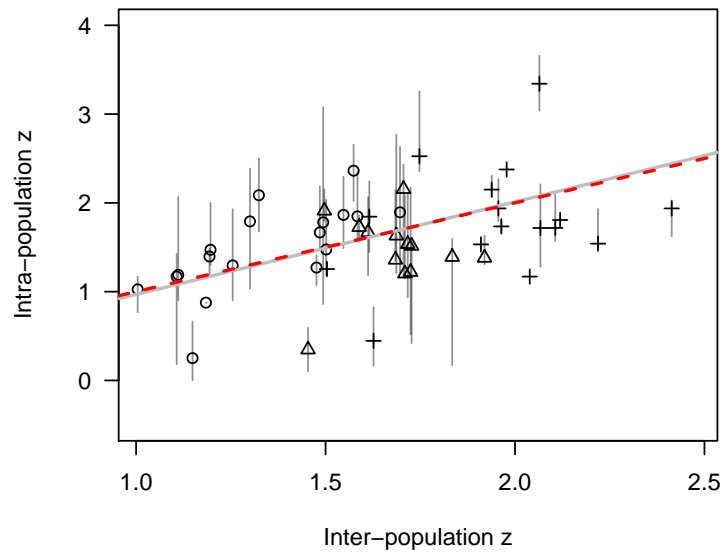


Figure 2.11: Intra- vs. inter-subpopulation mean-variance scaling relationship (Taylor’s power law  $z$ -value). Our estimation of the empirical mean-variance PE assumes that the inter-subpopulation  $z$ -value can approximate the intra-subpopulation  $z$ -value. We use the inter-subpopulation  $z$ -value throughout our paper. Here, we have also calculated the intra-subpopulation  $z$ -value for subpopulation time series in which the mean abundance in the 1<sup>st</sup> or 2<sup>nd</sup> half of the time series is twice the magnitude of the other half. Points represent median intra-subpopulation  $z$ -values within each metapopulation and vertical line segments represent 1<sup>st</sup> and 3<sup>rd</sup> quartile values. The dashed-red line represents a one-to-one relationship and the solid-grey line (under the one-to-one line) represents a linear regression of the median intra-subpopulation  $z$ -values with inter-subpopulation  $z$ -values. Symbols represent salmon (crosses), moths (triangles), and reef fishes (circles).

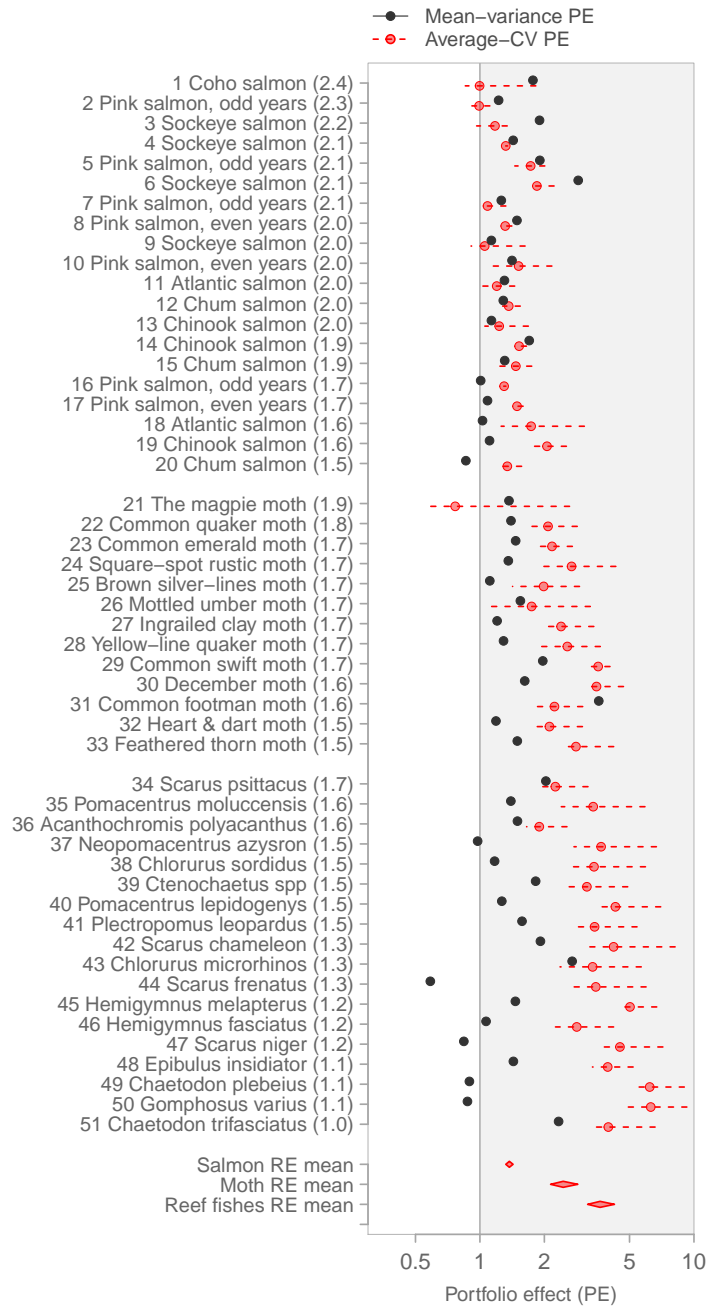


Figure 2.12: PEs with the mean-variance PEs estimated from a quadratic model. See Figure 2.3 for details.

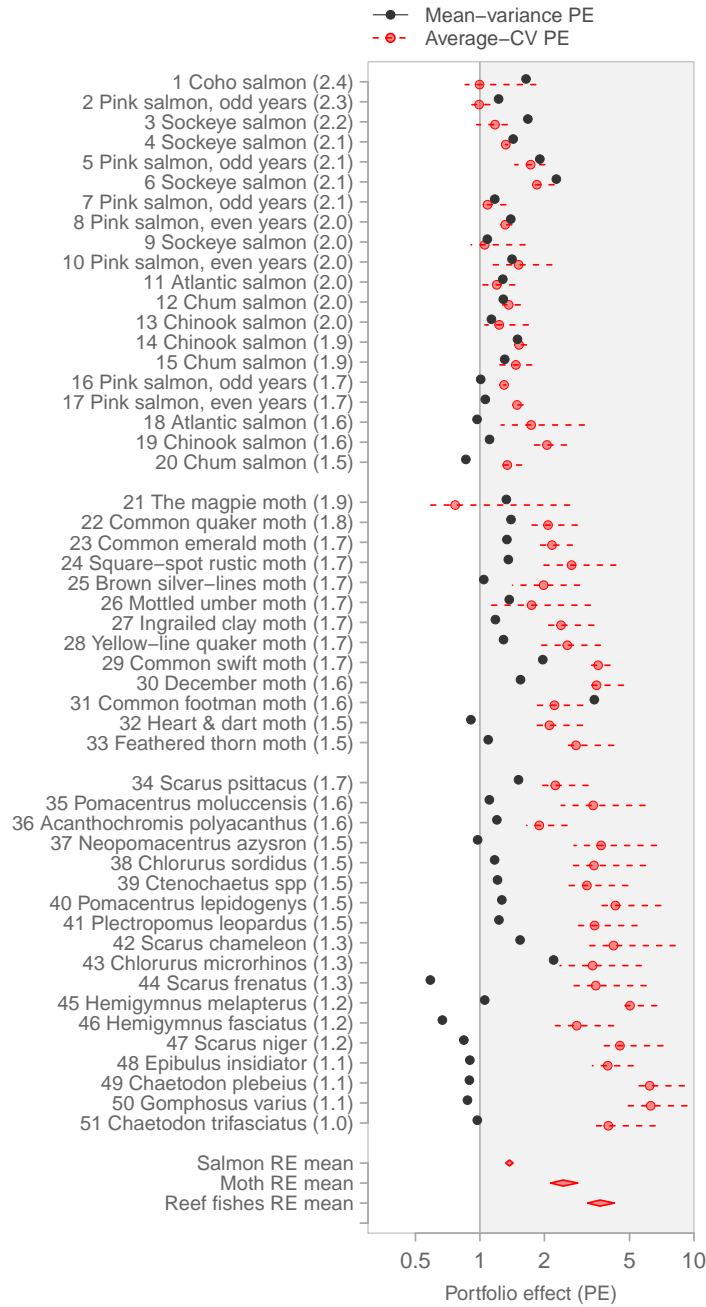


Figure 2.13: PEs with the mean-variance PEs estimated from a linear-quadratic averaged model. See Figure 2.3 for details.



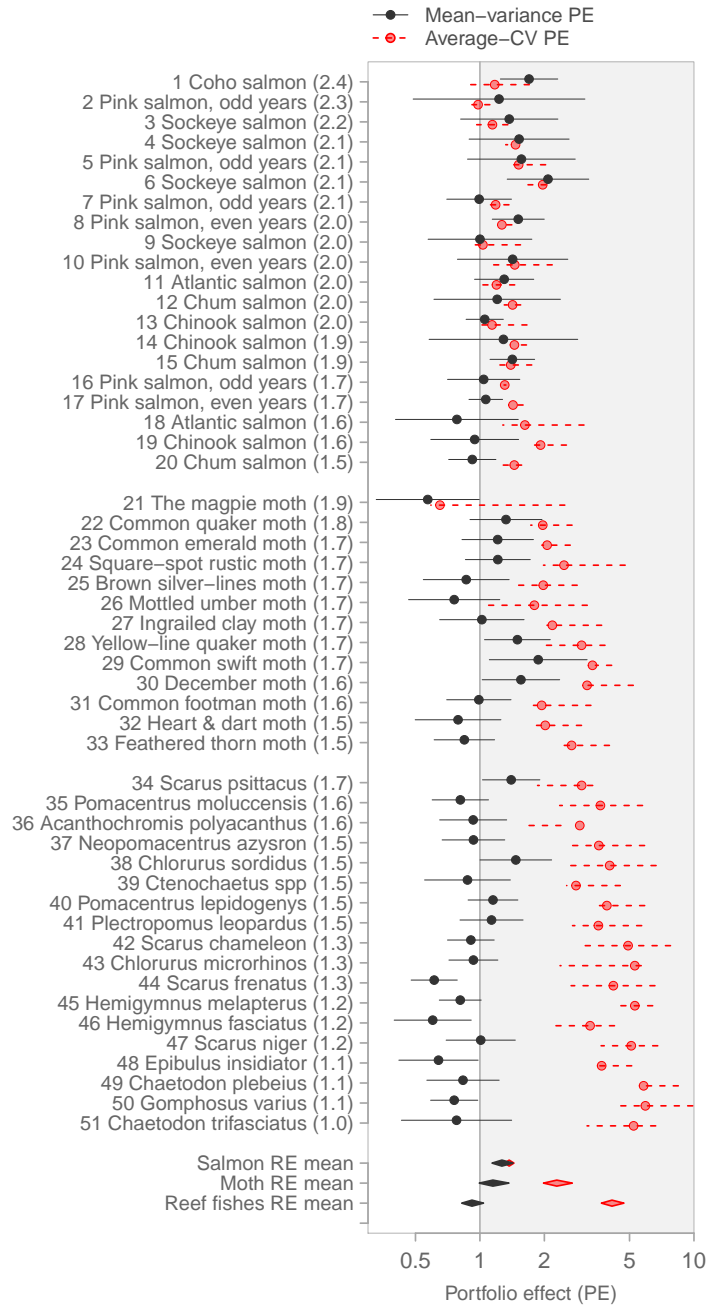


Figure 2.14: PEs from linear detrended time series. See Figure 2.3 for details.

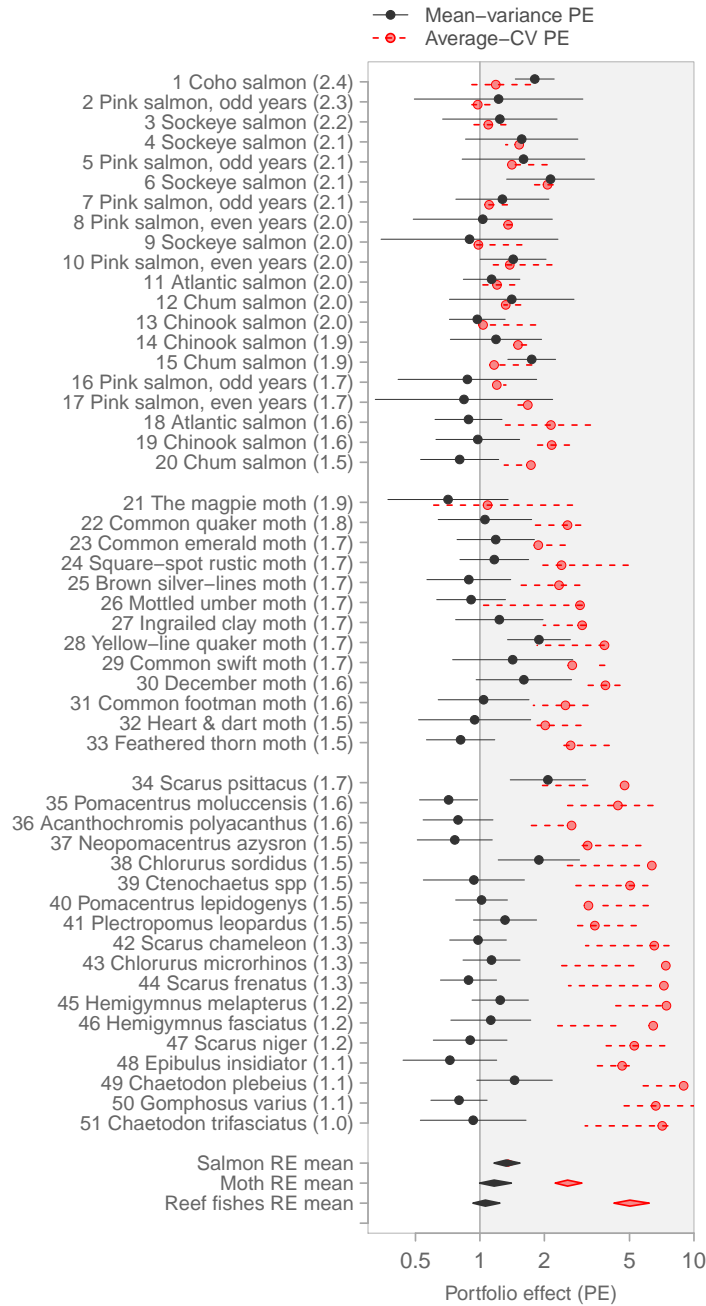


Figure 2.15: PEs from loess detrended time series. See Figure 2.3 for details.

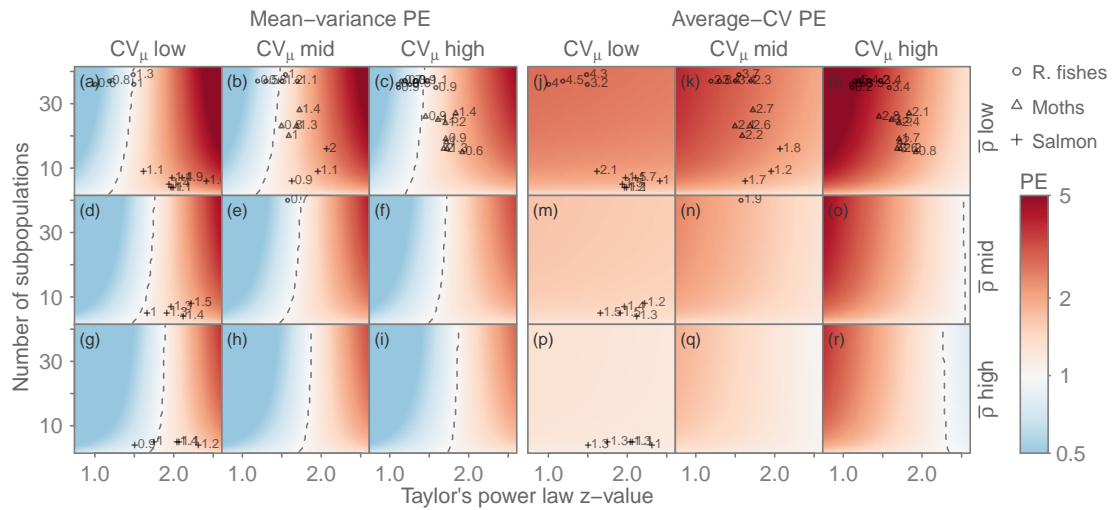


Figure 2.16: Empirical ecological PEs (points) overlaid in theoretical PE parameter space (colour shading). This is the same as Figure 2.5 except that here we indicate the empirical PE values beside the points. The colour shading indicates the stabilizing-effect of the theoretical mean-variance PEs (a–i) and average-CV PEs (j–r): red indicates a stabilizing effect and blue indicates a destabilizing effect. The dashed lines indicate neutral PEs. Columns from left to right show systems with increasingly uneven subpopulation sizes, and rows from top to bottom show systems with increasingly strong mean correlation between subpopulation

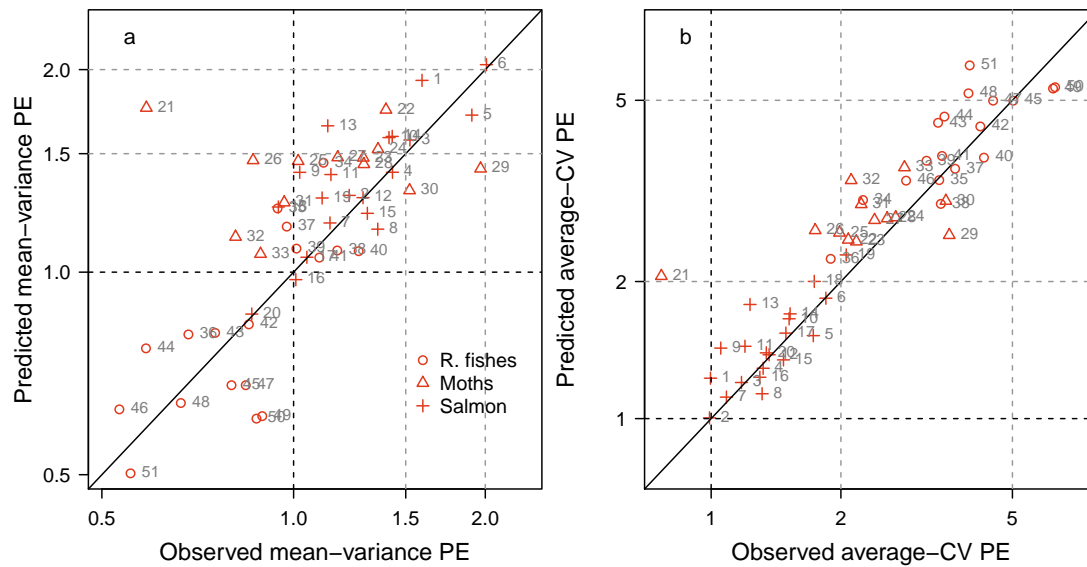


Figure 2.17: Predicted vs. observed mean-variance (a) and average-CV PEs (b). Predicted PEs correspond to the colour underlying the metapopulations displayed in Figure 2.5; observed PEs to the values calculated directly from the empirical data and shown in Figure 2.3. The predicted PEs are approximate due to other statistical properties of the data beyond the four examined in Figure 2.5, and due to grouping the  $CV_{mu}$  and correlation values from the metapopulations to match the displayed theoretical values in the bins. Numbers indicate the metapopulation IDs used throughout the paper (Table 2.1). The solid sloped lines indicate one-to-one relationships. Note that all axes have been log transformed and the two panels have separate axis limits.

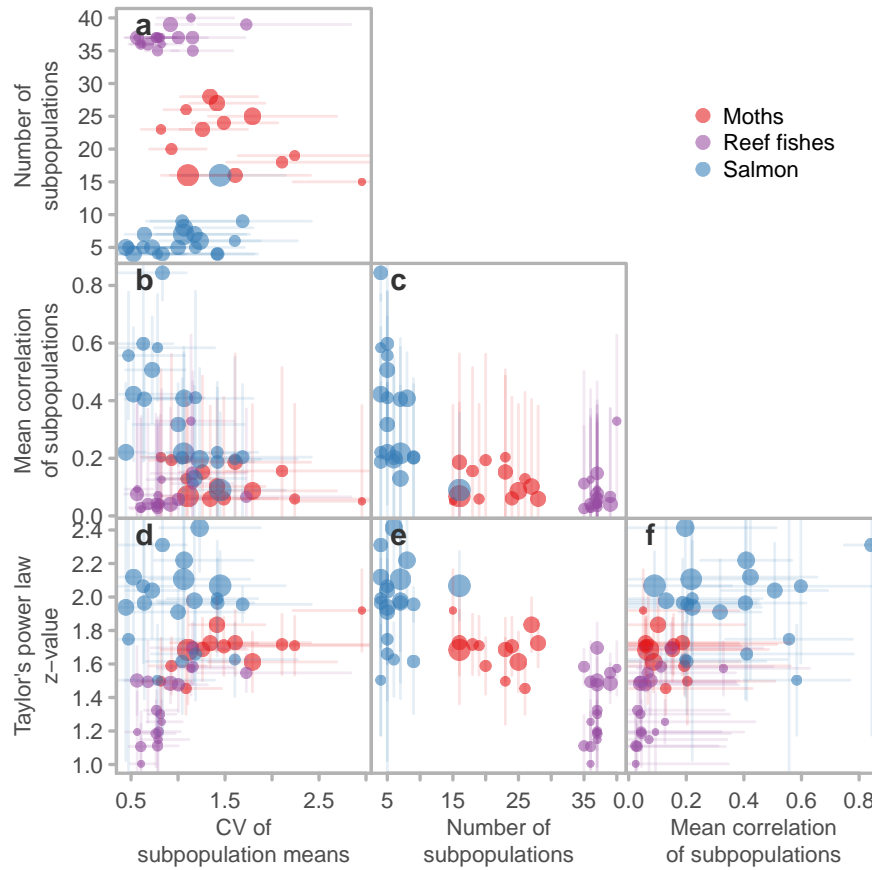


Figure 2.18: Relationship between the drivers of the PE in empirical systems for moths (red), reef fishes (purple), and salmon (blue). The area of the filled circles corresponds to the strength of the mean-variance PE with larger circles corresponding to more stabilizing PEs. Line segments indicate 95% confidence intervals.

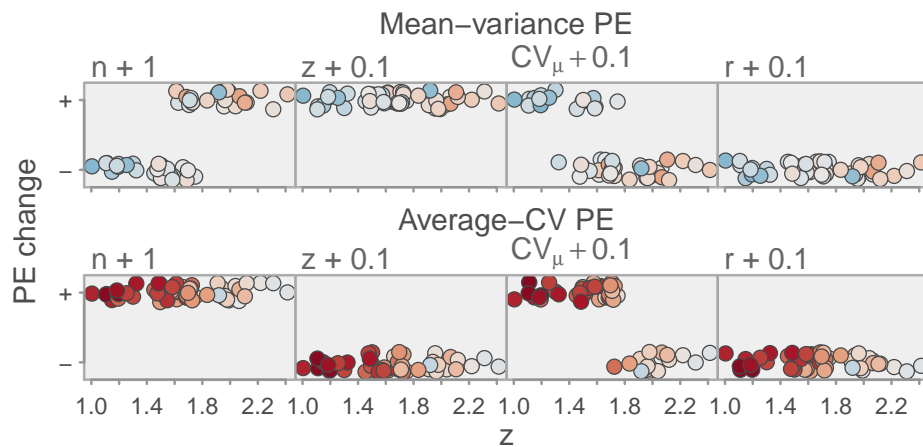


Figure 2.19: The PE used as an index of ecosystem change. The upper panel shows the mean-variance PE and the lower panel the average-CV PE. The horizontal axis shows Taylor's power law  $z$ -value. The vertical axis shows the change in the PE (more stabilizing = +, less stabilizing = -). The panels from left to right indicate an increase in the number of subpopulations ( $n + 1$ ), Taylor's power law  $z$ -value ( $z + 1$ ), subpopulation unevenness ( $CV_{\mu} + 0.1$ ), or the correlation between subpopulations ( $r + 0.1$ ). The quantities added are arbitrary and the results would look the same for any quantity added greater than zero. Each dot represents an empirical metapopulation and the colour indicates the observed empirical PE using the same colour scale as Figs. 4 and 5. The dots are jittered vertically slightly for visual clarity.

## Chapter 3

# Portfolio conservation of metapopulations under climate change<sup>2</sup>

### 3.1 Abstract

Climate change will likely lead to increasing population variability and extinction risk. Theoretically, greater population diversity should buffer against rising climate variability, and this theory is often invoked as a reason for greater conservation. However, this has rarely been quantified. Here we show how a portfolio approach to managing population diversity can inform metapopulation conservation priorities in a changing world. We develop a salmon metapopulation model where productivity is driven by spatially-distributed thermal tolerance and patterns of short- and long-term climate change. We then implement spatial conservation scenarios that control population carrying capacities and evaluate the metapopulation portfolios as a financial manager might—along axes of conservation risk and return. We show that preserving a diversity of thermal tolerances minimizes risk given environmental stochasticity and ensures persistence given long-term environmental change. When the thermal tolerances of populations are unknown, doubling the number of populations conserved may nearly halve metapopulation variability. However, this reduction in variability can come at the expense of long-term persistence if climate change increasingly restricts available habitat—forcing ecological managers to balance society’s desire for short-term stability and long-term viability. Our

---

<sup>2</sup>A version of this chapter appears as Anderson, S.C., J.W. Moore, M.M. McClure, N.K. Dulvy, A.B. Cooper. Portfolio conservation of metapopulations under climate change. *Ecological Applications*. In press. <http://doi.org/10.1890/14-0266.1>.

findings suggest the importance of conserving the processes that promote thermal-tolerance diversity, such as genetic diversity, habitat heterogeneity, and natural disturbance regimes, and demonstrate that diverse natural portfolios may be critical for metapopulation conservation in the face of increasing climate variability and change.

## 3.2 Introduction

Untangling the mechanisms that underpin the stability of ecological systems is a critical focus of ecology (e.g. Ives and Carpenter 2007; de Mazancourt et al. 2013). Decades of research has focused on the role of species richness and functional diversity in driving stability; however, recent research has highlighted that the drivers of ecological stability are more complex and multidimensional than previously thought (e.g. Balvanera et al. 2006; Ives and Carpenter 2007; de Mazancourt et al. 2013). Two key drivers of population stability that have been comparatively understudied are response diversity (Winfree and Kremen 2009; Mori et al. 2013)—different responses to the environment by functionally similar species or populations (Elmqvist et al. 2003)—and the role of metapopulations (Schtickzelle and Quinn 2007). Here, we examine the role of response diversity conservation in stabilizing metapopulations given projected changes in climate. With unprecedented loss of biodiversity and levels of anthropogenic environmental change, it is more critical than ever to consider conservation approaches that maintain system stability in the face of environmental uncertainty (Lee and Jetz 2008; Ando and Mallory 2012).

Typically, conservation actions to maintain system stability and thereby reduce risk are driven by an ad hoc combination of scientific information, political influences, and feasibility (Margules and Pressey 2000); the management of financial portfolios provides another way of considering risk (e.g. Figge 2004; Koellner and Schmitz 2006; Ando and Mallory 2012; Haak and Williams 2012). Economists work to minimize risk and maximize returns by building a portfolio of individual investments (called assets) with different attributes. For example, different financial sectors can be expected to perform uniquely in some economic conditions; when one rises in value another may fall. Modern portfolio theory proposes that out of all possible portfolios, there is a small subset of portfolios that maximizes expected return for a level of risk or minimizes risk for a level of return (called the efficient frontier), and that only by considering risk and return in tandem can an investor achieve maximum benefit from a portfolio (Markowitz 1952).



Similarly, expected growth rate and variance of a metapopulation is a function of the variance, covariance, and size of the individual populations (Moore et al. 2010; Carlson and Satterthwaite 2011; Anderson et al. 2013). An ecological portfolio approach to managing risk for a metapopulation might therefore consider how conservation actions affect the weight of each population in a metapopulation portfolio. This investment weight could represent the conservation budget or the habitat conserved for each population. The population growth rate is then analogous to the financial rate of return and the variability of that growth rate a metric of risk. Environmental conditions could represent the financial market conditions. Given this interpretation, ecological managers could consider how various conservation strategies affect the expected risk and return of their ecological portfolio. These risk and return elements are central to ecological management and conservation—management aims to ensure stability over environmental variability (risk), and increase population abundance (return). Different scenarios may suggest different desired trade-offs between the two. For example, a manager with a healthy population might prioritize short-term stability, while a manager with an endangered population might try to balance the two, or prioritize population growth initially.

Managing Pacific salmon under the uncertainty of climate change is an ideal scenario to consider through the lens of portfolio theory for four reasons. (1) The migration of Pacific salmon biomass profoundly influences aquatic and terrestrial coastal ecosystems throughout the North Pacific ocean from Korea to California (Quinn 2005). (2) Pacific salmon form metapopulations (e.g. Policansky and Magnuson 1998; Cooper and Mangel 1999; Schtickzelle and Quinn 2007) and we can consider, for example, the metapopulation in a river-catchment as a portfolio and the stream populations as assets (Schindler et al. 2010; Moore et al. 2010; Carlson and Satterthwaite 2011; Anderson et al. 2013; Yeakel et al. 2014). Fisheries often integrate across multiple populations, acting as investors in the salmon portfolio (Hilborn et al. 2003). Fisheries managers and conservation agencies can act as portfolio managers by choosing which salmon habitat to prioritize for protection or restoration. (3) Many Pacific salmon metapopulations are highly threatened (e.g. Gustafson et al. 2007) and will likely become more at risk as threats such as overfishing, damming, logging, and particularly changing climate, intensify (e.g. Lackey 2003). Indeed, recovery goals for Pacific salmon are often set at the metapopulation level (McElhany et al. 2000), and knowing what minimizes risk to the metapopulation can help choose efficient conservation actions (Policansky and Magnuson 1998; McElhany et al. 2000). (4) Given the scale and variety of the threats facing salmon, some prioritization will be required to recover these highly-valued, even iconic species (Allendorf et al. 1997; Ruckelshaus

et al. 2002).

Two key mechanisms can generate the asynchrony in metapopulation dynamics that is critical to a diversified portfolio. First, localized habitat features can filter larger-scale environments, generating unique conditions for populations (Schindler et al. 2008) (*sensu* the Moran effect). Second, salmon populations may respond differently to environmental variability (i.e. response diversity (Elmqvist et al. 2003) and biocomplexity (Hilborn et al. 2003)) arising from unique local adaptations and traits (Fraser et al. 2011; Eliason et al. 2011; Thorson et al. 2014c). In reality, these mechanisms can interact. For example, salmon response diversity in the marine environment can be driven by adaptation to localized freshwater environments (Johnson and Schindler 2013).

In addition to posing perhaps the greatest threat to global biodiversity in general (Thomas et al. 2004), climate warming poses a particular threat to riverine species whose ranges are largely confined to existing habitat (Thomas 2010). Among these species, salmon are strongly affected by climate warming (e.g. Patterson et al. 2007). Warmer water can lead to massive mortality of salmon populations (e.g. Patterson et al. 2007) and indirectly impact salmon productivity through alterations to snow-melt timing and extreme hydrological events (Crozier et al. 2008). Due to these effects, adverse stream temperatures are already impeding recovery of some Pacific salmon populations (McCullough 1999) and are expected to make recovery targets more difficult to achieve (Battin et al. 2007). However, despite the evidence that warming impacts salmon, salmon also show evidence of response diversity and local adaptation to temperature. For example, thermal tolerance of sockeye salmon in the Fraser River, British Columbia, Canada, varies within streams according to historical environmental conditions (Eliason et al. 2011).

Here we ask how portfolio theory can inform spatial approaches to prioritizing metapopulation conservation in a changing world. To answer this, we develop a salmon metapopulation simulation in which spatially-distributed thermal tolerance and patterns of short- and long-term climatic change drive population-specific productivity. We then implement scenarios that prioritize alternative sets of populations and evaluate the salmon portfolios along risk-return axes, as a financial portfolio manager might. We show that conserving a diversity of thermal tolerances buffers metapopulation risk given short-term climate forcing and ensures metapopulation persistence given long-term climate warming. We then show that dividing conservation among more populations buffers risk regardless of thermal-tolerance diversity or climate trend, but possibly at the expense of long-term growth rate and persistence when

available habitat declines over time. We conclude that considering metapopulations through portfolio theory provides a useful additional dimension through which we can evaluate conservation strategies.

### 3.3 Methods

We developed a 100-year salmon metapopulation simulation model that includes both population dynamics and harvesting along with process, observation, and implementation uncertainty (Fig. 3.1). We tested different conservation scenarios under two kinds of environmental regimes (short-term climate variability and long-term climate change) and in cases where habitat capacity remained constant or declined over time. We provide a package metafolio (Anderson 2014) for the statistical software R (R Core Team 2013) as an appendix, to carry out the simulations and analyses described in this paper (Supporting materials).

#### 3.3.1 Defining the ecological portfolio

In our ecological portfolios, we defined assets as stream-level populations and portfolios as salmon metapopulations. The specific configuration of our model refers to salmon that spend extended time rearing in freshwaters (e.g. steelhead [*Oncorhynchus mykiss*], sockeye salmon [*O. nerka*], coho salmon [*O. kisutch*], and stream-type Chinook salmon [*O. tshawytscha*]), which will likely be more impacted by changes to stream temperature and flow (Mantua et al. 2010). We use the terms *stream* and *populations* interchangeably to represent the portfolio assets. We defined the portfolio investors as the stakeholders in the fishery and metapopulation performance. For example, the investors could be conservation agencies, First Nations groups, or civil society as a whole. The fisheries management agency then becomes the portfolio manager. We defined the asset value as the abundance of returning salmon in each stream and the value of the portfolio as the overall metapopulation abundance.

In this scenario, the equivalent to financial rate of return is the generation-to-generation metapopulation growth rate, calculated as the first difference of the log salmon returns. We defined the financial asset investment weights as the capacity of the stream populations—specifically the unfished equilibrium stock size—since maintaining or restoring habitat requires money, time, and resources and habitat size itself is a strong predictor of the occupancy of salmon (Isaak et al. 2007). Investment in a population therefore represents investing in salmon

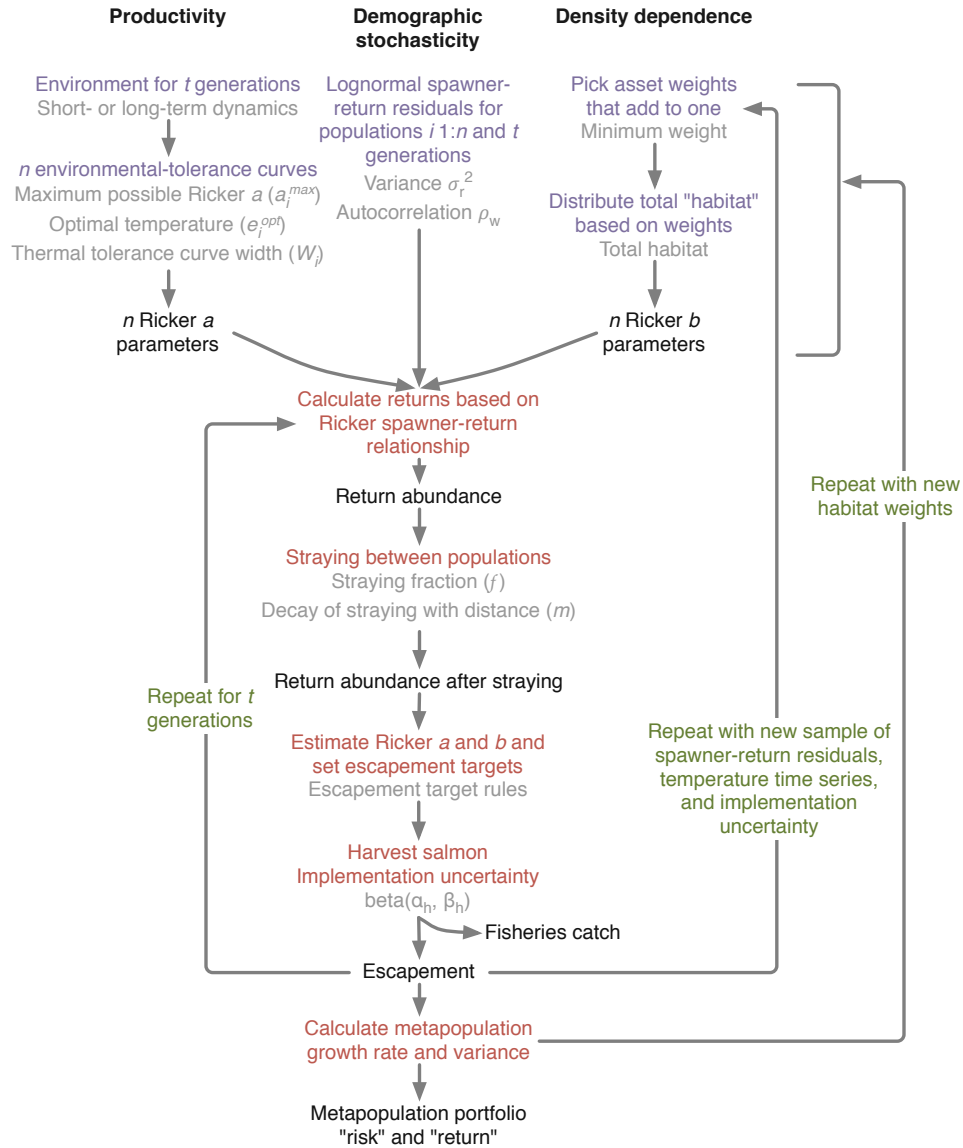


Figure 3.1: Flow chart of the salmon-metapopulation simulation. There are  $n$  salmon populations and  $t$  generations. Blue text indicates values that are generated before the simulation progresses through time. Red text indicates steps in which calculations are performed through time. Black text indicates values that are calculated. Grey text indicates parameters that can be set. Green text indicates the looping structure of the simulation.

habitat conservation or restoration and the risk and return from investment strategies become emergent properties of our metapopulation model.

### 3.3.2 Salmon metapopulation dynamics

The salmon metapopulation dynamics in our simulation were governed by a spawner-return relationship with demographic stochasticity and straying between populations. We defined the spawner-return relationship with a Ricker model,

$$R_{i(t+1)} = S_{i(t)} e^{a_{i(t)}(1 - S_{i(t)}/b_i) + w_{i(t)}}$$

where  $i$  represents a population,  $t$  a generation time,  $R$  the number of returns,  $S$  the number of spawners,  $a$  the productivity parameter (which can vary with the environment), and  $b$  the density-dependent term (which is used as the asset weights in the portfolios). The term  $w_{i(t)}$  represents first-order autocorrelated error. Formally,  $w_{i(t)} = \rho_w w_{i(t-1)} + r_{i(t)}$ , where  $r_{i(t)}$  represents independent and normally-distributed error with standard deviation of  $\sigma_r$ , mean of  $-\sigma_r^2/2$  (bias corrected so the expected value after exponentiation is 1), and correlation between subsequent generation values of  $\rho_w$ . We set  $\sigma_r = 0.7$  and  $\rho_w = 0.4$  to match the mean values for salmonids in Thorson et al. (2014a).

We manipulated the capacity and productivity parameters  $b_i$  and  $a_{i(t)}$  as part of the portfolio simulation. The capacity parameters  $b_i$  were controlled by the investment weights in the populations. For example, a large investment in a stream was represented by a larger unfished equilibrium stock size  $b$  for stream  $i$ . The productivity parameters  $a_{i(t)}$  were controlled by the interaction between a temperature time series and the population thermal-tolerance performance curves. In a different context, investment could represent improving the productivity ( $a_i$ ) parameters, say through culling, to offset mortality increases due to changing temperatures. However, such a scenario is unlikely in the case of an endangered species where population levels are often well below levels where culling would increase productivity.

We generated the thermal-tolerance curves according to

$$a_{i(t)} = \begin{cases} a_i^{\max} - W_i(e_t - e_i^{\text{opt}})^2, & \text{if } a_{i(t)} > 0 \\ 0, & \text{if } a_{i(t)} \leq 0 \end{cases}$$

where  $W_i$  controls the width of the curve for population  $i$ ,  $e_t$  represents the environmental value at generation  $t$ ,  $e_i^{\text{opt}}$  represents the optimal temperature for population  $i$ , and  $a_i^{\max}$  represents the maximum possible  $a$  value for population  $i$ . We set the  $W_i$  parameters (evenly spaced values

increasing and decreasing between 0.08 and 0.04) to generate widths approximately as shown in Eliason et al. (2011). We set the area under each curve to 30 units to create  $a_i^{\max}$  values ranging roughly between 2.2 and 2.9 as in Dorner et al. (2008). These parameter values created some warm-tolerant populations, some cold-tolerant populations, and some populations with a wider range of thermal-tolerance but a lower maximum productivity (Fig. 3.2a). Although we refer to a thermal-tolerance curve because temperature is a dominant driver of salmon productivity (e.g. McCullough 1999; Patterson et al. 2007; Eliason et al. 2011), our model could apply to any environmental tolerance (e.g. tolerance to stream flow volume or changes in snow melt timing; Crozier et al. 2008).

We implemented straying as in Cooper and Mangel (1999). We arranged the populations in a line and salmon were more likely to stray to streams near their natal stream (Supporting materials Fig. 3.7). Two parameters controlled the straying: the fraction of fish  $f_{\text{stray}}$  (0.02) that stray from their natal stream in any generation and the rate  $m$  (0.1) at which this straying between streams decays with distance

$$\text{strays}_{ij(t)} = f_{\text{stray}} R_{j(t)} \frac{e^{-m|i-j|}}{\sum_{\substack{k=1 \\ k \neq j}}^n e^{-m|k-j|}}$$

where  $R_{j(t)}$  is the number of returning salmon at generation  $t$  whose natal stream was stream  $j$ . The subscript  $k$  represents a stream ID and  $n$  the number of populations. The denominator is a normalizing constant to ensure the desired fraction of fish stray. Our simulation did not account for the homogenization of diversity due to straying. For example, all salmon in one population maintained the same thermal-tolerance curve regardless of how many salmon it received from another stream.

### 3.3.3 Fishing

Our simulation used a simple set of rules to establish the exploitation rate of fisheries and the remainder left to spawn (escapement target). First, to establish a range of spawner-return values and to mimic the start of an open-access fishery, for the first 30 years we drew the fraction of fish harvested randomly from a uniform distribution between 0.1 and 0.9. We discarded these initial 30 years as a burn-in period. Then, every five years for the remaining 100 years of our simulation, we fitted a spawner-return function to the cumulative data for individual

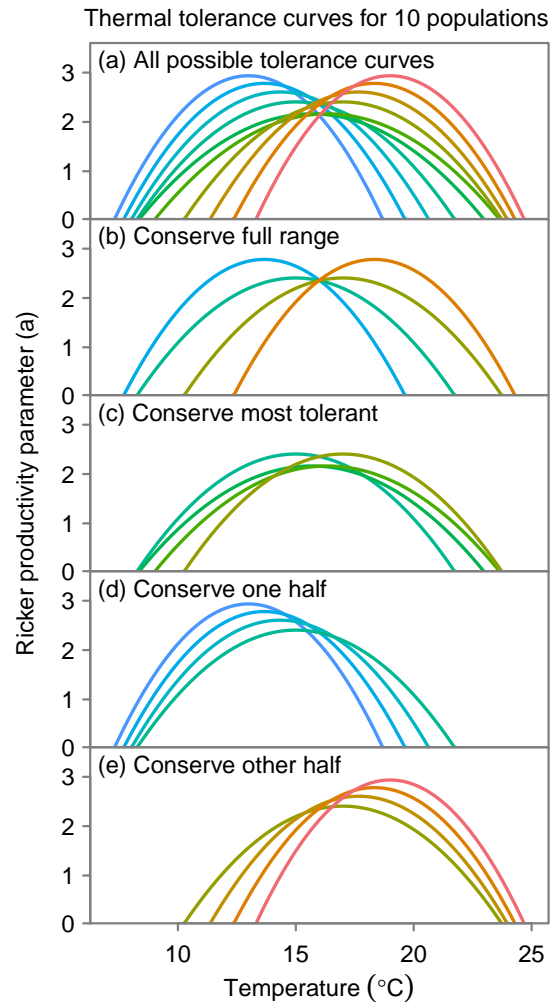


Figure 3.2: Different ways of prioritizing thermal-tolerance conservation. Panel a shows thermal-tolerance curves for ten possible populations and panels b–e show different ways of prioritizing four of those populations. The curves describe how productivity varies with temperature for a given population. Some populations thrive at low temperatures (blue shades) and some at warm temperatures (red shades). Some are tolerant to a wider range of environmental conditions (green-yellow shades) but with a lower maximum productivity. The total possible productivity (the area under the curves) is the same for each population.

populations. The target escapement rate  $E_{\text{tar}}$  (a proportion per year) was set based on Hilborn and Walters (1992) as

$$E_{\text{tar}} = \frac{R}{b(0.5 - 0.07a)}$$

where  $R$  represents the return abundance and  $a$  and  $b$  represent the Ricker model parameters. The target harvest rate is then a function of returns and the escapement target ( $H_{\text{tar}} = R - E_{\text{tar}}$ ). We included implementation uncertainty in the actual harvest rate  $H_{\text{act}}$  as a function of the target harvest rate and a beta distribution with location parameter  $\alpha_h$ , shape parameter  $\beta_h$ , and standard deviation of  $\sigma_h$  (set to 0.1 as observed for similar data in Pestes et al. (2008)).

$$\alpha_h = H_{\text{tar}}^2 \left( \frac{1 - H_{\text{tar}}}{\sigma_h^2} - \frac{1}{H_{\text{tar}}} \right)$$

$$\beta_h = \alpha_h \left( \frac{1}{H_{\text{tar}}} - 1 \right)$$

$$H_{\text{act}} = \text{beta}(\alpha_h, \beta_h).$$

### 3.3.4 Environmental dynamics

Environmental dynamics typically have both short- and long-term fluctuations, such as annual variability and directional climatic warming. We evaluated portfolio performance under these two components separately in our initial scenarios and combined in our final scenario. We did not explicitly model a cyclical climate trend, such as the Pacific Decadal Oscillation, but the effect of such a trend would largely be a product of the short-term variability and long-term trend. We represented short-term dynamics  $e_{\text{short}(t)}$  as a stationary first-order autoregressive process, AR(1), with correlation  $\rho_e$  (0.1)

$$e_{\text{short}(t)} = e_{t-1}\rho_e + d_t, d_t \sim N(\mu_d, \sigma_d^2)$$

where  $d_t$  represents normally distributed deviations of some mean  $\mu_d$  and standard deviation  $\sigma_d$ . We set  $\mu_d$  to 16 °C and  $\sigma_d$  to 2 °C, to approximately match the stream temperature variation in Eliason et al. (2011). We represented long-term environmental dynamics  $e_{\text{long}(t)}$  as a linear shift in the temperature through time

$$e_{\text{long}(t)} = e_0 + \beta_e t$$



where  $e_0$  represents the starting temperature up until the burn-in period ends and  $\beta_e$  represents the annual increase in temperature. We set  $e_0 = 15^\circ\text{C}$  and  $\beta_e = 0.04^\circ\text{C}/\text{generation}$  to obtain an increase in stream temperature of  $4^\circ\text{C}$  over the next century (assuming one generation equals one year) ending at or above the optimum thermal optimum of all populations. This increase approximately matches predicted increases in stream temperature—relative to the 1980s, stream temperatures in the Pacific Northwest have already increased by approximately  $0.2^\circ\text{C}/\text{decade}$  (Isaak et al. 2012), and are predicted to increase 2 to  $5^\circ\text{C}$  by 2080 (Mantua et al. 2010).

We summarize the chosen parameter values in Supporting materials Table 3.1. Combining salmon population dynamics, fishing, and environmental dynamics, we illustrate the components of an example simulation in Fig. 3.3 and the effect of varying population, fishing, and environmental parameters from their base values on metapopulation abundance in Supporting materials Fig. 3.8.

### 3.3.5 Conservation scenarios

*Spatial conservation scenarios:* We evaluated four spatial conservation scenarios (Fig. 3.2b–e). We conserved four populations ( $b_i = 1000$ ) and set the unfished equilibrium abundance of the six remaining populations to near elimination ( $b_i = 5$ ) at the start of the simulation. These reduced populations could still receive straying salmon but were unlikely to rebuild on their own to a substantial abundance. The four spatial scenarios we considered were:

1. Conserve a full range of thermal tolerances (conserve some cool-, some intermediate-, and some warm-tolerant populations; Fig. 3.2b).
2. Conserve the middle section of the metapopulation (conserve the most thermal-tolerant populations with the widest response curves; Fig. 3.2c).
3. Conserve the lower half of the metapopulation (conserve cool-tolerant populations; Fig. 3.2d).
4. Conserve the upper half of the metapopulation (conserve warm-tolerant populations; Fig. 3.2e).

*Unknown thermal tolerances:* In reality we rarely know precise levels of thermal response diversity. We therefore also considered cases where conservation was randomly assigned with

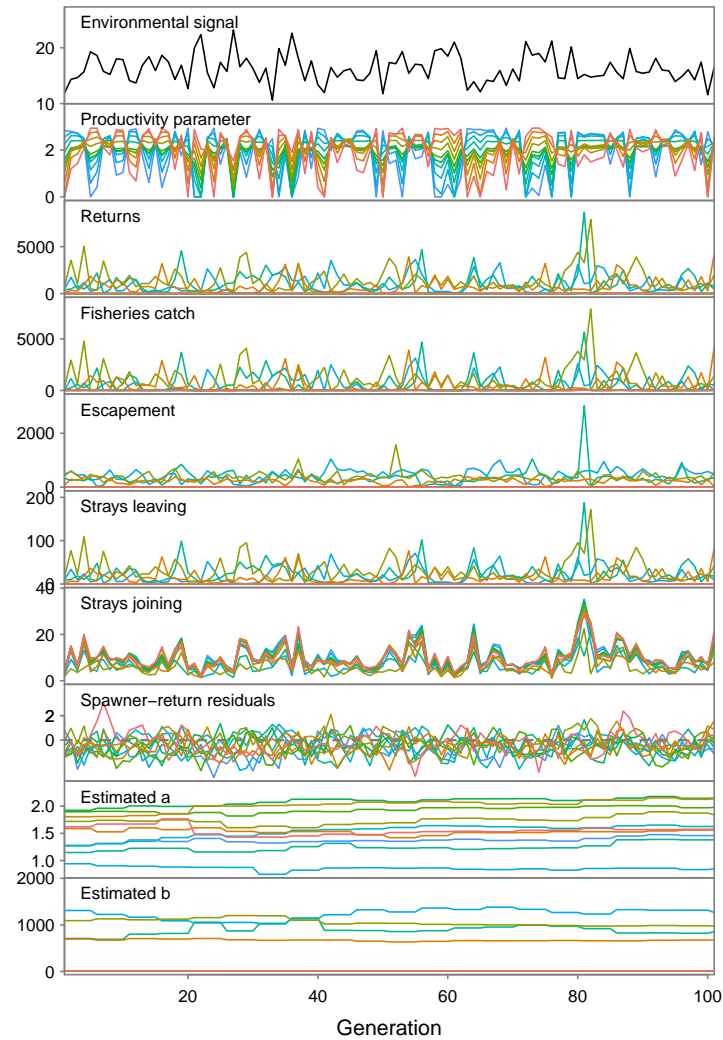


Figure 3.3: The components of an example metapopulation simulation. We show, from top to bottom, the temperature signal, the resulting productivity parameter (Ricker  $a$ ), the salmon returns, fisheries catch, salmon escapement, salmon straying from their natal streams, salmon joining from other streams, spawner-return residuals on a log scale, and the estimated  $a$  and  $b$  parameters in the fitted Ricker curve. The shaded lines indicate populations that thrive at low (blue-green) to high (orange-red) temperatures.

respect to thermal tolerance but where conservation effort ( $\sum_{i=1}^n b_i = 2000$ ) could be distributed across different numbers of streams. We considered conserving from two to 16 streams with thermal tolerance distributed along the same range as in the spatial scenarios. As in the spatial strategies, we reduced the capacity of the remaining streams to the nominal level of  $b_i = 5$ .

*Declining habitat availability:* Habitat capacity in the Pacific Northwest is likely shrinking over time as salmon populations are squeezed between warming temperatures reducing habitat from below and declining stream flows reducing the habitat that remains from above. For example, temperature isotherms are shifting upstream at 1–10 km/decade in low gradient streams that Chinook use for spawning (Isaak and Rieman 2013). At the same time, summer-fall stream flow volumes have been decreasing 10–30% across the Pacific Northwest over the past 50 years (Luce and Holden 2009) and are likely to continue declining (Luce et al. 2013). We therefore considered a scenario where habitat capacity declined by a constant amount across all populations. We reduced the  $b$  parameters by 0.85 units per generation so that some of the smaller populations would reach near extinction by the end of the simulation, as is likely for smaller isolated populations within this century (e.g. Gustafson et al. 2007). In this scenario, we considered cases where thermal tolerance was unknown but conservation effort could be distributed across between 16 and two streams. Climate followed a combination of the same long-term warming and short-term variability as before. For many Pacific salmon metapopulations, this scenario represents the most realistic scenario investigated.

## 3.4 Results

### 3.4.1 Spatial conservation scenarios

*Given short-term environmental fluctuations* (strong interannual variation), conserving a wide range of thermal tolerances is the safest choice because it reduces overall risk to an ecological portfolio (Figs 3.3, 3.4a, Supporting materials Fig. 3.10). The average variance of metapopulation growth rate was 1.6 times lower given balanced thermal tolerance conservation (conserving a full range of thermal tolerances or the middle section vs. the upper or lower half). Thermal tolerance diversity also led to more consistent stability—there was less spread in variance across simulated metapopulations (width of quantiles from left to right in Fig. 3.4a). These increases in stability occurred despite the portfolios being comprised of warm- and cool-thriving populations that individually showed greater variation in response to environmental variability than populations with wide thermal tolerance curves. We can see the mechanism behind these

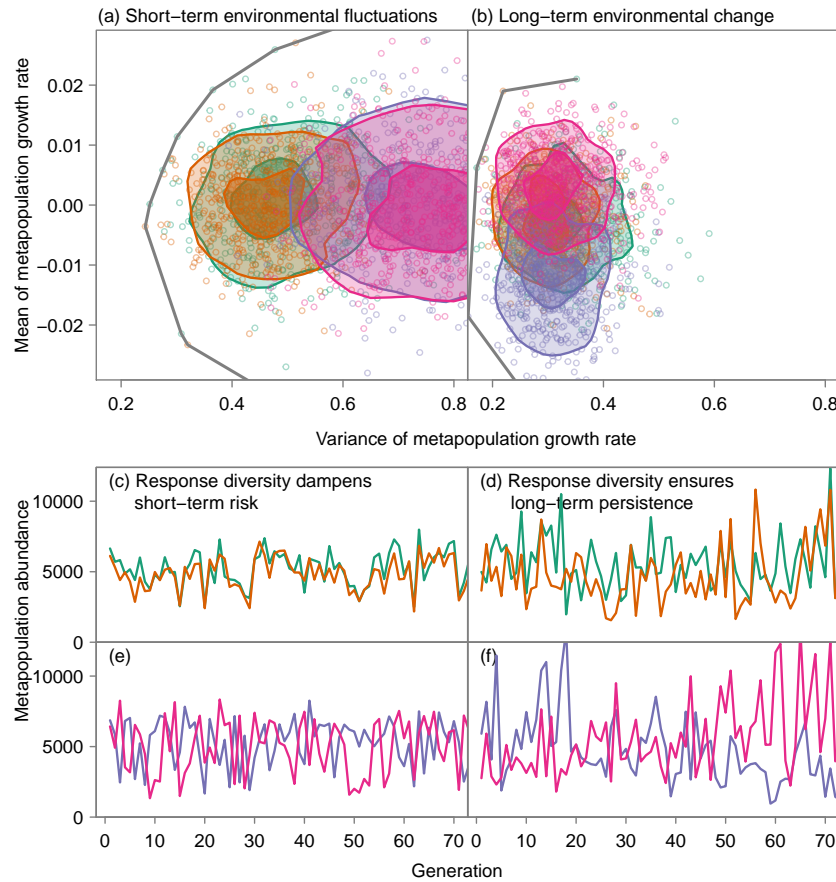


Figure 3.4: The importance of preserving thermal-tolerance diversity through spatial conservation strategies. The conservation strategies correspond to figure 2 and represent conserving a range of responses (green), the most stable populations only (orange), or one type of environmental response (purple and pink). In risk-return space we show environmental scenarios that are comprised primarily of (a) short-term and (b) long-term environmental fluctuations. The dots show simulated metapopulations and the contours show 25% and 75% quantiles across 500 simulations per strategy. We also show example metapopulation abundance time series for the (c, e) short-term and (d, f) long-term environmental-fluctuation scenarios. The thick grey line (a, b) indicates the efficient frontier across all simulated metapopulations—metapopulations with the minimum variability for a given level of growth rate.

portfolio properties by inspecting example population time series (Fig. 3.4c, d). If only the upper or lower half of thermal tolerances is conserved, the portfolio tends to alternate between performing well and poorly, depending on the environmental conditions, resulting in a riskier portfolio (Fig. 3.4e). This risk is buffered when a diversity of thermal tolerances is conserved (Fig. 3.4c) and the resulting asynchrony in population abundance (Supporting materials).

*Given long-term environmental change*, such as climate warming, an ecological manager is hedging his or her bets on the environmental trend and how the populations will respond by conserving a range of thermal tolerances. The choice of which populations to conserve affects the “rate of return” (metapopulation growth rate) properties of an ecological portfolio (Fig. 3.4b; Supporting materials Figs 3.11, 3.12). The typical metapopulation growth rate when thermal tolerances were balanced was near zero—the metapopulation neither increased nor decreased in abundance in the long run. The example metapopulation abundance time series (Fig. 3.4d, f) illustrate the mechanism: by conserving a range of thermal tolerances, when one population is doing poorly, another is doing well and the metapopulation abundance remains stationary through time. If a manager had invested only in the populations that were doing well at the beginning they would have had the lowest metapopulation growth rate at the end (purple portfolios in Fig. 3.4f).

### 3.4.2 Unknown thermal tolerances

In a scenario where the distribution of population-level thermal tolerances are unknown, portfolio optimization informs us that investing in more populations buffers portfolio risk regardless of environmental trend (Fig. 3.5). *Given short-term environmental fluctuations*, conserving more populations buffers portfolio risk (Fig. 3.5a, c, d; Supporting materials Figs 3.13, 3.14). For example, a metapopulation with 16 conserved populations is on average 1.7 times less variable than a metapopulation with only eight. At the same time, the random conservation of thermal tolerances creates an increased spread of possible metapopulation risk given fewer populations conserved (increasing quantile width from left to right in Fig. 3.5a).

*Given long-term environmental change*, conserving more populations also buffers portfolio risk (Fig. 3.5b; Supporting materials Figs 3.15, 3.16). Furthermore, in comparison to the short-term environmental noise scenario, the long-term environmental change creates a greater spread of possible metapopulation growth rates. For example, the height of the 75% quantile of the mean metapopulation growth rate for the two-population systems (light grey polygons) is larger given long-term change than short-term change.

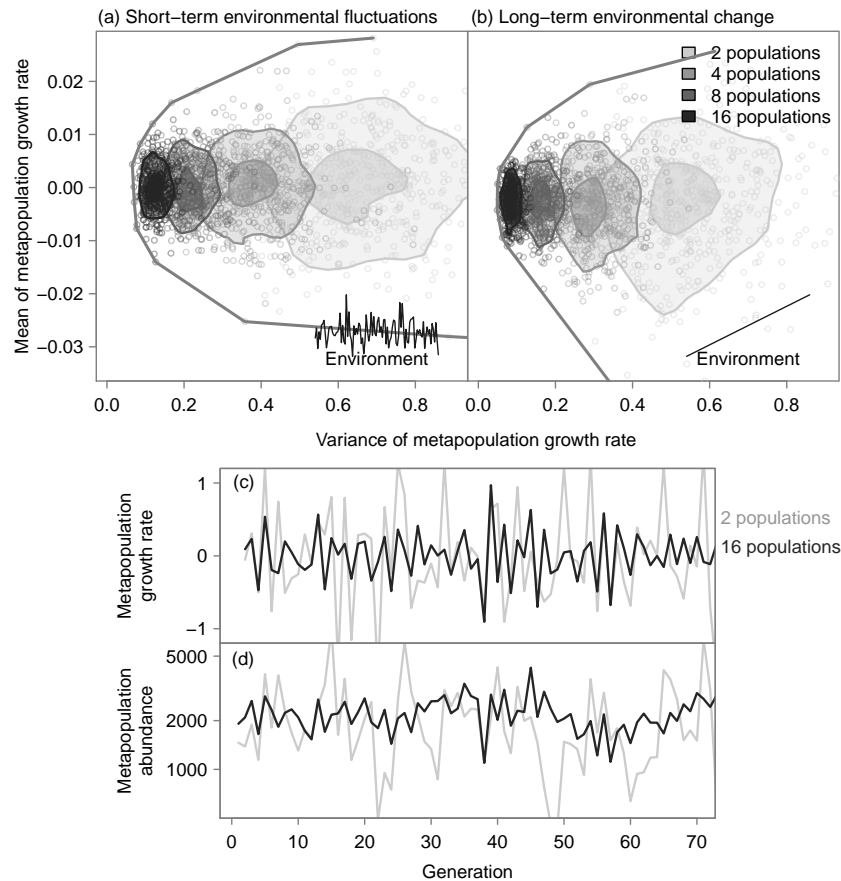


Figure 3.5: The importance of preserving as many populations as possible when we do not know how thermal-tolerance is distributed. In risk-return space we show environmental scenarios that are comprised primarily of (a) short-term and (b) long-term environmental fluctuations. We show metapopulations in which two through 16 populations are conserved. The dots show simulated metapopulations and the contours show 25% and 75% quantiles across 500 simulations per strategy. We also show example metapopulation (c) rate-of-change and (d) abundance time series for the short-term environmental-fluctuation scenario. The thick grey line (a, b) indicates the efficient frontier across all simulated metapopulations—metapopulations with the minimum variability for a given level of growth rate.

### 3.4.3 Declining habitat availability

Given a reduction in stream flow over time along with climate change and climate variability, a manager encounters a risk-return trade-off when deciding how many populations to distribute conservation efforts across (Fig. 3.6; Supporting materials Figs 3.17, 3.18). Conserving more populations buffers portfolio risk, but at the expense of expected metapopulation growth rate. For example, the mean metapopulation variance was 2.7 times lower when 12 populations were conserved instead of four, but the expected metapopulation growth rate was 2.0 times lower when 16 populations were conserved instead of eight. The conservation scenarios represent an efficient frontier where a manager must choose whether to hedge his or her bets on a smaller number of populations and take on greater expected variability or conserve more populations and accept a lower expected metapopulation growth rate.

## 3.5 Discussion

The importance of conserving populations with a diversity of responses to the environment is a key assumption of conservation ecology, but has rarely been tested quantitatively (Mori et al. 2013). We show how maintaining populations with a variety of thermal tolerances reduces risk caused by short-term environmental stochasticity and optimizes chances for long-term persistence given climate change. Further, conserving more populations reduces metapopulation variability but possibly at the expense of long-term metapopulation growth rate if available habitat is squeezed by climate change. In this discussion, we begin by linking our model with real-world conservation issues for Pacific Northwest salmon. We then consider broader implications for metapopulation conservation of any species and ecological stability in general.

### 3.5.1 Implications for salmon conservation

Our results emphasize the importance of promoting ecological conditions that promote diversity of environmental response to the environment if stability is to be maintained in the face of environmental uncertainty. This suggests three clear conservation actions. First, since habitat heterogeneity can lead to local adaptation (e.g. Fraser et al. 2011), our results emphasize the need to maintain a diversity of salmon habitat (Rogers and Schindler 2008). Second, if conservation actions must be prioritized, then our model suggests we should focus on populations that aren't spatially contiguous to maximize diversity of response to the environment. Third,

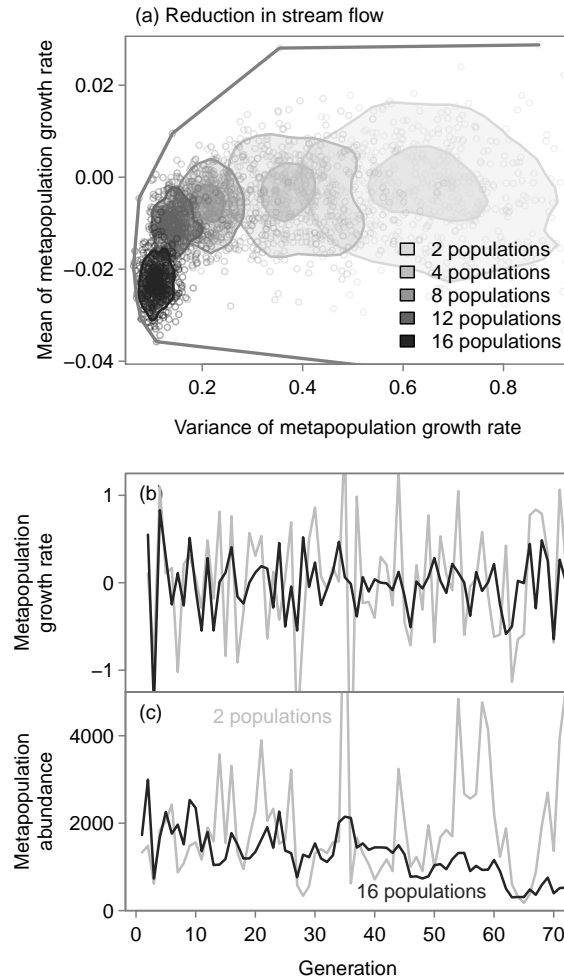


Figure 3.6: Risk-return trade-off in the case where habitat is lost over time through stream flow reduction. The temperature follows both short-term fluctuations and a long-term increase. Thermal tolerance is randomly conserved. Shading indicates conservation plans where two through 16 populations are conserved. (a) Conserving more populations decreases expected variance but also decreases expected growth rate. Dots show simulated metapopulations and contours show 25% and 75% quantiles across 500 simulations per strategy. The thick grey line indicates the efficient frontier across all simulated metapopulations—metapopulations with the minimum variability for a given level of growth rate. Also shown are (b) example metapopulation growth rate and (c) abundance time series from the 2 and 16 population scenarios. Regression lines in (b) illustrate a decreasing growth rate through time.



our results demonstrate the advantages of avoiding structures that artificially remove diversity of environmental response. For salmon, dams are a prominent example (McClure et al. 2008a). Dams can have a double impact whereby their introduction selectively eliminates a large swath of contiguous habitat, perhaps analogous to our upper- or lower-half scenarios in Fig. 3.4, and then mitigation approaches such as hatcheries can further reduce response diversity if not carefully managed (McClure et al. 2008b). In fact, salmon habitat lost to dams in the western U.S. has been biased towards warmer, drier, higher habitats (McClure et al. 2008a) and our findings suggest the resulting loss of warm-tolerant species may compound the risk to current metapopulations in the face of global warming.

The goals of existing salmon management structures in the western US and Canada support a portfolio conservation perspective. In the US, salmon populations are divided into Evolutionarily Significant Units (ESUs), groups of populations that are reproductively isolated and share a common evolutionary heritage, and finer-scale Viable Salmonid Populations (VSPs), populations that are demographically independent of other populations over a 100-year time frame (McElhany et al. 2000). In Canada, the rough equivalent to the ESU is a Conservation Unit (CU), which consists of a group of salmon that are reproductively isolated and that if lost would be unlikely to recolonize in a reasonable time frame (DFO 2005). A salmon portfolio in our model could represent an ESU or CU and the lessons learned from our models are thus directly applicable to management guidelines in the Pacific Northwest. In fact, a number of VSP guidelines agree with our findings. For example, VSP guidelines suggest maintaining diversity in a variety of forms, focusing conservation efforts not just where salmon are currently abundant, and maintaining metapopulations with some populations near each other and others further apart (McElhany et al. 2000).

However, salmon populations in the Pacific Northwest are already heavily impacted (e.g. Gustafson et al. 2007) and VSP and CU recovery goals have not yet been achieved for most populations. Since European-Americans arrived, 29% of 1400 historical salmon populations in the Pacific Northwest and California have been lost (Gustafson et al. 2007). Furthermore, 44% of salmon habitat in the western US (in the lower 48 states) has been lost to dams and other freshwater blockages (McClure et al. 2008a). Changes to habitat, combined with increasing climate variability, has led to disturbance regimes that differ substantially in the frequency, magnitude, and duration from historical patterns, and threaten the resilience of salmon populations (Waples et al. 2009). Many remaining populations rely on hatcheries for long-term population viability—creating substantial evolutionary risks such as outbreeding depression,

genetic homogenization, reduced effective population size, and domestication of fish (adaption to artificial environments and reduced fitness in wild environments) (McClure et al. 2008b). Reduction of long-term reliance on hatcheries, accompanied by habitat restoration through, for example, restoring connectivity of floodplains and stream flow regimes, remains a critical component of long-term salmon sustainability in the Pacific Northwest—particularly given predicted patterns of climate change (Beechie et al. 2013).

Our model complements other simulation-based salmon-habitat prioritization models. While these other models tend to focus on detailed assessment of individual fish stocks, our model is the first to consider the role of response diversity in buffering risk for metapopulations as a whole. The Shiraz model is one complementary prioritization scheme (Scheuerell et al. 2006). It focuses on detailed conditioning of the habitat-population-dynamics relationship at multiple life-history stages for a single salmon population. Whereas the Shiraz model can be applied to an entire watershed, it combines the populations together as a single unit thereby ignoring the role of population-level environmental response diversity. A second salmon prioritization model proposes combining population viability measures with an assessment of the genetic consequences of losing particular populations (Allendorf et al. 1997). This model, however, also focuses on the assessment of individual stocks without considering their covariance and therefore the performance of the salmon portfolio as a whole. Our model does not replace these prioritization schemes. Rather, it proposes an additional focus on prioritization that optimizes metapopulation growth *and* risk and that considers diversity of tolerance to environmental conditions.

While our model captures many relevant aspects of salmon life history and environmental dynamics, it ignores others that could be investigated in future analyses and might improve our understanding of salmon portfolio conservation. First, some salmon populations, such as ocean-type Chinook, tend to spawn further downstream than stream-type salmon. Ocean-type Chinook may therefore be less affected by declining stream flow and be able to shift upstream to avoid shifting isotherms (Mantua et al. 2010). A model could consider evolutionary adaptation by having populations adopt more ocean-type-like characteristics. Second, our model ignores lost thermal-tolerance diversity from populations that reach low population sizes and are reestablished by straying from nearby streams. An individual-based model might more accurately penalize for this lost diversity and emphasize the need to define lower limits on the investment weights in a salmon conservation portfolio. Third, our model ignores fine-scale

within-stream spatial and temporal environmental fluctuations. Fine-scale extremes in temperature and stream flow may be particularly important to population dynamics (Mantua et al. 2010) and could be incorporated into a future analysis. Such a model might show an increased benefit of portfolio optimization if the impact of increased magnitude and frequency of local climate extremes is important in addition to the mean trend (Jentsch et al. 2007).

### 3.5.2 Broad ecological implications and conservation priorities

To promote the stabilizing effect of a diversified ecological portfolio, there are two key components to identify: (1) the environmental drivers to which a varied response might occur, and (2) the conservation actions that can increase or decrease the diversity of response. A third component, identifying the traits and behaviours that mediate population responses to the environment may provide further insight into the mechanisms. Environmental drivers of response can include, for example, changes to temperature, habitat availability, air quality, water chemistry, or extreme weather (Elmqvist et al. 2003). Identifying conservation actions that promote environmental response diversity is critical to developing stable ecological systems (Mori et al. 2013). However, merely measuring environmental response diversity in real ecological systems is challenging (albeit possible; Thibaut et al. 2012). Therefore, one realistic solution may be to create general guidelines from a small number of intensively-monitored systems in which we can associate changes in synchrony of populations with changes in conservation regimes (e.g. Moore et al. 2010; Carlson and Satterthwaite 2011). Another solution may be to monitor the diversity of environmental conditions themselves (e.g. temperature, stream flow, and gravel size in the case of salmon) since we know that traits affecting response to environmental conditions are heritable and are likely to adapt to local conditions (Carlson and Satterthwaite 2011) possibly producing diversity of response to subsequent disturbances.

We suggest a number of specific extensions to our simulation model. First, the environment-thermal-tolerance mechanism could be expanded—the distribution of environmental tolerance across a metapopulation does not necessarily follow a linear gradient, different forms of environmental tolerance could interact, and environmental conditions could affect populations through mechanisms other than productivity. Second, in addition to other taxa, our model could be extended to ecological communities or meta-communities after accounting for species interactions. Third, without any modifications, our model could consider the Moran or environmental-filter concept whereby populations experience increasingly different environmental forces at further distances (Schindler et al. 2008; Rogers and Schindler 2008). Fourth, a model

could consider the contribution of contemporary evolution (Stockwell et al. 2003). These rapid adaptations to changes in the environment could strongly influence portfolio performance and emphasize the importance of maintaining genetic diversity and a variety of local habitat. Finally, our model could be conditioned on a system of interest—say a particular river basin in our example—and the metapopulation portfolio could be optimized across conservation and restoration options as part of a formal decision analysis.

Management decisions for exploited species often come with a trade-off between conservation and revenue generation. Our findings when habitat capacity declined over time illustrate another kind of trade-off more similar to the trade-off described by Markowitz (1952) in his seminal financial portfolio work. In this case, managers must navigate a trade-off between expected risk and return of the metapopulation/portfolio growth rate itself. No position along this trade-off is inherently better than another unless considered in the context of societal values. Does society value short-term stability or a greater assurance of long-term persistence? The optimal choice likely lies somewhere in the middle and parameterizing our model to a specific metapopulation could illustrate the nature of the trade-off and aid conservation decision making. However, if environmental tolerance could be targeted for conservation as in Fig. 3.4, a manager could likely achieve portfolios closer to the efficient frontier in Fig. 3.6. In other words, a manager could achieve a lower expected variance for the same expected growth rate or a higher expected growth rate for the same expected variance—a better conservation outcome in either case.

Conservation planning is inherently a spatial activity (Pressey et al. 2007) and our results can inform how we approach spatial conservation planning. First, our results suggest focusing on conserving the processes and mechanisms underlying stability, not just biodiversity itself (Pressey et al. 2007; Beechie et al. 2013). In particular, our results suggest that response diversity should be a mainstream element of conservation, not just species and functional diversity (Mori et al. 2013). Our analysis also illustrates how conserving a portfolio of populations, ideally selected for a wide range of environmental tolerance, can help integrate across environmental uncertainty when spatial planning (Ando and Mallory 2012). This is particularly important given the uncertainty surrounding the future ecological responses to climate change (Walther et al. 2002). Finally, the increasing rapidness and variability of environmental change necessitates a dynamic approach in which spatial planning is reevaluated at regular intervals (Hannah et al. 2002)—perhaps testing for changes in population and species asynchrony in addition to changes in local productivity and variability. Combined, our results detail a pathway through

which population diversity in environmental tolerance can underpin the stability of ecological systems. This pathway highlights that diverse natural portfolios may be critical for the conservation of metapopulations in the face of increasing climate variability and change.

### **3.6 Acknowledgements**

We thank T.A. Branch, J.D. Yeakel, S.M. O'Regan, S.A. Pardo, L.N.K. Davidson, and C.C. Phillis for helpful discussions and comments on earlier drafts. We thank D.J. Isaak, an anonymous reviewer, and O.P. Jensen for suggestions that greatly improved the manuscript. We are particularly grateful to D.J. Isaak for suggesting and carefully outlining the declining stream flow scenario. Funding was provided by Simon Fraser University, NSERC (ABC, NKD, SCA), the Canada Research Chairs Program (NKD), the Liber Ero Chair of Coastal Science and Management (JWM), Fulbright Canada (SCA), and a Garfield Weston Foundation/B.C. Packers Ltd. Graduate Fellowship in Marine Sciences (SCA).

### 3.7 Supporting materials

The metafolio R package contains the functions and code to carry out the analyses in our paper.

The package can be installed from CRAN with:

```
install.packages("metafolio")
```

Alternatively, you can view the code and install the package from

<http://github.com/seananderson/metafolio>.

The included vignette describes the package and illustrates some example simulations. You can view the vignette with:

```
vignette("metafolio")
```

You can view the help for the package with:

```
?metafolio
```

```
help(package = "metafolio")
```

The figures from this paper can be re-created by downloading the code from GitHub and sourcing the file `README.R` in the `inst/examples` folder:

```
setwd("metafolio/inst/examples")
```

```
source("README.R")
```

## 3.7.1 Supporting Tables and Figures

Table 3.1: Input parameters to the salmon metapopulation simulation with default values.

Description	Symbol	Value	Reference
<i>Population dynamics parameters</i>			
Stock-recruit residual standard deviation (on log scale)	$\sigma_r$	0.7	Thorson et al. 2014a
AR(1) serial correlation of stock-recruit residuals	$\rho_w$	0.4	Thorson et al. 2014a
Fraction of fish that stray from natal streams	$f_{\text{stray}}$	0.02	Quinn 2005 and references therein
Exponential rate of decay of straying with distance	$m$	0.1	Cooper and Mangel 1999
Range of maximum productivities	$a_i^{\text{max}}$	2.2–2.9	Dorner et al. 2008
<i>Environmental parameters</i>			
Width parameter for thermal-tolerance curves for populations $i = 1$ to $n$ (values generate widths in line with listed references)	$W_i$	0.08–0.04–0.08	Brett 1952; Eliason et al. 2011
Optimum environmental value for populations $i = 1$ to $n$	$e_i^{\text{opt}}$	13–19	Eliason et al. 2011
Standard deviation of annual temperature fluctuations	$\sigma_d$	2	Eliason et al. 2011
AR(1) autocorrelation of annual temperature fluctuations	$\rho_e$	0.1	
Annual increase in stream temperature in degrees Celcius	$\beta_e$	0.04	Mantua et al. 2010
<i>Fishery parameters</i>			
Standard deviation of beta distribution for implementation error	$\sigma_h$	0.1	Pestes et al. 2008
Frequency of assessment (years)	$f_{\text{assess}}$	5	

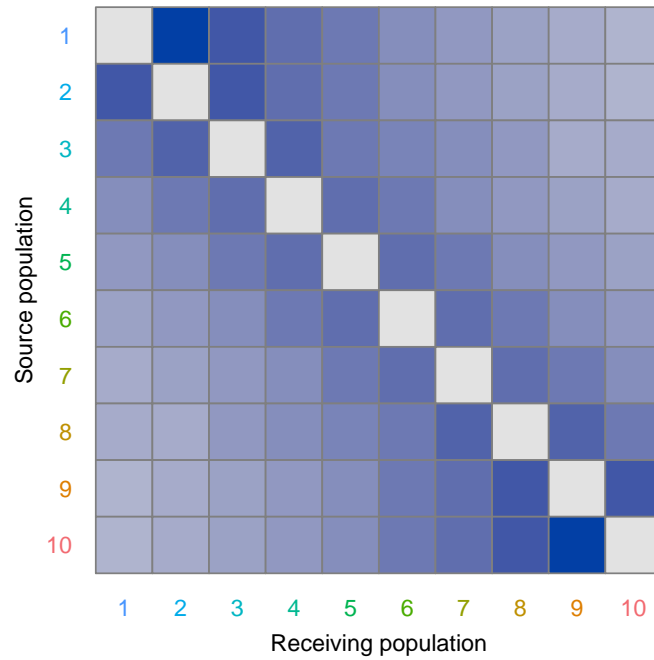


Figure 3.7: An example straying matrix. The rows and columns represent different populations (indicated by population number). Dark blue indicates a high rate of straying and light blue indicates a low rate of straying.



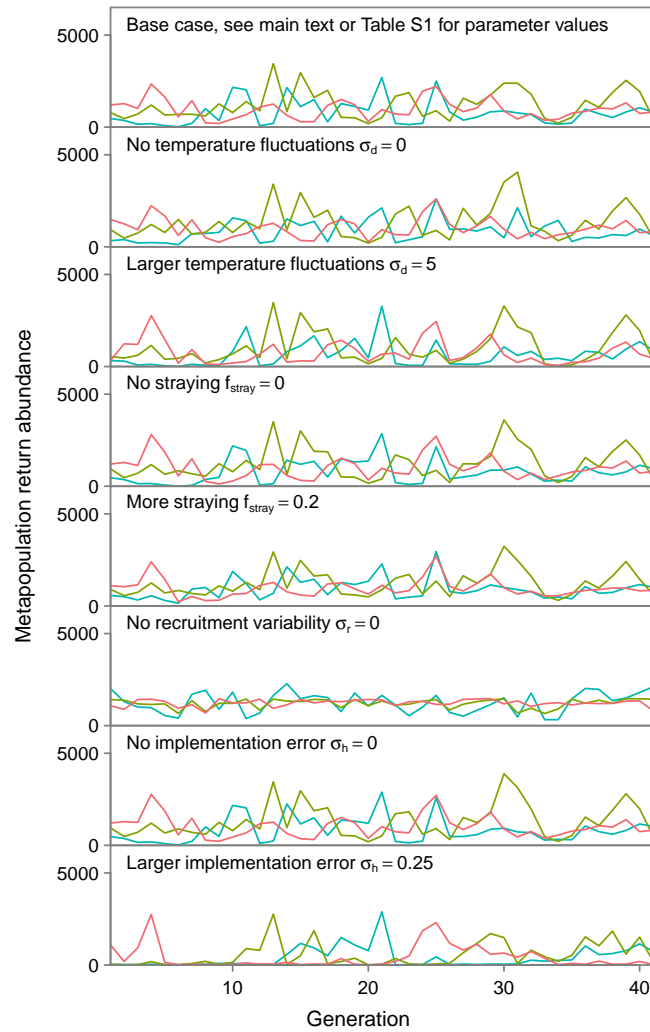


Figure 3.8: The impact of increasing or decreasing various parameter values on metapopulation return abundance. The different coloured lines represent three example salmon populations. The base case represents the base-case values for the short-term environmental fluctuation scenario.

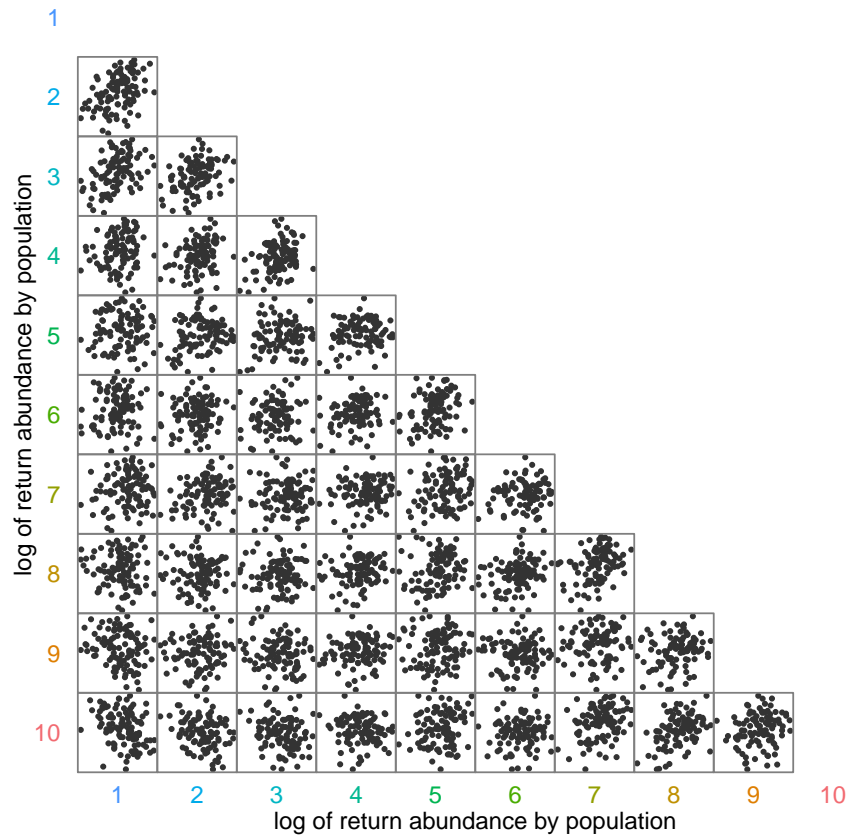


Figure 3.9: A comparison of the  $\log(\text{returns})$  between populations. The subpopulation IDs are coloured from warm tolerant (warm colours) to cool tolerant (cool colours). Note how populations 1 and 10 have asynchronous returns whereas populations with more similar thermal-tolerance curves (say populations 9 and 10) have more synchronous dynamics. Populations with thermal tolerance curves in the middle (e.g. population 6) are less correlated with other populations. Their population dynamics end up primarily driven by demographic stochasticity and less so by temperature-induced systematic changes in productivity.

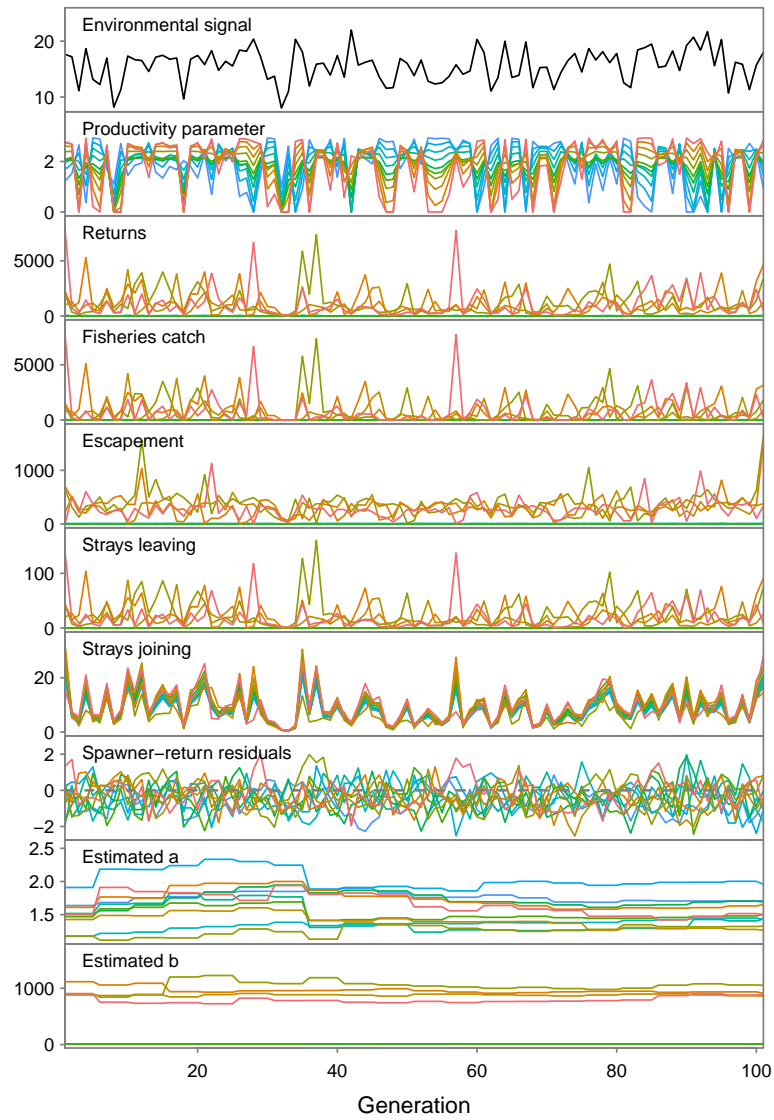


Figure 3.10: Conserving **one half** of response diversity (spatial conservation strategy) with **short-term** environmental fluctuations.

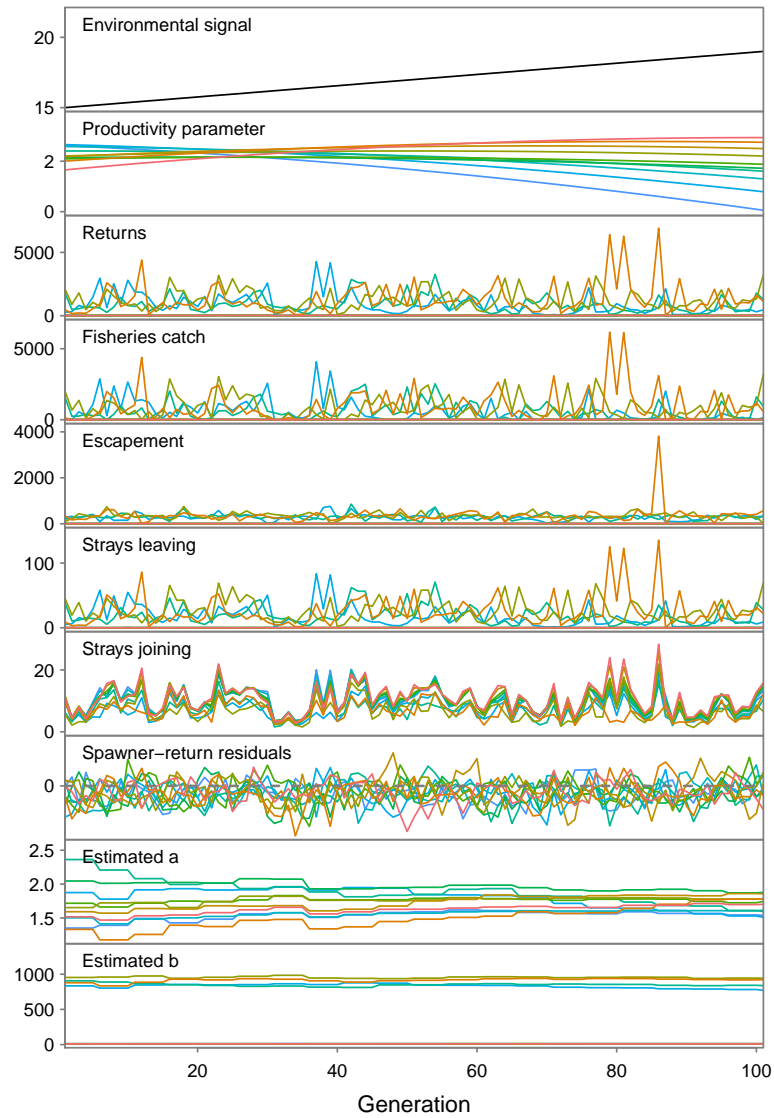


Figure 3.11: Conserving a **full range** of response diversity (spatial conservation strategy) with **long-term** environmental change.

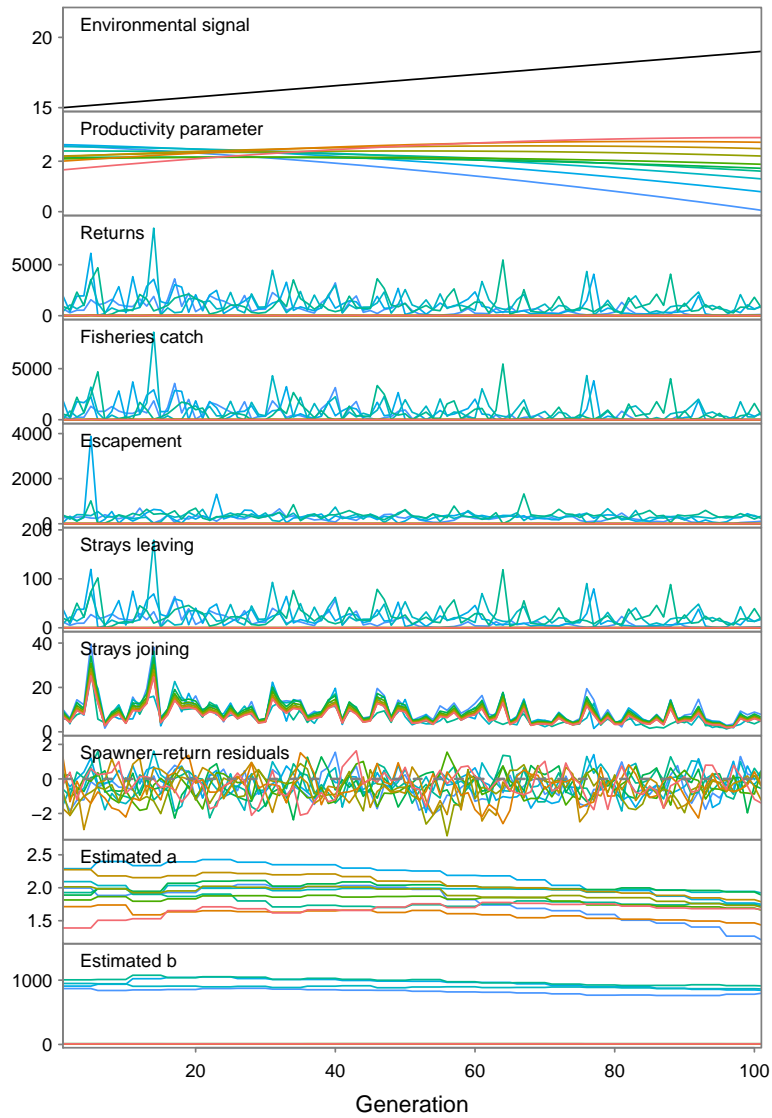


Figure 3.12: Conserving **one half** of response diversity (spatial conservation strategy) with **long-term** environmental change.

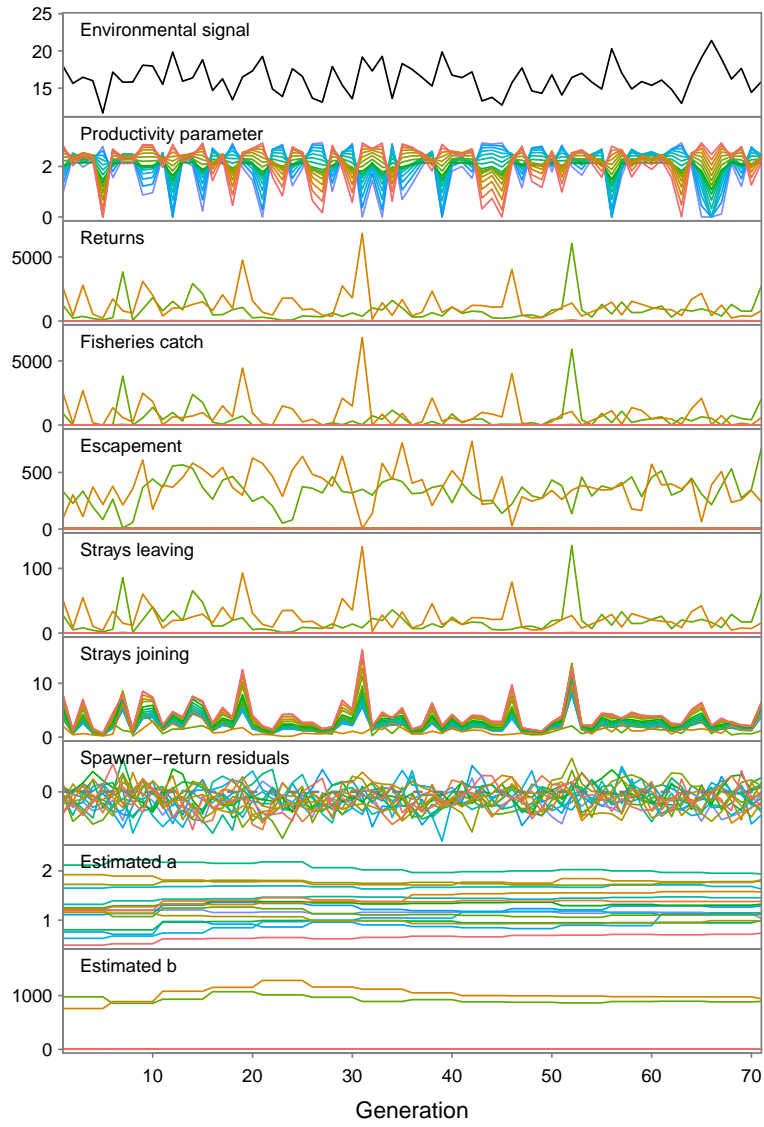


Figure 3.13: **Two populations** conserved with random response diversity and **short-term** environmental fluctuations.

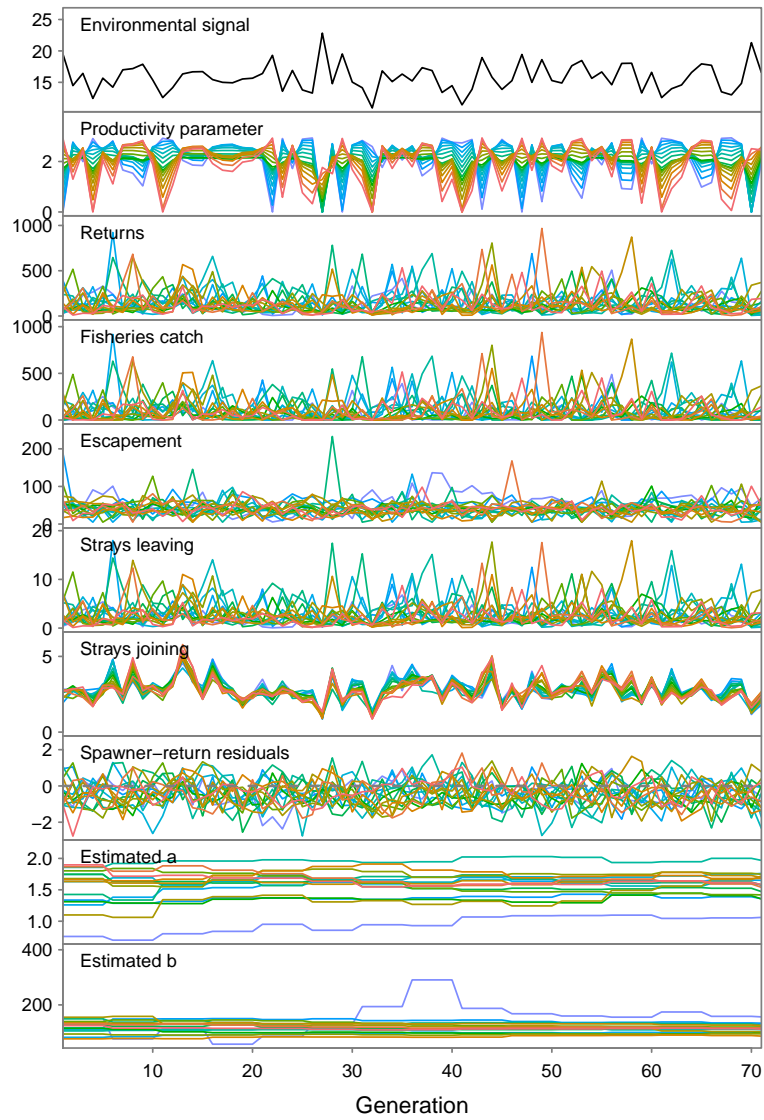


Figure 3.14: **Sixteen populations** conserved with random response diversity and **short-term** environmental fluctuations.

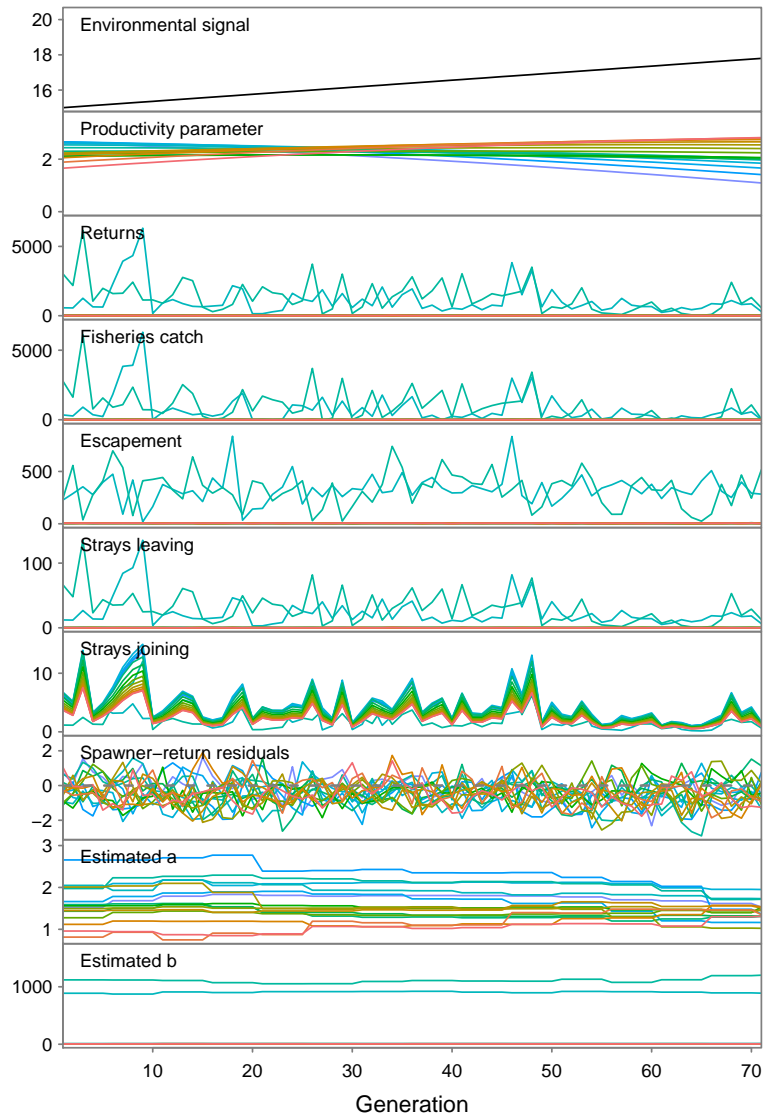


Figure 3.15: **Two populations** conserved with random response diversity and **long-term** environmental change.



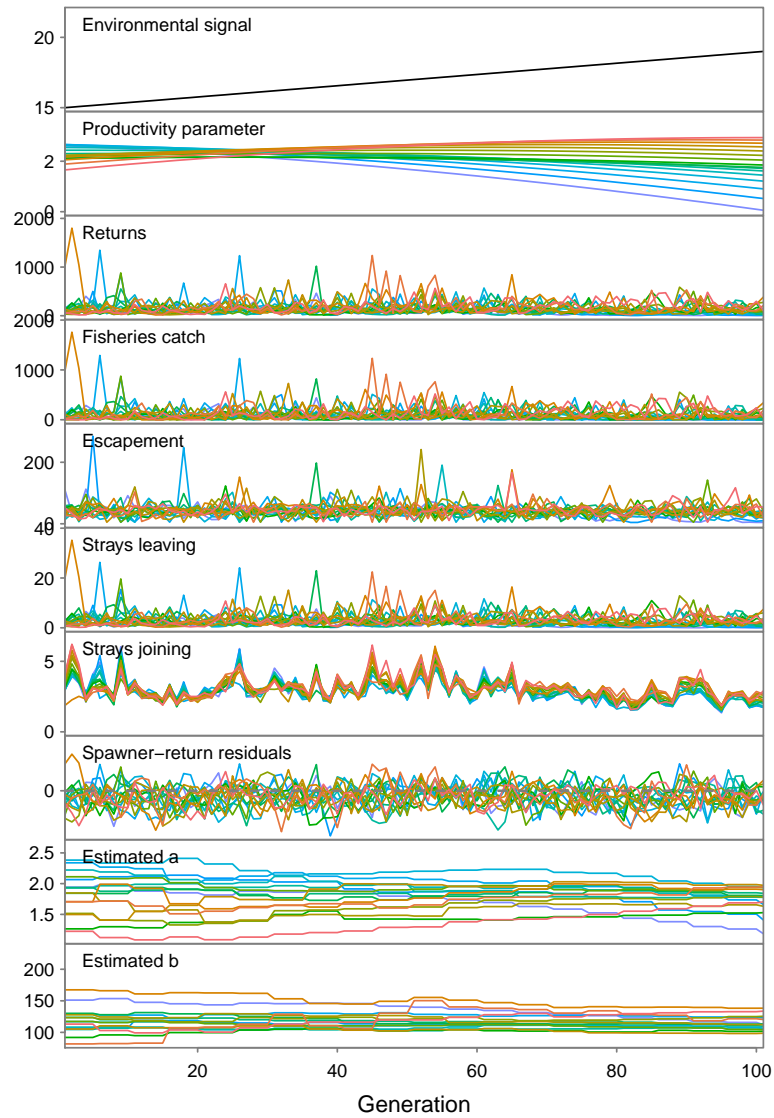


Figure 3.16: **Sixteen populations** conserved with random response diversity and **long-term environmental change**.

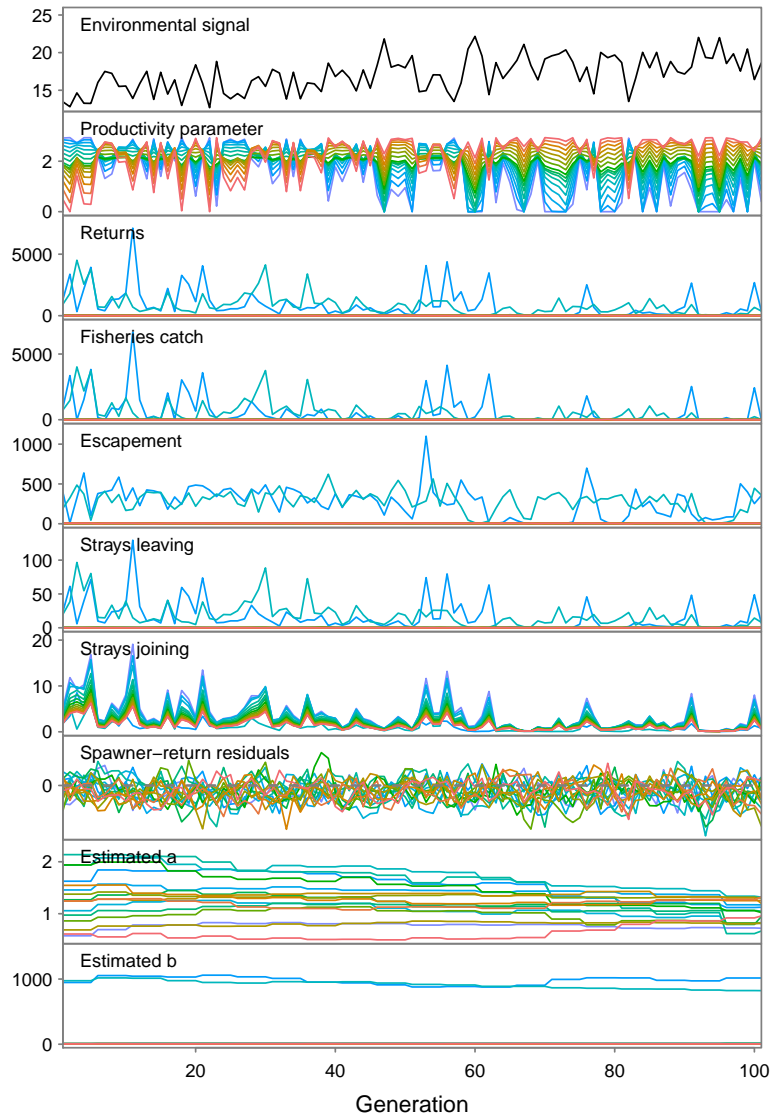


Figure 3.17: Two populations conserved with random response diversity and long-term declining stream flow.

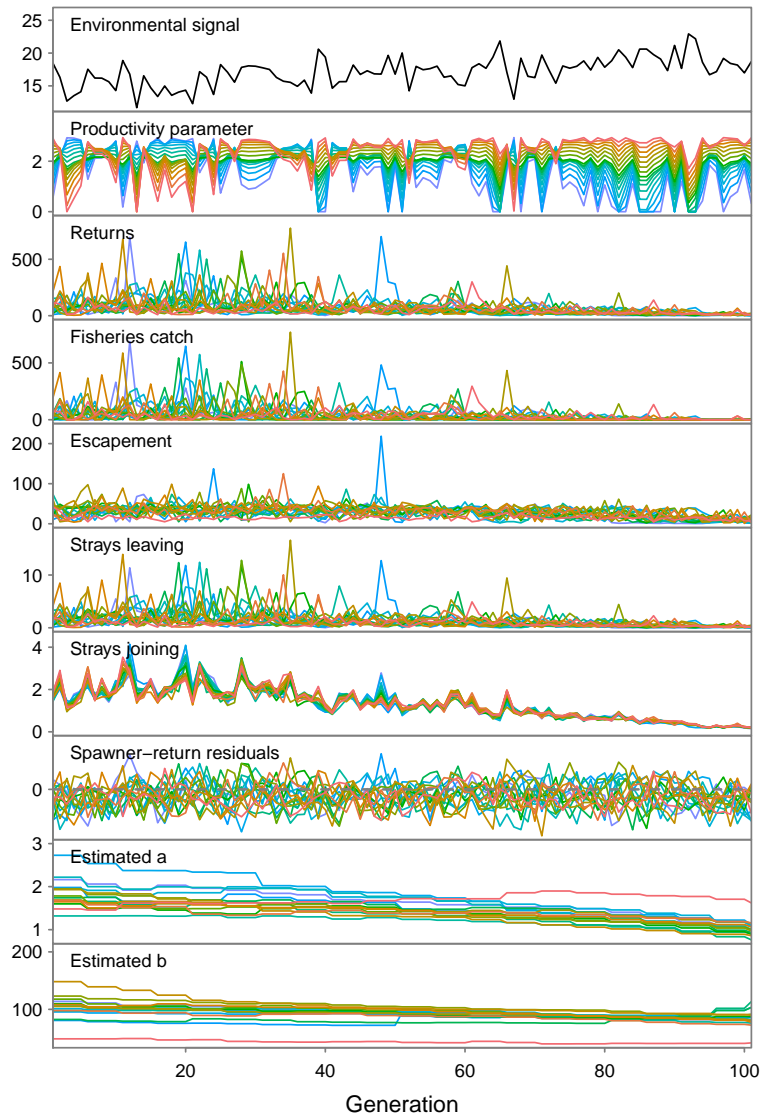


Figure 3.18: Sixteen populations conserved with random response diversity and long-term declining stream flow.

## Chapter 4

# Evidence for black-swan events in animal populations<sup>3</sup>

### 4.1 Abstract

Black swans are statistically improbable events that nonetheless occur—often with profound consequences. While extremes in the physical environment, such as monsoons and heat waves, are widely studied and increasing in magnitude and frequency, it remains unclear the extent to which ecological populations buffer or suffer from such extremes. Here, we estimate the degree of heavy-tailedness (presence of black swans) in ecological process noise by applying a probability model to 609 time series from around the world across 39 taxonomic orders and seven classes. We find strong evidence of black swans, but they are rare, occurring in 3–5% of populations: most frequently for birds (4–8%) followed by mammals (4–6%) and insects (2–3%). Black swans were predominantly (87%) downward events and were not explained by any life-history covariates, but tended to be driven by external perturbations such as climate, severe winters, predator or parasite cycles, and the combined effects of multiple factors. Extreme events were more frequently detected for populations with longer time series and lower levels of process noise; for shorter and noisier time series, our simulations suggested black-swan dynamics are often not identifiable as such. The presence of black swans in population dynamics highlights the importance of developing robust conservation and management strategies—particularly as the frequency and magnitude of climate extremes increase over the next century.

---

<sup>3</sup>T.A. Branch, A.B. Cooper, and N.K. Dulvy are co-authors on this chapter, which is in preparation for submission to a journal.

## 4.2 Introduction

Black swans are unexpected extreme events with potentially dramatic consequences (Taleb 2007; Sornette 2009). One of the most striking black swans in ecology is the asteroid collision that may have marked the end-Cretaceous mass extinction 65 million years ago (Alvarez et al. 1980; Harnik et al. 2012). Today, climate extremes, in concert with shifts in mean temperature, are expected to cause the greatest ecological and societal damage (IPCC 2012). But, while extremes in the physical environment such as wave height, storm severity, and temperature are frequent events (Gaines and Denny 1993; Katz et al. 2005), it remains unclear the extent to which ecological systems buffer or suffer from black swans (Nuñez and Logares 2012).

There is compelling anecdotal evidence for ecological black swans, but systematic evidence across taxa has been elusive. A survey of ecologists indicated that surprising outcomes of field experiments are far more common than we assume (Doak et al. 2008), and events such as the global invasion of Argentine ants and the mutation of viruses to infect new hosts could be considered black swans (Nuñez and Logares 2012). In fact, anecdotes of population catastrophes are numerous and catastrophes may be the most important element affecting population persistence (Mangel and Tier 1994). For marine mammal populations, we have compelling evidence of catastrophes (Gerber and Hilborn 2001; Ward et al. 2007), and recently, time-series of marine microbe abundance (Segura et al. 2013) and time to extinction for experimental water-flea populations (Drake 2014) have been found to follow heavier tailed distributions than the normal. Despite these examples, as far as we can tell there have been two systematic surveys for ecological black swans: one with North American breeding birds and the other with the Global Population Dynamics Database, which uncovered little clear evidence for them (Keitt and Stanley 1998; Allen et al. 2001; Halley and Inchausti 2002). Nevertheless there are methodological challenges to their detection (Allen et al. 2001; Ward et al. 2007).

There are two key reasons why we may find little evidence of ecological black swans. First, they might not exist in higher taxa. Indeed, the majority of model fitting and risk forecasting assumes that population dynamics are normal tailed on a log scale (e.g. Brook et al. 2006; Dennis et al. 2006; Knappe and de Valpine 2012). Alternatively, black-swan dynamics might exist, but our ability to detect them requires further development of statistical tools. One such tool is the generalized extreme value distribution, which has been applied to environmental data (e.g. Katz et al. 2005). This distribution describes the most extreme event per time interval (e.g. heaviest rainfall per year), but requires time series that are sufficiently long to be condensed into time intervals. Another statistical tool involves fitting a catastrophic mixture distribution in a

state space model to quantify the probability that population events are extreme, although this is also data intensive (Ward et al. 2007). A third tool is to compare the support for fits of thin- and heavy-tailed distributions (Halley and Inchausti 2002), but this analysis did not quantify the probability of black swans or allow for population dynamics.

Here, we assess the frequency and magnitude of black-swan dynamics across 609 populations from a wide array of taxonomic groups—mostly birds, mammals, insects, and fishes. We then identify characteristics of time series or intrinsic life-history characteristics that are associated with the detection of black-swan events and attempt to verify known causes. To accomplish this, we develop a framework for identifying heavy-tailed process noise in population dynamics, i.e. whether the largest stochastic jumps in abundance from one time step to the next are more extreme than typically seen with a log-normal distribution. Our framework allows for a range of population dynamic models, can incorporate observation uncertainty, and can be easily applied to abundance time series.

### 4.3 Methods

To obtain estimates of the probability and magnitude of black-swan events, we fit population dynamic models to abundance time series from around the world. For each population, we estimated the shape of the process noise tails by measuring the degrees of freedom ( $\nu$ ) of a Student t-distribution.

#### 4.3.1 Time-series data

We selected abundance time series from the Global Population Dynamics Database (GPDD; NERC Centre for Population Biology, Imperial College 2010), which contains nearly 5000 time series of abundance from  $\sim 1000$  species and  $\sim 100$  taxonomic orders. We filtered the data (Supporting materials) to remove populations from less reliable data sources, and those without sufficient data for our models, and then interpolated some missing values (*sensu* Brook et al. 2006). Our interpolation affected only  $\sim 1\%$  of the final data points (Supporting materials Table 4.3) and none of the data points that were later considered black-swan events. Our final dataset contained 609 populations across 39 taxonomic orders and seven taxonomic classes, with a median of 26 time steps (range of 20–117) (Supporting materials Table 4.3, Fig. 4.5).

### 4.3.2 Population models

Our main analysis focuses on the commonly applied Gompertz population dynamics model (e.g. Knappe and de Valpine 2012; Dennis and Ponciano 2014; Connors et al. 2014). The Gompertz model represents population growth as a linear function in log space. If we let  $x_t$  represent the log abundance ( $N$ ) at time  $t$ , we can represent the Gompertz model as:

$$x_t = \lambda + bx_{t-1} + \epsilon_t$$

$$\epsilon_t \sim \text{Student-t}(\nu, 0, \sigma).$$

The growth parameter  $\lambda$  represents the expected growth rate if  $N_t = 1$ . The model is density independent if  $b = 1$ , maximally density dependent if  $b = 0$ , and inversely density dependent if  $b < 0$ . Usually, the process noise  $\epsilon_t$  is modelled as normally distributed, but in our paper we assume it is drawn from a t distribution with scale parameter  $\sigma$  and degrees of freedom  $\nu$ . In previous analyses of the GPDD, the Gompertz was most often identified as the most parsimonious population model fit to these data (Brook and Bradshaw 2006).

By allowing the process noise to be drawn from a Student-t distribution we can estimate the degree to which the process deviations have heavy tails and are therefore evidence of black-swan events (Fig. 4.1a, b). For example, at  $\nu = 2$ , the probability of drawing a value more than five standard deviations below the mean is 0.02, whereas the probability of drawing such a value from a normal distribution is tiny ( $2.9 \cdot 10^{-7}$ ). As the value of  $\nu$  approaches infinity, the distribution approaches the normal distribution (Fig. 4.1a, b). While, across populations, the extreme process deviations might tend to be more frequently upwards or downwards events, a small random sample from a heavy-tailed distribution can have many outliers on one side and appear asymmetric (Gelman 2013). Therefore, fitting a symmetric t distribution is appropriate for the relatively short population time series in our dataset and is agnostic towards the detection of upwards or downwards black swans.

We fit all models in a Bayesian framework using Stan (Stan Development Team 2014) via the R computing environment (R Core Team 2014). Stan samples from the posterior distribution with an adaptive version of Hamiltonian Markov chain Monte Carlo called the No-U-Turn Sampler and generally obtains less correlated samples than algorithms such as the Gibbs sampler (Hoffman and Gelman 2014). We tested to ensure that the chains had sufficiently converged and that the sampler had obtained sufficient independent samples from the posterior ( $\widehat{R} < 1.05$ ,  $n_{\text{eff}} > 200$ ; Supporting materials).

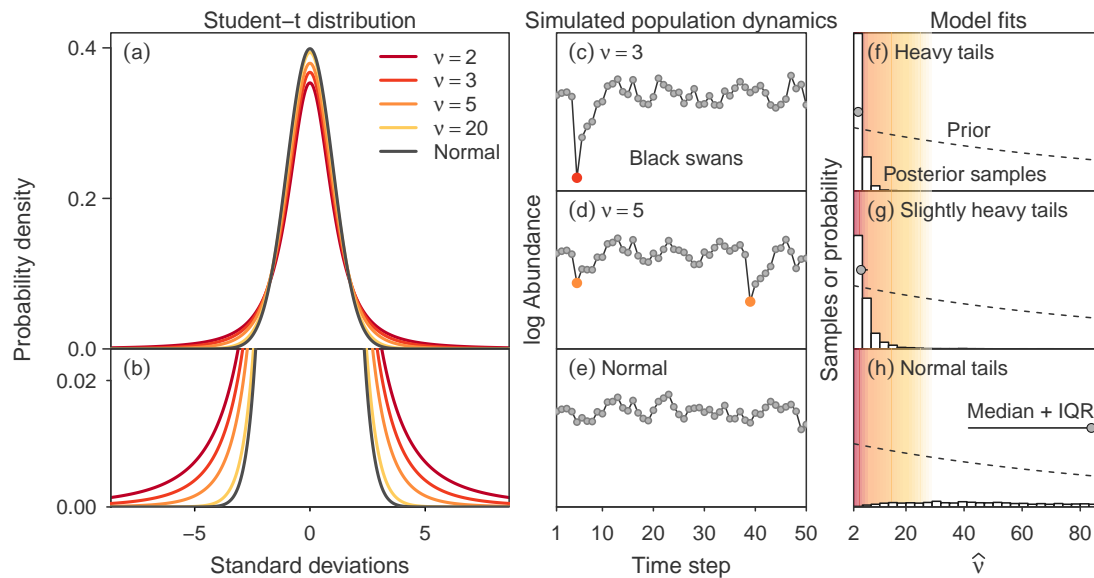


Figure 4.1: An illustration of fitting population dynamic models that allow for heavy tails, represented by the Student- $t$  degrees of freedom parameter  $\nu$ . (a, b) The probability density for  $t$  distributions with a scale parameter of 1 and different values of  $\nu$ . Small values of  $\nu$  create heavy tails. As  $\nu$  approaches infinity the distribution approaches the normal distribution. For example, at  $\nu = 2$ , the probability of drawing a value more than five standard deviations below the mean is 0.02, whereas the probability of drawing such a value from a normal distribution is nearly zero ( $2.9 \cdot 10^{-7}$ ). (c–e) Simulated population dynamics from a Gompertz model with process noise drawn from  $t$  distributions with three different values of  $\nu$ . Coloured dots in panels c and d represent jumps with less than a 1 in 1000 chance of occurring in a normal distribution. (f–h) Estimates of  $\nu$  from models fit to the times series in panels c–e. Shown are the posterior samples (histograms), median and interquartile range of the posterior (IQR) (dots and line segments), and the exponential prior on  $\nu$  (dashed lines). Colour shading behind panels f–h illustrates the region of heavy tails.



We chose weakly informative priors to incorporate our understanding of plausible population dynamics (Gelman et al. 2014; Figs 4.1f–h, 4.6). For  $\nu$ , we chose an exponential prior with rate parameter of 0.01 truncated at values above two—a slightly less informative prior than suggested by Fernandez and Steel (1998). This prior gives only a 7.7% probability that  $\nu < 10$  but constrains the sampling sufficiently to avoid wandering off towards infinity. In any case, for  $\nu > 20$  the t distribution is almost indistinguishable from the normal distribution (Fig. 4.1). Based on the shape of the t distribution, we chose the probability that  $\nu < 10$ ,  $\Pr(\nu < 10)$ , to define the probability of heavy-tailed dynamics. When categorizing a population as heavy or normal tailed, we used a threshold of 0.5 probability.

We fit alternative population models to test if four key phenomena systematically changed our conclusions. Autocorrelation has been suggested as a reason for increased observed variability of abundance time series through time, which could create apparent heavy tails (Inchausti and Halley 2002); therefore, we fit a model that included serial correlation in the residuals. Additionally, previous work has modelled abundance or growth rates without accounting for density dependence (Halley and Inchausti 2002; Segura et al. 2013); therefore, we fit a simpler model in which we assumed density independence. Third, observation error could bias parameter estimates (Knape and de Valpine 2012) or mask our ability to detect heavy tails (Ward et al. 2007); therefore, we fit a model where we allowed for a fixed quantity of observation error (0.2 standard deviations on a log scale). Finally, the Gompertz model assumes that population growth rate declines linearly with log abundance. Therefore, we also fit an alternative model, the Ricker-logistic model, which assumes that population growth rate declines linearly with abundance itself (Supporting materials).

In addition to alternative population models, we investigated the sensitivity of our results to weaker and stronger priors (exponential rate parameter = 0.005, 0.02; Supporting materials Fig. 4.6, Supporting materials). We used simulated data to test how easily we could detect  $\nu$  given different sample sizes and to ensure we could recover unbiased parameter estimates from the Gompertz model (Supporting materials).

### 4.3.3 Covariates of population dynamic black swans

We investigated possible covariates of heavy-tailed population dynamics visually and through multilevel modelling. We plotted characteristics of the time series ( $\sigma$ ,  $\lambda$ ,  $b$ , and time-series length) along with two life-history characteristics (body length and maximum lifespan obtained from Brook et al. (2006)) against our estimated probability of heavy tails,  $\Pr(\nu < 10)$ . We

formally investigated these relationships by fitting beta regression multilevel models (Ferrari and Cribari-Neto 2004). The beta probability distribution can represent continuous response data that range between zero and one; we fit our models with a logit link as is common for beta and logistic regression (Ferrari and Cribari-Neto 2004). We incorporated standard deviations around the means for covariates that were derived from Gompertz model parameter estimates. To account for broad patterns of phylogenetic relatedness, we allowed for hierarchical intercepts at the taxonomic class, order, and species level (Supporting materials). We fit our model in Stan with weakly informative priors on the coefficients (Gelman et al. 2008) and variance parameters (Gelman 2006; Gelman et al. 2014; Supporting materials).

Finally, we investigated a sample of populations that our method categorized as having a high probability of heavy tails ( $\Pr(\nu < 10) > 0.5$ ). Where possible, we found the documented causes of ecological black swans in the primary data source cited in the GPDD or in other literature describing the population.

## 4.4 Results

We found strong, but rare, evidence for black-swan population dynamics. By defining black-swan dynamics as a greater than 0.5 probability that  $\nu < 10$ , our main Gompertz model found evidence for heavy tails most frequently for birds (7%) followed by mammals (5%), and insects (3%) (Fig. 4.2, Supporting materials Table 4.4). Black swans were taxonomically widespread, occurring in 38% of taxonomic orders. Accounting for time series length and partially pooling inference across taxonomic class and order with a multilevel model (Supporting materials), there was stronger evidence for black swans in insect populations than is visually apparent in Fig. 4.2—four of 10 orders with the highest median probability of heavy tails were insect orders—however, there was considerable uncertainty in these estimates (Fig. 4.3a).

The majority of our heavy-tailed estimates were robust to alternative population models, observation error, and choice of priors. Our conclusions were not systematically altered when we included an autocorrelation structure in the residuals, modelled population growth rates without density dependence, or modelled the population dynamics as Ricker-logistic (Supporting materials Fig. 4.7). However, setting observation error standard deviation to 0.2 increased the median estimate of  $\nu$  from  $< 10$  to  $\geq 10$  in 8 of 26 populations, although the majority of  $\nu$  estimates remained qualitatively similar (Supporting materials Fig. 4.7). The strength of the prior on  $\nu$  had little influence on estimates of black-swan dynamics (Supporting materials Fig. 4.8). Our simulation testing shows that, if anything, our models underpredict the true magnitude

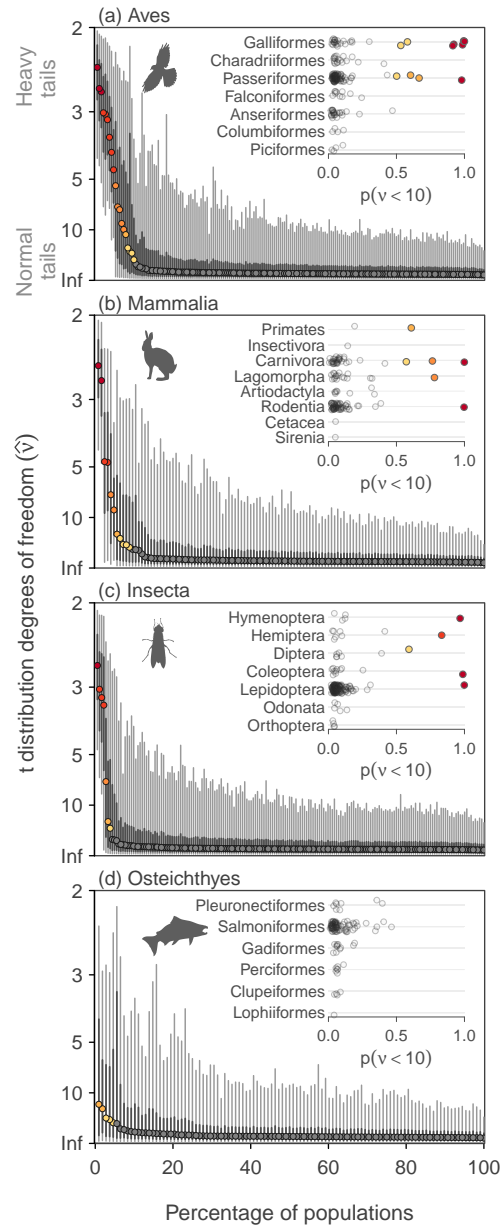


Figure 4.2: Estimates of population dynamics heavy-tailedness for 606 populations of birds, mammals, insects, and fishes. Small values of  $\nu$  approximately ( $< 10$ ) suggest heavy-tailed black-swan dynamics; larger values of  $\nu$  suggest approximately normal-tailed dynamics. Vertical points and line segments represent posterior medians and 50% / 90% credible intervals for individual populations. Inset plots show probability that  $\nu < 10$  (probability of heavy tails) for populations arranged by taxonomic order and sorted by decreasing mean  $\Pr(\nu < 10)$ . Taxonomic orders with three or fewer populations in panel a are omitted for space. Red to yellow points highlight populations with a high to moderately high probability of heavy-tailed black-swan dynamics.

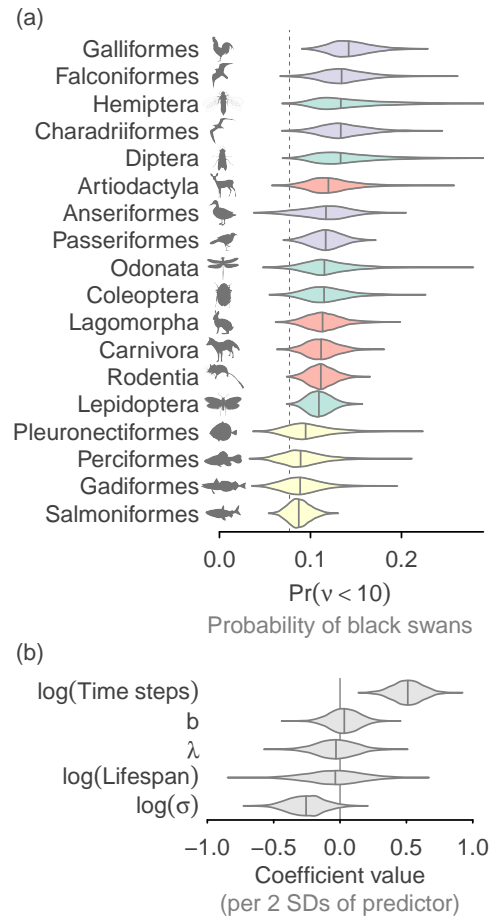


Figure 4.3: Posterior probability distributions from beta regression multilevel models. (a) Taxonomic-order-level posterior densities of  $\Pr(v < 10)$  (approximately the probability of heavy tails) after accounting for time-series length. Estimates are at the geometric mean of time series length across all the data (approximately 27 time steps). Colour shading refers to taxonomic class (yellow: fishes, green: insects, purple: birds, and red: mammals). Dotted vertical line in panel a indicates the  $\Pr(v < 10)$  from the prior distribution. (b) Main effect posterior densities for potential covariates of  $\Pr(v < 10)$ . The beta regression models were fit on a logit scale with hierarchical intercepts for taxonomic class, taxonomic order, and species. All covariates were standardized by subtracting their mean and dividing by twice their standard deviation. In both panels, short vertical line segments within the density polygons indicate median posterior estimates.

and probability of heavy tailed events—especially given the length of the time series in the GPDD (Supporting materials Figs 4.9, 4.10).

Across populations, the probability of observing black-swan dynamics was positively related to time-series length and negatively related to magnitude of process noise ( $\sigma$ ) but not clearly related to population growth rate ( $\lambda$ ), density dependence ( $b$ ), or maximum lifespan (Figs 4.3b, 4.4). Longer time-series length was the strongest covariate of observing black-swan dynamics. For instance, the expected probability density below  $v = 10$  was about 1.6 times greater for a population with 60 time steps compared to one with 30 time steps. However, the absolute change in probability with increased time series length was small (0.20 vs. 0.13 in the previous example, Fig. 4.4).

We examined all time series with published explanations of why the black-swan events occurred (Table 4.1 and Supporting materials Table 4.4). The majority of documented events (87%) were downward black swans and involved a combination of multiple factors. For example, a synchronization of environmental- and predation-mediated population cycles are thought to have caused a downward black-swan event for a water vole (*Arvicola terrestris*) population (Saucy 1994). Other black swans were the result of a sequence of extreme climate events on their own. For instance, severe winters in 1929, 1940–1942, and 1962–1963 were associated with black-swan downswings in grey heron (*Ardea cinerea*) abundance in the United Kingdom (Stafford 1971). Our analysis finds that the last event was a combination of two black-swan events in a row and it took the population three times longer to recover than predicted (Stafford 1971). Downwards black swans were sometimes followed by upwards black swans. For example, during a period of population crowding and nest shortages, a population of European shag cormorants (*Phalacrocorax aristotelis*) on the Farne Islands, United Kingdom, declined suddenly following a red tide event in 1968 (Potts et al. 1980). This freed quality nest sites for first-time breeders, productivity rapidly increased, and the population experienced a rapid upswing in abundance (Potts et al. 1980).

## 4.5 Discussion

We found strong evidence for black swans (heavy-tailed process noise) in 3–5% of ecological time series. Black swans were usually (87%) downward events and were detected more frequently in longer time series and in populations with a smaller magnitude of process noise. Black swans were not associated with density dependence, population growth rate, or lifespan. In verified cases, black-swan events were often a result of the combination of extreme

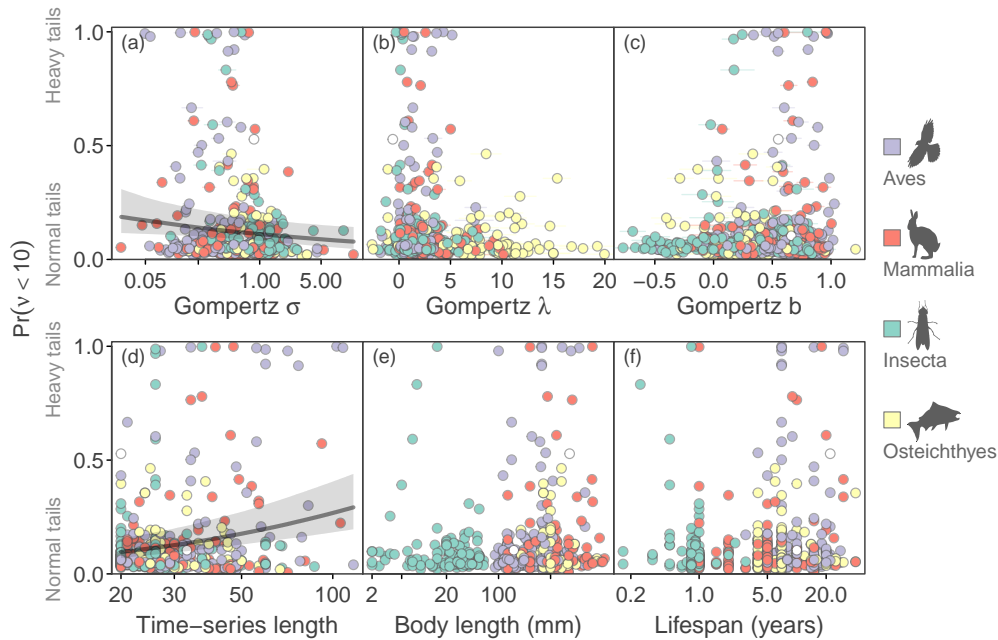



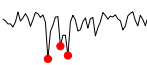


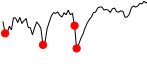


Figure 4.4: Potential covariates of heavy-tailed population dynamics (indicated by a high probability that  $v < 10$ ). Shown are (a–c) parameters from the Gompertz heavy-tailed population model ( $\sigma$ ,  $\lambda$ ,  $b$ ), (b) number of time steps, (c) body length, and (d) lifespan. For the Gompertz parameters,  $\sigma$  refers to the scale parameter of the Student-t process-noise distribution,  $\lambda$  refers to the expected log abundance at the next time step at an abundance of one,  $b$  refers to the density dependence parameter (1 is maximally density independent, 0 is maximally density dependent, and  $< 0$  is inversely density dependent). Circles representing a few sharks, crustaceans, and gastropods are filled in white. Median and 90% credible interval posterior predictions of a beta regression multilevel model are shown in panels a and d where there was a high probability the slope coefficient was different from zero (Fig. 4.3b).

Table 4.1: Example population dynamic black swans from the Global Population Dynamics Database and a description of their causes. Red and blue dots indicate downward and upward events that have a  $10^{-4}$  probability or less of occurring if the population dynamics were explained by a Gompertz model with normally distributed process noise. These populations are a sample from the heavy-tailed populations we could verify (Table 4.4).

Time series (log scale)	Population	Black swan description	Reference
	Shag, <i>Phalacrocorax aristotelis</i> , UK	Shortage of nest sites reduced productivity; red-tide event in 1968 caused extreme mortality; no longer a nest shortage; population rapidly increased	Potts et al. 1980
	Water vole, <i>Arvicola terrestris</i> , UK	Short-term population cycles from predator interactions combined with long-term environmental cycle caused sharp downswing	Saucy 1994
	Fur seal, <i>Arctocephalus pusillus</i> , South Africa	Strong decreases in harvesting, loss of predators, and diamond mining regulations reducing human traffic caused sharp upswings	Shaughnessy 1982
	Willow grouse, <i>Lagopus lagopus</i> , UK	Parasite and predation effects interacted to cause low years	Dobson and Hudson 1995
	Red grouse, <i>Lagopus lagopus scoticus</i> , UK	Good environmental conditions produced high numbers and vulnerable populations; bad conditions and overcrowding combined to create crashes	Mackenzie 1952
	Wren, <i>Troglodytes troglodytes</i> , UK	Severe winters where food was buried under snow caused population crash	Newton et al. 1998
	Grey heron, <i>Ardea cinerea</i> , UK	Severe winters in 1929, 1940–1942, and 1962–1963; 1963 event so severe that recovery took three times longer than expected	Stafford 1971

climate, predators and parasite cycles, and strong changes in human pressures. Our empirical results, sensitivity analyses, and simulation tests suggest that estimating the tail shape of process noise is a viable method of detecting black-swan population dynamics and if anything will underestimate the probability of black-swan events. The presence of black swans highlights the importance of developing management strategies that detect quickly, respond to, and are robust to extremes in population dynamics—particularly as the frequency and magnitude of climatic extremes increase over the next century (Easterling et al. 2000; IPCC 2012).

Our results clarify previous related analyses. An analysis with an older version of the GPDD assessed the distribution of abundance time series but focused on identifying if the log-normal distribution was the most frequently parsimonious model (Halley and Inchausti 2002). For heavy-tailed distributions, Halley and Inchausti (2002) fit the extremely heavy-tailed Cauchy distribution and the four-parameter Levy stable distribution and found little information criteria support for these distributions in longer time series. However, black-swan events are by definition rare, and the majority of time series in the GPDD are short for these purposes. Therefore, we would not expect to observe black swans in a large proportion of populations. By quantifying the probability of heavy-tails and allowing for non-stationary time series and density dependence, our analysis allows for a more nuanced description of the evidence of ecological black swans. In an earlier study, Keitt and Stanley (1998) described heavy (power law) tails in breeding bird population abundance. However, this finding was challenged by Allen et al. (2001), who showed that mixing data across species could falsely generate heavy tails.

We might expect to observe black-swan dynamics in ecological time series because of unmodelled intrinsic properties of populations or extrinsic forces acting on populations. Since a t-distribution can be formed by a mixture of normal distributions (with the same mean and inverse-gamma-distributed variances, Gelman et al. 2014), we could observe heavy tails if we miss some underlying mixture of intrinsic processes (Allen et al. 2001). That process might be an aggregation of populations across space, or population diversity, or an intrinsic change in population variability through time. Extrinsic forces could also cause black-swan dynamics (e.g. Nuñez and Logares 2012). These forces could be extreme themselves. For example, extreme climate, predation from (or competition with) other species experiencing black swans, or sharp changes in human pressure such hunting, fishing, or habitat destruction might cause black swans. Alternatively, the synchrony of multiple “normal” extrinsic forces could give rise to black-swan ecological dynamics. This could occur with a synergistic interaction (e.g. Kirby



et al. 2009) or even if non-synergistic forces experience a rare alignment (Denny et al. 2009).

There are a number of caveats when considering the generality of our results. The GPDD data represent a taxonomically and geographically biased sample of populations—the longer time series we focus on are dominated by commercially and recreationally important species and a disproportionate number of populations are located in the United Kingdom. Although we would expect to find qualitatively similar evidence for black swans in many other large taxonomic or geographic samples of populations, the common forces driving those black swans would likely differ (e.g. severe winters in Table 4.1). In addition to a possibly biased sample of populations, some black-swan detections could just be recording mistakes, or conversely, some extreme observations may have been discarded or altered if they were erroneously suspected of being recording mistakes. Indeed, we discarded three of the populations that our method initially identified as heavy tailed because they turned out to be data-entry errors (Supporting materials). A final caveat is that the temporal scales of observation and population dynamics vary considerably across populations in the GPDD and this likely influences the detection of heavy tails. As an example, if we make frequent observations relative to generation time (e.g. for many large-bodied mammals) we will average across generations and perhaps miss black swans. Conversely, if we census populations infrequently relative to generation time (e.g. many insects in the GPDD) the recorded data may average across extreme and less-extreme events and also dampen black-swan dynamics.

Recognizing the prevalence of heavy-tailed dynamics suggests a number of policy directions. Ecological resource management can draw from other disciplines that focus on heavy tails. For example, earthquake preparedness and response is focussed on black-swan events. Similarly to ecological black swans, we can rarely predict the specific location and timing of large earthquakes. But, earthquake preparedness involves spatial planning based on forecast probabilities to focus early detection efforts and develop disaster response plans. A similar focus might benefit resource management once our ability to predict the spatial probability and covariates of ecological black swans improves. The presence of black swans also suggests that we develop management policy that is robust to heavy tails. For instance, setting target population abundances that are appropriately set back from critical limits may buffer black-swan events (e.g. Caddy and McGarvey 1996), and maintaining genetic, phenotypic, and behavioural diversity may allow some components of populations to persist when others are affected by disease or extreme environmental forces (e.g. Hilborn et al. 2003; Schindler et al. 2010; Anderson et al. 2014). Finally, extreme and unexpected, surprising, or counterintuitive ecological

dynamics offer a tremendous opportunity to learn about ecological systems, evaluate when our models break down, and adjust future management policy (Doak et al. 2008; Pine III et al. 2009; Lindenmayer et al. 2010).

Our results suggest a number of research questions related to ecological black swans. Given that black swans do occur, can we forecast the probability of black swans in space and time? Furthermore, what management policies allow us to detect them quickly after they happen? Can we isolate the components of ecological dynamics that experience black swans by moving from phenomenological models such as the Gompertz to mechanistic models that, for example, take into account recruitment dynamics? We expect that greater insight into the mechanisms and covariates of ecological black swans may be best obtained through specific geographic and taxonomic subsets of data where longer time series with low levels of observation error are available (e.g. Segura et al. 2013).

Most importantly, what is the impact of allowing for black swans in forecasts of ecological risk? Even extremely rare catastrophes can have a profound influence on population persistence (Mangel and Tier 1994). In recent decades, ecology has moved toward focussing on aspects of variance in addition to mean responses (e.g. Loreau 2010; Thompson et al. 2013). Our results suggest that an added focus on ecological extremes represents the next frontier, particularly in the face of increased climate extremes (Meehl and Tebaldi 2004; IPCC 2012; Thompson et al. 2013). Financial analysts are concerned with the shape of the downward tails of financial returns because these directly impact estimates of risk—the probability of a specific magnitude of undesired event occurring (Rachev et al. 2008). A comparable focus in ecology would increase our estimates of extinction risk, since these would be disproportionately impacted by downward black-swan events.

## 4.6 Acknowledgements

We thank J.W. Moore, J.D. Yeakel, and other members of the Earth to Ocean research group for helpful discussions and comments. We are grateful to the contributors and maintainers of the Global Population Dynamics Database and to Compute Canada's WestGrid high-performance computing resources. Silhouette images were obtained from [phylopic.org](http://phylopic.org) under Creative Commons licenses; sources are listed in the Supporting materials. Funding was provided by a Simon Fraser University Graduate Fellowship (SCA), the Natural Sciences and Engineering Research Council of Canada (NKD, ABC), the Canada Research Chairs Program (NKD).

## 4.7 Supporting materials

### 4.7.1 Data selection

We applied the following data selection and quality-control rules to the Global Population Dynamics Database (GPDD):

1. To remove populations with unreliable population indices that could be strongly confounded with economics and sampling effort, we removed all populations with a sampling protocol listed as harvest as well populations with the words harvest or fur in the cited reference title.
2. We removed all populations with uneven sampling intervals, i.e. we removed populations that did not have a constant difference between the “decimal year begin” and “decimal year end” columns.
3. We removed all populations rated as  $< 2$  in the GPDD quality assessment (on a scale of 1 to 5, with 1 being the lowest quality data) (following Sibly et al. 2005; Ziebarth et al. 2010).
4. Populations with negative abundance values were removed. Of the populations that remained at the end of our other filtering rules, the remaining populations with negative abundances listed were all from time series that had been standardized by subtracting the mean and dividing by the standard deviation. We verified this by locating the original papers the datasets were extracted from: Colebrook (1978) for zooplankton and Lindström et al. (1995) for grouse. Since the papers did not include the original mean time-series values we could not back transform these data points.
5. We filled in all missing time steps with NA values and imputed single missing values with the geometric mean of the previous and following values. We chose a geometric mean to be linear on the log scale that the Gompertz and Ricker-logistic models were fit on.
6. We filled in single recorded values of zero with the lowest non-zero value in the time series (following Brook et al. 2006). This assumes that single values of zero result from abundance being low enough that censusing overlooked individuals that were actually present. We turned multiple zero values in a row into NA values. This implies that multiple zero values were either censusing errors or caused by emigration. Regardless, our

population models were fit on a multiplicative (log) scale and so could not account for zero abundance. To avoid distorting the original data too strongly, we removed populations in which we filled in more than four zeros.

7. We removed all populations without at least four unique values (following Brook et al. 2006).
8. We removed all populations with four or more identical values in a row since these suggest either recording error or extrapolation between two observations.
9. We then wrote an algorithm to find the longest unbroken window of abundance (no NAs) with at least 20 time steps in each population time series. If there were any populations with multiple windows of identical length, we took the most recent window. This is a longer window than used in some previous analyses (e.g. Brook et al. 2006), but since our model attempts to capture the shape of the distribution tails, our model requires more data.
10. We removed GPDD Main IDs 20531 and 10139, which we noticed were duplicates of 20579 (a heron population). 20579 contained additional years of data not present in 10139. We removed a limited number of populations from class Angiospermopsida and Bacillariophyceae to focus the taxonomy in our analysis on animals. We also removed any populations with an Unknown taxonomic class.
11. Finally, we removed populations with the following GPDD Main IDs, which we discovered were data entry errors when verifying the populations with suspected black swans: 1207 because the 1957 data point was entered as 2 but should have been 27 (Kendeigh 1982), 6531 because the 1978 data point was entered as 7 but should have been 47 (Minot and Perrins 1986), and 6566 because some of the data did not match the graph (Heessen 1996).

We provide a supplemental figure of all the time series included in our analysis and indicate which values were interpolated (non-zero interpolations) (17% of populations had at least one point interpolated but only 0.7% of the total observations were interpolated) (Fig. 4.5). Note that interpolation is highly unlikely to lead to black-swan detections, since black swans involve extreme increases or decreases. Table 4.3 shows the final taxonomic breakdown and the number of populations with interpolated values.

### 4.7.2 Details on the heavy-tailed Gompertz probability model

For the Gompertz model, our weakly-informative priors (Fig. 4.6) were:

$$\begin{aligned} b &\sim \text{Uniform}(-1, 2) \\ \lambda &\sim \text{Normal}(0, 10^2) \\ \sigma &\sim \text{Half-Cauchy}(0, 2.5) \\ \nu &\sim \text{Truncated-Exponential}(0.01, \text{min.} = 2). \end{aligned}$$

Our prior on  $b$  was uninformative between values of  $-1$  and  $2$ . We would not expect values of  $b$  with levels of density dependence as low as  $-1$  (very strong inverse density dependence), nor would we generally expect values above  $1$ . We allowed values of  $b$  above  $1$  to allow for non-stationary time series of growth rates. The estimates of  $b$  were well within these bounds. Our prior on  $\lambda$  was very weakly informative within the range of expected values for population growth and is similar to the default priors suggested by Gelman et al. (2008) for intercepts of regression models. Our Half-Cauchy prior on  $\sigma$  follows Gelman (2006) and Gelman et al. (2008) and the specific scale parameter of  $2.5$  is based on our expected range of the value in nature from previous studies (e.g. Connors et al. 2014). In our testing of a subsample of populations, our parameter estimates were not qualitatively changed by switching to an uninformative uniform prior on  $\sigma$ , but the weakly informative Half-Cauchy prior substantially sped up chain convergence.

Our prior on  $\nu$  was based on Fernandez and Steel (1998). They chose an exponential rate parameter of  $0.1$ . We chose a less informative rate parameter of  $0.01$  and truncated the distribution at  $2$ , since at  $\nu < 2$  the variance of the  $t$  distribution is undefined. This prior gives only a  $7.7\%$  probability that  $\nu < 10$  but constrains the sampling sufficiently to avoid wandering off towards infinity—above approximately  $\nu = 20$  the  $t$  distribution is so similar to the normal distribution (Fig. 4.1) that time series of the length considered here are unlikely to be informative about the precise value of  $\nu$ . In the scenario where the data are uninformative about heavy tails (e.g. Fig. 4.1e, h), the posterior will approximately match the prior (prior median =  $71$ , mean =  $102$ ) and the metrics used in our paper (e.g.  $\Pr(\nu < 10) > 0.5$ ) are unlikely to flag the population as heavy tailed.

We fit our models with Stan 2.4.0 (Stan Development Team 2014), and R 3.1.1 (R Core Team 2014). We began with four chains and 2000 iterations, discarding the first 1000 as warm up (i.e. 4000 total samples). If  $\hat{R}$  (the potential scale reduction factor—a measure of chain convergence) was greater than  $1.05$  for any parameter or the minimum effective sample size,  $n_{\text{eff}}$ , (a

measure of the effective number of uncorrelated samples) for any parameter was less than 200, we doubled both the total iterations and warm up period and sampled from the model again. These thresholds are in excess of the minimums recommended by Gelman and Hill (2006) of  $\hat{R} < 1.1$  and effective sample size  $> 100$  for reliable point estimates and confidence intervals. In the majority of cases our minimum thresholds were greatly exceeded. We continued this procedure up to 8000 iterations (16000 total samples) by which all chains were deemed to have sufficiently converged. These chain lengths may seem low to those familiar with software such as WinBUGS or JAGS, but the No-U-Turn Hamiltonian Markov chain Monte Carlo Sampler in Stan generally requires far fewer iterations to obtain equivalent effective sample sizes (Stan Development Team 2014).

### 4.7.3 Alternative priors

To test if the prior on  $\nu$  influenced our estimate of black-swan dynamics, we refit our models with weaker and stronger priors. Our base model used a prior on  $\nu$  of Truncated-Exponential(0.02, min. = 2). For a weaker prior we used Truncated-Exponential(0.005, min. = 2) and for a stronger prior we used Truncated-Exponential(0.02, min. = 2) (Fig. 4.6). Note that the base and weaker priors are relatively flat within the region of  $\nu < 20$ , which is the region we are mostly concerned about when categorizing populations as heavy- or thin-tailed.

Our results show that these weaker and stronger priors would have little influence on our conclusions about heavy-tailed dynamics (Fig. 4.8). When the data are informative about tail behaviour (i.e. when there is strong evidence of low  $\nu$  values, upper-right of Fig. 4.8), the prior has little impact on the estimate of  $\nu$ . When the data are less informative about  $\nu$  (i.e. when there are no or few tail events and time series are short or noisy), the prior can pull the estimate of  $\nu$  towards larger or smaller values (Fig. 4.8). The vast majority of the populations with  $\Pr(\nu < 10)$  in the base prior were not altered qualitatively by this range of prior strength.

### 4.7.4 Alternative population models

We fit four alternative population models to the time-series data to check how they would influence our conclusions. Our alternative models allowed for autocorrelation in the residuals, assumed no density dependence, allowed for observation error, or assumed a Ricker-logistic functional form. The range of percentages of black swans by taxonomic class cited in the abstract and results are based on lower and upper limits across our main Gompertz model and these four alternative models.

### Autocorrelated residuals

We considered a version of the Gompertz model in which an autoregressive parameter was fit to the process noise residuals:

$$x_t = \lambda + bx_{t-1} + \epsilon_t$$

$$\epsilon_t \sim \text{Student-t}(\nu, \phi\epsilon_{t-1}, \sigma).$$

In addition to the parameters in the original Gompertz model, this model estimates an additional parameter  $\phi$ , which represents the correlation of subsequent residuals. Based on the results of previous analyses with the GPDD (e.g. Connors et al. 2014) and the chosen priors in previous analyses (e.g. Thorson et al. 2014a) and to greatly speed up chain convergence when running our model across all populations, we placed a weakly informative prior on  $\phi$  that assumed the greatest probability density near zero with the reduced possibility of  $\phi$  being near  $-1$  or  $1$ . Specifically, we chose  $\phi \sim \text{Truncated-Normal}(0, 1, \text{min.} = -1, \text{max.} = 1)$ . The MCMC chains did not converge for 75 populations according to our criteria ( $\widehat{R} < 1.05, n_{\text{eff}} > 200$ ) after 8000 iterations of four chains. This included only 1 populations in which  $\text{Pr}(\nu < 10) > 0.5$  categorized them as heavy in the main Gompertz model. We did not include these models in Fig. 4.7.

### Assumed density independence

We fit a simplified version of the Gompertz model in which the density dependence parameter  $b$  was fixed at 1 (density independent). This is equivalent to fitting a random walk model (with drift) to the log abundances or assuming the growth rates are drawn from a stationary distribution. The model was as follows:

$$x_t = \lambda + x_{t-1} + \epsilon_t$$

$$\epsilon \sim \text{Student-t}(\nu, 0, \sigma).$$

We fit this model for three reasons: (1) it is computationally simpler and so provides a check that our more complicated full Gompertz model was obtaining reasonable estimates of  $\nu$ , (2) it provides a test of whether density dependence was systematically affecting our perception of heavy tails, (3) it matches how some previous authors have modelled heavy tails without accounting for density dependence (Segura et al. 2013).

### Assumed observation error

Observation error can bias parameter estimates (e.g. Knappe and de Valpine 2012) and is known to affect the ability to detect extreme events (Ward et al. 2007). In our main analysis, we fit a model that ignored observation error. One way to account for observation error would be to fit a full state-space model that simultaneously estimates the magnitude of process noise and observation error. However, simultaneously estimating observation and process noise is a challenging problem (e.g. because the observation and process noise parameters tend to negatively covary in model fitting) and is known to sometimes result in identifiability issues with the Gompertz population model (Knappe 2008). Furthermore, our model was applied to hundreds of time series, often of short length (as few as 20 time steps) and our model estimates an additional parameter—the shape of the process deviation tails—potentially making identifiability and computational issues even greater. Therefore, we considered a version of the base Gompertz model that allowed for a fixed level of observation error:

$$\begin{aligned} U_t &= \lambda + bU_{t-1} + \epsilon_t \\ x_t &\sim \text{Normal}(U_t, \sigma_{\text{obs}}^2) \\ \epsilon_t &\sim \text{Student-t}(\nu, 0, \sigma_{\text{proc}}), \end{aligned}$$

where  $U$  represents the unobserved state vector,  $\sigma_{\text{obs}}$  represents the standard deviation of observation error (on a log scale), and  $\sigma_{\text{proc}}$  represent the process noise scale parameter. We set  $\sigma_{\text{obs}}$  to 0.2, which represents the upper limit of values often used in simulation analyses (e.g. de Valpine and Hastings 2002; Thorson et al. 2014b).

### Ricker-logistic

We also fit a Ricker-logistic model:

$$\begin{aligned} x_t &= x_{t-1} + r_{\text{max}} \left( 1 - \frac{N_{t-1}}{K} \right) + \epsilon_t \\ \epsilon_t &\sim \text{Student-t}(\nu, 0, \sigma), \end{aligned}$$

where  $r_{\text{max}}$  represents the theoretical maximum population growth rate that is obtained when  $N_t$  (abundance at time  $t$ ) = 0. The parameter  $K$  represents the carrying capacity and, as before,  $x_t$  represents the log transformed abundance at time  $t$ . The Ricker-logistic model assumes a linear decrease in population growth rate with increases in abundance. In contrast, the Gompertz model assumes a linear decrease in population growth rate with increases in *log* abundance ( $x_t$ ) (e.g. Thibaut et al. 2012).



To fit the Ricker-logistic models, we chose a prior on  $K$  uniform between zero and twice the maximum observed abundance (Clark et al. (2010) chose uniform between zero and maximum observed, which is more informative). We set the prior on  $r_{\max}$  as uniform between 0 and 20 as in Clark et al. (2010). We used the same priors on  $\nu$  and  $\sigma$  as in the Gompertz model.

#### 4.7.5 Simulation testing the model

We performed two types of simulation testing. First, we tested how easily the Student-t distribution  $\nu$  parameter could be recovered given different true values of  $\nu$  and different sample sizes. Second, we tested the ability of the heavy-tailed Gompertz model to obtain unbiased parameter estimates of  $\nu$  given that a set of process deviations was provided in which the effective  $\nu$  value was close to the true  $\nu$  value.

We separated our simulation into these two components to avoid confounding two issues. (1) With smaller sample sizes, there may not be a stochastic draw from the tails of a distribution. In that case, no model, no matter how perfect, will be able to detect the shape of the tails. (2) Complex models may return biased parameter estimates if there are conceptual, computational, or coding errors. Our first simulation tested the first issue and our second simulation tested the latter. In general, our simulations show that, if anything, our model under predicts the magnitude and probability of heavy tailed events—especially given the length of the time series in the GPDD.

#### Estimating $\nu$ from a stationary t distribution

First, we tested the ability to estimate  $\nu$  given different true values of  $\nu$  and different sample sizes. We took stochastic draws from t distributions with different  $\nu$  values ( $\nu = 3, 5, 10$ , and  $10^6$  [ $\approx$  normal]), with central tendency parameters of 0, and scale parameters of 1. We started with 1600 stochastic draws and then fit the models again at the first 800, 400, 200, 100, 50, and 25 draws. Each time we recorded the posterior samples of  $\nu$ .

We found that we could consistently and precisely recover median posterior estimates of  $\nu$  near the true value of  $\nu$  with large samples ( $\geq 200$ ) (Fig. 4.9 upper panels). At smaller samples we could still usually qualitatively distinguish heavy from not-heavy tails, but the model tended to underestimate how heavy the tails were. At the same time, at smaller sample sizes, the model tended to overestimate how large the scale parameter was (Fig. 4.9 lower panels).

### Heavy-tailed Gompertz model simulations

In the second part of our simulation testing, we tested the ability of the heavy-tailed Gompertz model to obtain unbiased parameter estimates when the process noise was chosen so that appropriate tail events were present. To generate these process deviations for the  $\nu = 3$  and  $\nu = 5$  scenarios, we repeatedly drew proposed candidate process deviations and estimated the central tendency, scale, and  $\nu$  values each time. We recorded when  $\hat{\nu}$  (median of the posterior) was within 0.2 CVs (coefficient of variations) of the true  $\nu$  value and used this set of random seed values in our Gompertz simulation. The following simplified R code illustrates this procedure (the actual code is available at <https://github.com/seananderson/heavy-tails>):

```
get_effective_nu_seeds <- function(nu_true = 5, cv = 0.2, N = 50, seed_N = 20) {
  # nu_true: The true nu value
  # cv:      The permitted effective nu coefficient of variation
  # N:       The length of time series
  # seed_N:  The number of seed values to generate
  seeds <- numeric(length = seed_N)
  seed_value <- 0
  for (i in seq_len(seed_N)) {
    nu_close <- FALSE
    while (!nu_close) {
      seed_value <- seed_value + 1
      set.seed(i)
      y <- rt(N, df = nu_true)
      sm <- rstan::stan(... # fit the Stan model here
      med_nu_hat <- median(rstan::extract(sm, pars = "nu")[[1]])
      if (med_nu_hat > (nu_true - cv) & med_nu_hat < (nu_true + cv)) {
        nu_close <- TRUE
        seeds[i] <- seed_value
      }
    }
  }
  seeds
}
```

```
nu_3_seeds_N50 <- get_effective_nu_seeds(nu_true = 3)
nu_5_seeds_N50 <- get_effective_nu_seeds(nu_true = 5)
```

We then fit our Gompertz models to the simulated datasets with all parameters (except  $\nu$ ) set near the median values estimated in the GPDD. We repeated this with 50 and 100 samples without observation error, 50 samples with observation error ( $\sigma_{\text{obs}} = 0.2$ ), and 50 samples

with the same observation error and a Gompertz model that allowed for correctly specified observation error magnitude. Our results indicate that the Gompertz model can recapture the true value of  $\nu$  when the process noise was chosen so that appropriate tail events were present (Fig. 4.10 upper panels). The addition of observation error caused the model to tend to underestimate the degree of heavy-tailedness. Fitting a model with correctly specified observation error did not make substantial improvements to model bias (Fig. 4.10).

When converting the posterior distributions of  $\nu$  into  $\Pr(\nu < 10)$ , the models distinguished heavy and not-heavy tails reasonably well (Fig. 4.10 lower panels). Without observation error, and using a probability of 0.5 as a threshold, the model correctly classified all simulated systems with normally distributed process noise as not heavy tailed. The model would have miscategorized only one of 40 simulations at  $\nu = 5$  across simulated populations with 50 or 100 time steps (Fig. 4.10, scenarios 1 and 2 in lower row, second panel from left). The model would have correctly categorized all cases where the process noise was not heavy tailed (Fig. 4.10 bottom-right panel) and all cases where  $\nu = 3$  and there was not observation error. With 0.2 standard deviations of observation error, the model still categorized 65% of cases as heavy tailed when  $\nu = 5$  and all but one case when  $\nu = 3$ . Allowing for observation error made little improvement to the detection of heavy tails. Therefore, we chose to focus on the simpler model without observation error in the main text, particularly given that the true magnitude of observation error was unknown in the empirical data.

#### 4.7.6 Modelling covariates of heavy-tailed dynamics

We fit a multilevel beta regression model to the predicted probability of heavy tails,  $\Pr(\nu < 10)$ , to investigate potential covariates of heavy-tailed dynamics. The beta distribution is useful when response data range on a continuous scale between zero and one (Ferrari and Cribari-Neto 2004). We used a logit link function as is typically used in logistic regression. The model was as follows:

$$\begin{aligned}
\Pr(v_i < 10) &\sim \text{Beta}(A_i, B_i) \\
\mu_i &= \text{logit}^{-1}(\alpha + \alpha_{j[i]}^{\text{class}} + \alpha_{k[i]}^{\text{order}} + \alpha_{l[i]}^{\text{species}} + X_i\beta), \text{ for } i = 1, \dots, 617 \\
A_i &= \phi_{\text{disp}}\mu_i \\
B_i &= \phi_{\text{disp}}(1 - \mu_i) \\
\alpha_j^{\text{class}} &\sim \text{Normal}(0, \sigma_{\alpha}^2_{\text{class}}), \text{ for } j = 1, \dots, 6 \\
\alpha_k^{\text{order}} &\sim \text{Normal}(0, \sigma_{\alpha}^2_{\text{order}}), \text{ for } k = 1, \dots, 38 \\
\alpha_l^{\text{species}} &\sim \text{Normal}(0, \sigma_{\alpha}^2_{\text{species}}), \text{ for } l = 1, \dots, 301,
\end{aligned}$$

where  $A$  and  $B$  represent the beta distribution shape parameters;  $\mu_i$  represents the predicted value for population  $i$ , class  $j$ , order  $k$ , and species  $l$ ;  $\phi_{\text{disp}}$  represents the dispersion parameter; and  $X_i$  represents a vector of predictors (such as lifespan) for population  $i$  with associated  $\beta$  coefficients. The intercepts are allowed to vary from the overall intercept  $\alpha$  by taxonomic class ( $\alpha_j^{\text{class}}$ ), taxonomic order ( $\alpha_k^{\text{order}}$ ), and species ( $\alpha_l^{\text{species}}$ ) with standard deviations  $\sigma_{\alpha \text{ class}}$ ,  $\sigma_{\alpha \text{ order}}$ , and  $\sigma_{\alpha \text{ species}}$ . Where possible, we also allowed for error distributions around the predictors by incorporating the standard deviation of the posterior samples for the Gompertz parameters  $\lambda$ ,  $b$ , and  $\log \sigma$  around the mean point value as normal distributions (not shown in the above equation).

We log transformed  $\sigma$ , time-series length, and lifespan to match the way they are visually represented in Fig. 4.4 and to make the relationship approximately linear on the logit-transformed response scale. All input variables were standardized by subtracting their mean and dividing by two standard deviations to make their coefficients comparable in magnitude (Gelman 2008). We excluded body length as a covariate because it was highly correlated with lifespan, and lifespan exhibited more overlap across taxonomy than body length. Lifespan is also more directly related to time and potential mechanisms driving black-swan dynamics.

We incorporated weakly informative priors into our model: Cauchy(0, 10) on the global intercept  $\alpha$ , Half-Cauchy(0, 2.5) on all standard deviation parameters, Half-Cauchy(0, 10) on the dispersion parameter  $\phi_{\text{disp}}$ , and Cauchy(0, 2.5) on all other parameters (Gelman 2006; Gelman et al. 2008). Compared to normal priors, the Cauchy priors concentrate more probability density around expected parameter values while allowing for a higher probability density far into the tails, thereby allowing the data to dominate the posterior more strongly if it disagrees with the prior. Our conclusions were not qualitatively changed by using uniform priors. We fit our models with 5000 total iterations per chain, 2500 warm-up iterations, four chains, and

discarding every second sample to save memory. We checked for chain convergence visually and with the same criteria as before ( $\widehat{R} < 1.05$  and  $n_{\text{eff}} > 200$  for all parameters).

To derive taxonomic-order-level estimates of the probability of heavy tails accounting for time-series length (Fig. 4.3a), we fit a separate multilevel model with the same structure but with only log time-series length as a predictor. (In this case, we did not want to control for intrinsic population characteristics such as density dependence.) Since our predictors were centered by subtracting their mean value, we obtained order-level estimates of the probability of heavy tails at mean log time-series length by adding the posteriors for  $\alpha$ ,  $\alpha_j^{\text{class}}$ , and  $\alpha_k^{\text{order}}$ .

#### 4.7.7 Additional acknowledgements

Many of the silhouette images used in Figs 4.2, 4.4 and 4.3 were obtained from `phylopic.org` under Creative Commons licenses. We vectorized the salmon in Fig. 4.2 and Fig. 4.4 ourselves. The bird in these figures was obtained from `phylopic.org` under a Creative Commons Attribution 3.0 Unported license with credit to Jean-Raphael Guillaumin [photography] and T. Michael Keeseey [vectorization]. The silhouettes in Fig. 4.3 were obtained from the following sources (metadata obtained with the help of the `rphylopic` R package, <https://github.com/sckott/rphylopic>):

Taxonomic order	Credit	License URL
Salmoniformes	Servien (vectorized by T. Michael Keeseey)	<a href="http://creativecommons.org/licenses/by-sa/3.0/">http://creativecommons.org/licenses/by-sa/3.0/</a>
Gadiformes		<a href="http://creativecommons.org/publicdomain/mark/1.0/">http://creativecommons.org/publicdomain/mark/1.0/</a>
Perciformes	Ellen Edmonson and Hugh Chrisp (vectorized by T. Michael Keeseey)	<a href="http://creativecommons.org/publicdomain/mark/1.0/">http://creativecommons.org/publicdomain/mark/1.0/</a>
Pleuronectiformes	Tony Ayling (vectorized by T. Michael Keeseey)	<a href="http://creativecommons.org/licenses/by-sa/3.0/">http://creativecommons.org/licenses/by-sa/3.0/</a>
Lepidoptera	Curtis (modified by T. Michael Keeseey)	<a href="http://creativecommons.org/publicdomain/mark/1.0/">http://creativecommons.org/publicdomain/mark/1.0/</a>
Rodentia	Mattia Menchetti	<a href="http://creativecommons.org/publicdomain/zero/1.0/">http://creativecommons.org/publicdomain/zero/1.0/</a>
Carnivora	Brian Gratwicke (photo) and T. Michael Keeseey (vectorization)	<a href="http://creativecommons.org/licenses/by/3.0/">http://creativecommons.org/licenses/by/3.0/</a>
Lagomorpha	Sarah Werning	<a href="http://creativecommons.org/licenses/by/3.0/">http://creativecommons.org/licenses/by/3.0/</a>
Coleoptera	Crystal Maier	<a href="http://creativecommons.org/licenses/by/3.0/">http://creativecommons.org/licenses/by/3.0/</a>

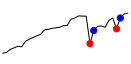

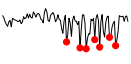

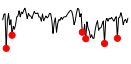

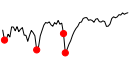

Odonata	Gareth Monger	<a href="http://creativecommons.org/licenses/by/3.0/">http://creativecommons.org/licenses/by/3.0/</a>
Passeriformes	Michael Scroggie	<a href="http://creativecommons.org/publicdomain/zero/1.0/">http://creativecommons.org/publicdomain/zero/1.0/</a>
Anseriformes	Sharon Wegner-Larsen	<a href="http://creativecommons.org/publicdomain/zero/1.0/">http://creativecommons.org/publicdomain/zero/1.0/</a>
Artiodactyla	Jan A. Venter, Herbert H. T. Prins, David A. Balfour and Rob Slotow (vectorized by T. Michael Keeseey)	<a href="http://creativecommons.org/licenses/by/3.0/">http://creativecommons.org/licenses/by/3.0/</a>
Diptera	Gareth Monger	<a href="http://creativecommons.org/licenses/by/3.0/">http://creativecommons.org/licenses/by/3.0/</a>
Charadriiformes	JJ Harrison (vectorized by T. Michael Keeseey)	<a href="http://creativecommons.org/licenses/by-sa/3.0/">http://creativecommons.org/licenses/by-sa/3.0/</a>
Hemiptera	T. Michael Keeseey	<a href="http://creativecommons.org/publicdomain/zero/1.0/">http://creativecommons.org/publicdomain/zero/1.0/</a>
Falconiformes	Liftarn	<a href="http://creativecommons.org/licenses/by-sa/3.0/">http://creativecommons.org/licenses/by-sa/3.0/</a>
Galliformes	Steven Traver	<a href="http://creativecommons.org/publicdomain/zero/1.0/">http://creativecommons.org/publicdomain/zero/1.0/</a>

---

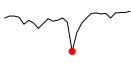
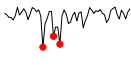

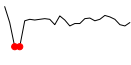



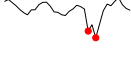

Table 4.3: Summary statistics for the filtered Global Population Dynamics Database time series arranged by taxonomic class. Columns are: number of populations, number of taxonomic orders, numbers of species, median time series length, total number of interpolated time steps, total number of substituted zeros, and total number of time steps.

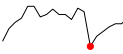




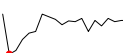
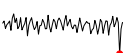

Taxonomic class	Populations	Orders	Species	Median length	Interpolated pts	Zeros pts	Total pts
Aves	191	15	112	27	68	32	6160
Insecta	182	7	91	25	26	55	4812
Mammalia	125	8	51	28	18	21	4027
Osteichthyes	108	6	35	26	13	3	3310
Chondrichthyes	1	1	1	20	1	0	20
Crustacea	1	1	1	33	0	0	33
Gastropoda	1	1	1	21	0	0	21

Table 4.4: All populations with  $\Pr(\nu < 10) > 0.5$  in the base heavy-tailed Gompertz population dynamics model. Shown are the log abundance time series, population descriptions, Global Population Dynamics Database Main IDs, citation for the data source or separate verification literature, a description of the cause of the black swan events (if known), the probability of heavy tails as calculated by our model, and median estimate of  $\nu$  from our model with 90% quantile credible intervals indicated in parentheses. Red dots on the time series indicate downward black-swan events and blue values indicate upward black-swan events that have a  $10^{-4}$  probability or less of occurring if the population dynamics were explained by a Gompertz model with normally distributed process noise with a standard deviation equal to the scale parameter in the fitted t distribution.

Time series	Population	ID	Citation	Description	$\Pr(\nu < 10)$	$\hat{\nu}$
	Shag, <i>Phalacrocorax aristotelis</i> , Farne Islands, Northumberland	6528	Potts et al. 1980	Red tide event combined with low productivity due to overcrowding	1.00	2 (2-4)
	South African fur seal, <i>Arctocephalus pusillus</i> , South Africa	7115	Shaughnessy 1982	Harvesting and predation changes	1.00	2 (2-4)
	Red grouse, <i>Lagopus lagopus scoticus</i> , Scotland - un-named area	10128	Potts et al. 1984	Environment- and parasite-caused cycles	1.00	3 (2-4)
	Pine looper or Bordered white, <i>Bupalus piniaria</i> , Kessock	9382	Broekhuizen et al. 1993	Unknown, but sampling intensity was decreasing	1.00	3 (2-5)
	Red grouse, <i>Lagopus lagopus scoticus</i> , Scotland - un-named area	10127	Potts et al. 1984	Environment- and parasite-caused cycles	0.99	3 (2-5)
	Water vole, <i>Arvicola terrestris</i> , Le Pont	10007	Saucy 1994	Predator-environment cycle interactions	1.00	3 (2-5)
	Grey heron, <i>Ardea cinerea</i> , Southern Britain	20579	Stafford 1971	Severe winter	0.98	3 (2-7)
	Flea beetle, <i>Chaetocnoma concinna</i> , Finland	9655	Markkula 1965	Cannot locate original source	0.99	3 (2-6)



	Wren, <i>Troglodytes troglodytes</i> , Eastern Wood, Bookham Common	1235	Newton et al. 1998	Severe winter	0.98	3 (2-8)
	Willow grouse, <i>Lagopus lagopus</i> , Northern England	10113	Dobson and Hudson 1995	Parasites and predators	0.99	3 (2-6)
	Gooseberry sawfly, <i>Nemastus ribesii</i> , Finland	9667	Markkula 1965	Cannot locate original source	0.97	3 (2-8)
	Unknown, <i>Trioza apicalis</i> , Finland	9679	Markkula 1965	Cannot locate original source	0.83	3 (2-88)
	Wandering albatross, <i>Diomedea exulans</i> , Taiaroa	20527	Robertson and Gales 1998	Unknown	0.99	4 (2-7)
	Red grouse, <i>Lagopus lagopus scoticus</i> , Northern Scotland	10039	Dobson and Hudson 1995	Parasites and predators	0.92	4 (2-12)
	Red grouse, <i>Lagopus lagopus scoticus</i> , Atholl Estate	10162	Mackenzie 1952	Bad environmental conditions and overcrowding combined to create crashes	0.91	5 (2-12)
	Fisher or Pekan, <i>Martes pennanti</i> , Manitoba	9503	Keith 1963	Unknown	0.76	5 (2-87)
	European rabbit, <i>Oryctolagus cuniculus</i> , Estate 2, East Anglia	7099	Barnes and Tapper 1986	Disease outbreak followed by years of good weather	0.78	5 (2-67)

	Wheat ear, <i>Oenanthe oenanthe</i> , Skokholm Island	2778	Lack 1969	Unknown, but decline noted specifically, cold winters caused some crashes	0.67	5 (2-141)
	Cabbage root fly or maggot, <i>Delia radicum</i> , Finland	9659	Markkula 1965	Cannot locate original source	0.59	7 (2-161)
	Blue jay, <i>Cyanocitta cristata</i> , Robert Allerton Park	1195	Kendeigh 1982	Unknown	0.60	7 (2-149)
	Barbary macaque, <i>Macaca sylvanus</i> , Queens Gate	5019	Fa 1984	Cannot locate original source	0.61	7 (2-132)
	Rock ptarmigan, <i>Lagopus mutus</i> , Iceland	9953	Clarke and Backhouse 1885; Williams 1954	Severe winters	0.58	7 (2-172)
	Lesser-spotted dogfish, <i>Scyliorhinus caniculus</i> , North Sea	6548	Heessen 1996	Unknown, not specifically mentioned	0.53	8 (2-190)
	American red fox, <i>Vulpes fulva</i> , Labrador	20546	D'Ancona 1954; Lindström et al. 1994	Predator-prey cycles	0.57	9 (3-65)
	Ruffed grouse, <i>Bonasa umbellus</i> , Connecticut	9470	Keith 1963	Unknown	0.53	9 (3-158)

---

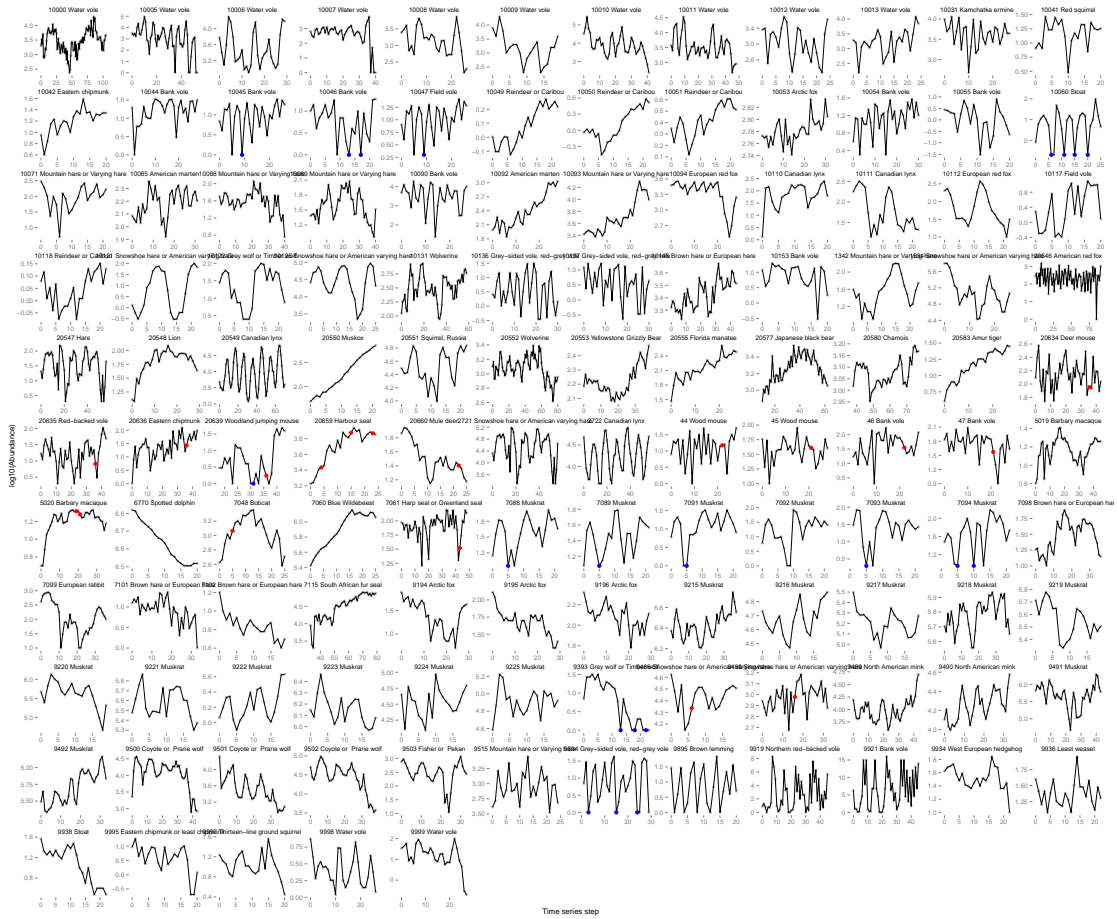


Figure 4.5 (mammals) continued on next page ...



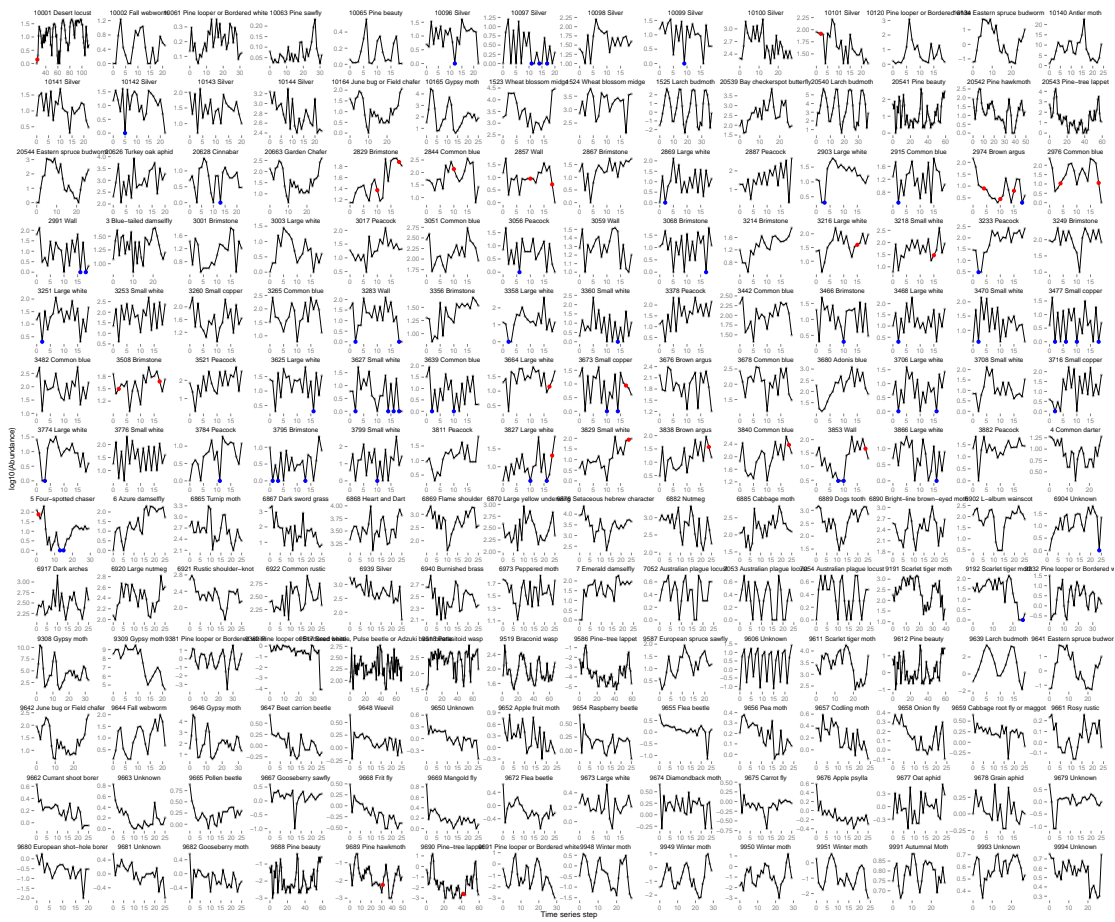


Figure 4.5 (insects) continued on next page ...

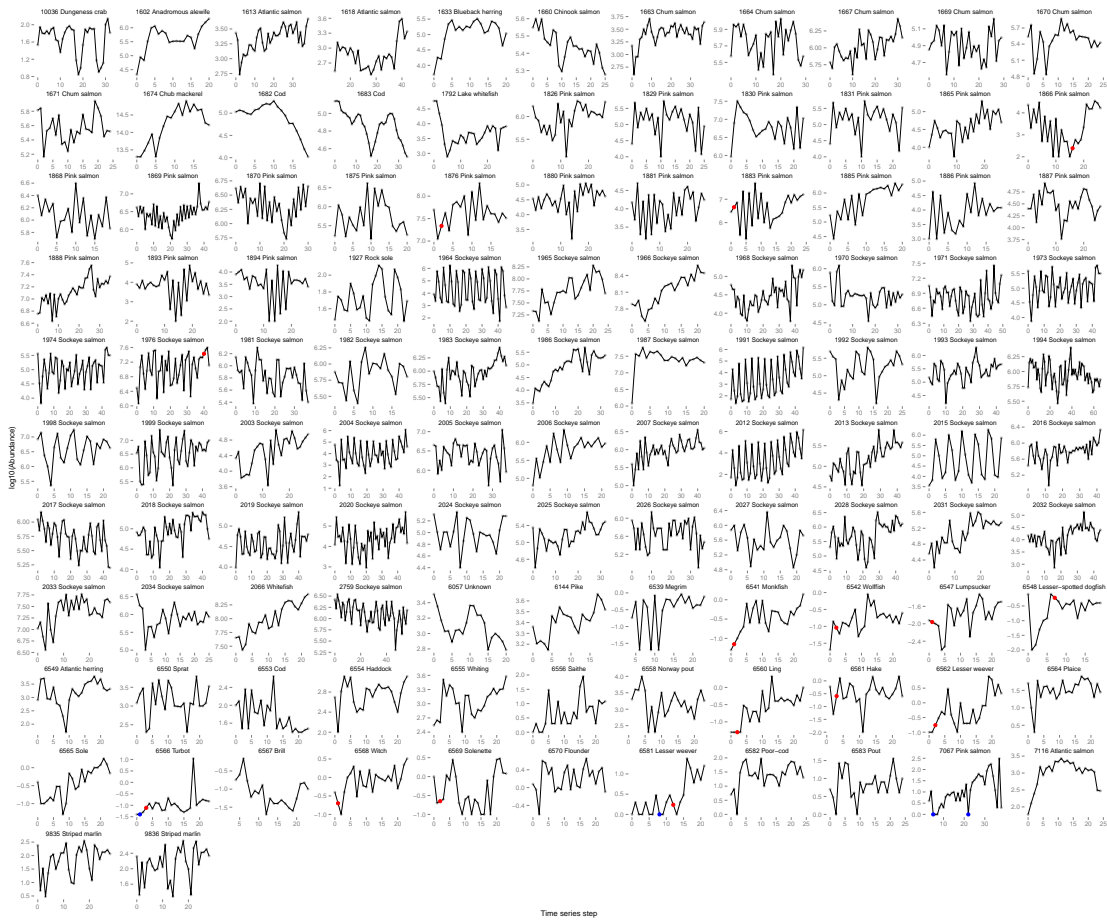


Figure 4.5: (fishes, crustaceans, gastropods, sharks). All filtered time series used in our analysis. The abundances are shown on a  $\log_{10}$  vertical axis. Throughout this figure, red dots indicate values that were interpolated and blue dots indicate values that were recorded as zero but were set to the next lowest observed abundance. Numbers before each species name are the GPDD Main ID numbers.

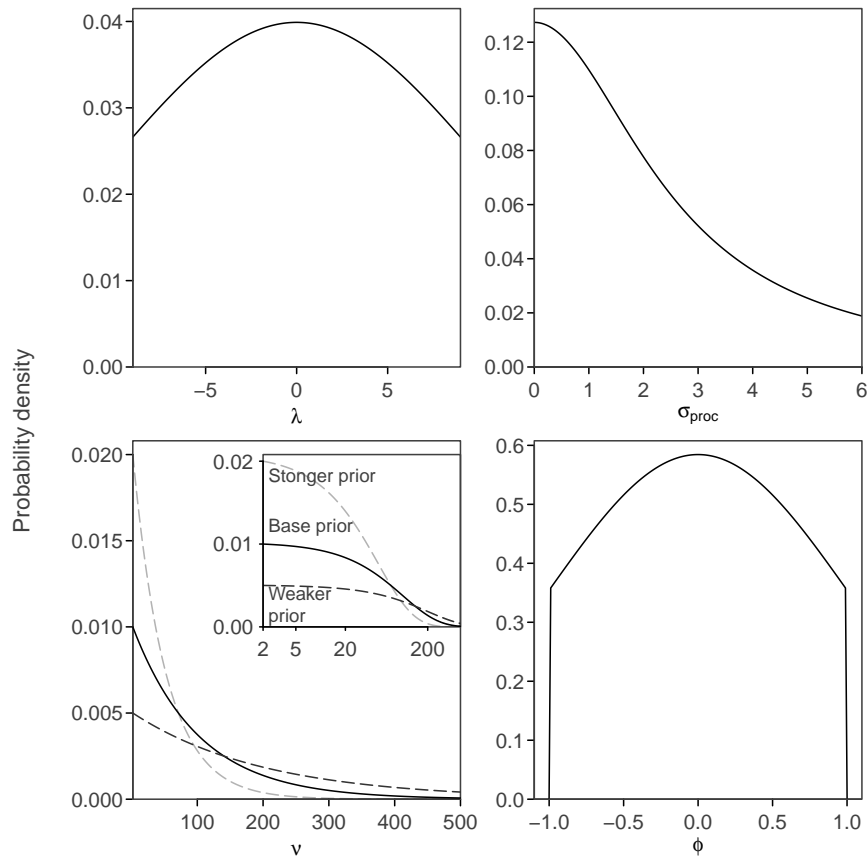


Figure 4.6: Probability density of the Bayesian priors for the Gompertz models. From left to right and then top to bottom: (1) per capita growth rate at  $\log(\text{abundance}) = 0$ :  $\lambda \sim \text{Normal}(0, 10^2)$ ; (2) scale parameter of t-distribution process noise:  $\sigma \sim \text{Half-Cauchy}(0, 2.5)$ ; (3) t-distribution degrees of freedom parameter:  $\nu \sim \text{Truncated-Exponential}(0.01, \text{min.} = 2)$ ; (4) AR1 correlation coefficient of residuals:  $\phi \sim \text{Truncated-Normal}(0, 1, \text{min.} = -1, \text{max.} = 1)$ . Not shown is  $b$ , the density dependence parameter:  $b \sim \text{Uniform}(-1, 2)$ . The  $\nu$  panel also shows two alternative priors: a weaker prior  $\nu \sim \text{Truncated-Exponential}(0.005, \text{min.} = 2)$ , and a stronger prior  $\nu \sim \text{Truncated-Exponential}(0.02, \text{min.} = 2)$ . The inset panel shows the same data but with a log-transformed x axis. Note that the base and weaker priors are relatively flat within the region of  $\nu < 20$  that we are concerned with.

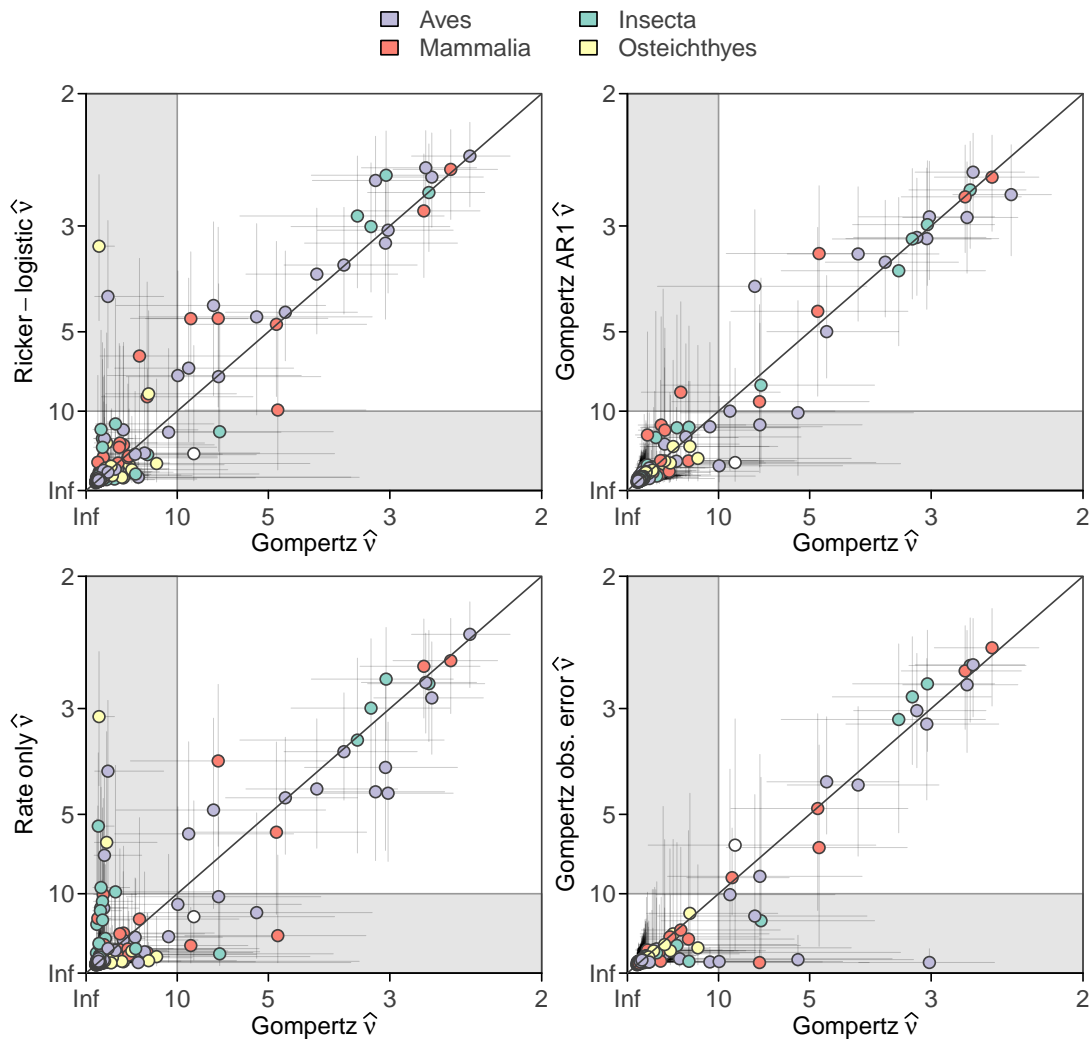


Figure 4.7: Estimates of  $\nu$  from alternative models plotted against the base Gompertz model estimates of  $\nu$ . Shown are medians of the posterior (dots) and 50% credible intervals (segments). The diagonal line indicates a one-to-one relationship. Different colours indicate various taxonomic classes. The grey-shaded regions indicate regions of disagreement if  $\nu = 10$  is taken as a threshold of heavy-tailed dynamics. The Gompertz observation error model assumes a fixed standard deviation of observation error of 0.2 on a log scale.



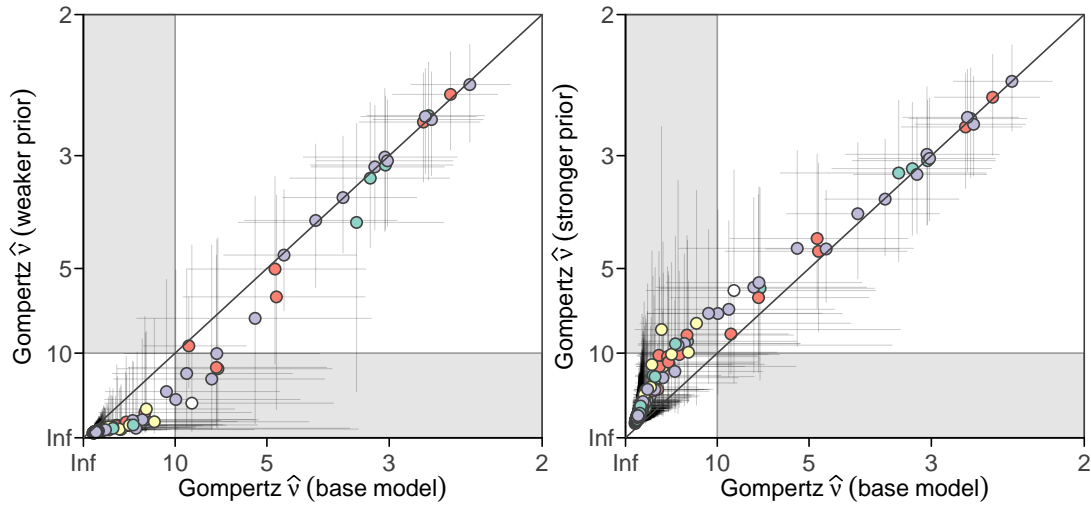


Figure 4.8: Estimates of  $\nu$  from Gompertz models with alternative priors on  $\nu$ . Shown are medians of the posterior (dots) and 50% credible intervals (segments). The diagonal line indicates a one-to-one relationship. Different colours indicate various taxonomic classes. The grey-shaded regions indicate regions of disagreement if  $\nu = 10$  is taken as a threshold of heavy-tailed dynamics. The base, weaker, and stronger priors on  $\nu$  are illustrated in Fig. 4.6. In general, the estimates are nearly identical in cases where the data are informative about low values of  $\nu$ . When the data are less informative about low values of  $\nu$ , the prior can slightly pull the estimates of  $\nu$  towards higher or lower values.

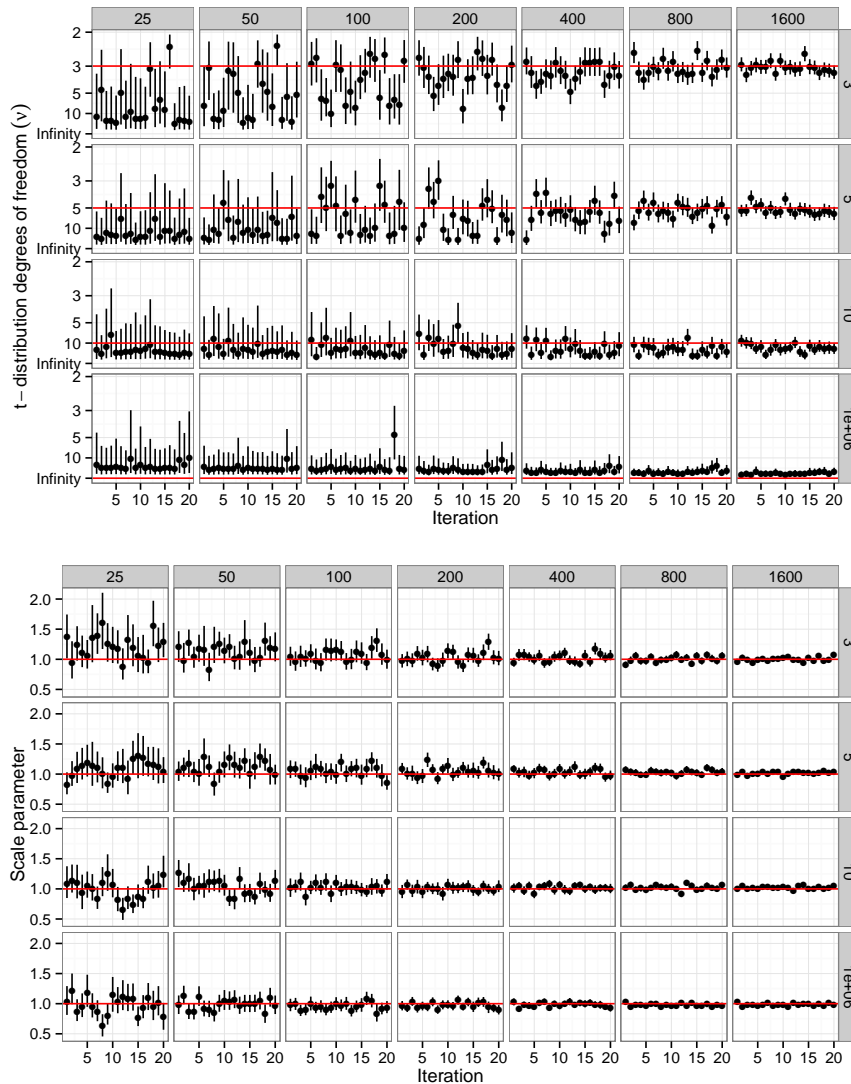


Figure 4.9: Testing the ability to estimate  $\nu$  (top panels) and the scale parameter of the process deviations (bottom panels) for a given number of samples (columns) drawn from a distribution with a given true  $\nu$  value (rows). The red lines indicate the true population value. When a small number of samples are drawn there may not be samples sufficiently far into the tails to recapture the true  $\nu$  value; however, heavy tails are still distinguished from normal tails in most cases, even with only 25 or 50 samples.

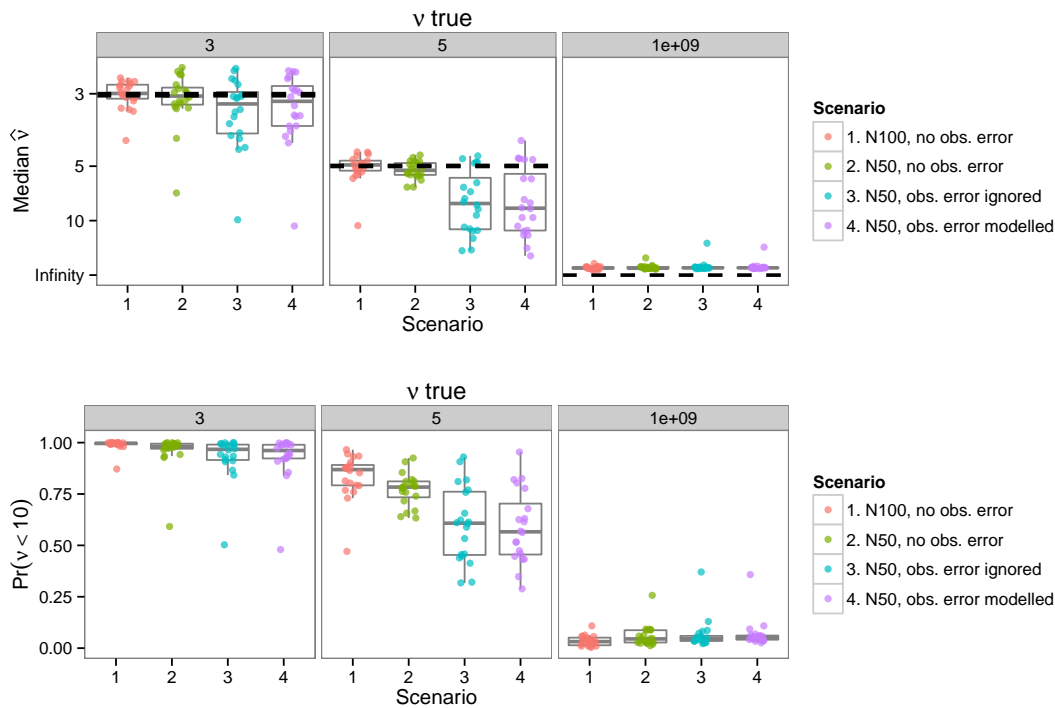


Figure 4.10: Simulation testing the Gompertz estimation model when the process deviation draws were chosen so that  $\nu$  could be estimated close to the true value outside the full population model (“effective  $\nu$ ” within a CV of 0.2 of specified  $\nu$ ). Upper panels show the distribution of median  $\hat{\nu}$  across 20 simulation runs. Lower panels show the distribution of  $\Pr(\nu < 10)$  across 20 simulation runs. We ran the simulations across three population (“true”)  $\nu$  values (3, 5, and  $1 \cdot 10^9$ , i.e. approximately normal) and four scenarios: (1) 100 time steps and no observation error, (2) 50 time steps and no observation error, (3) 50 time steps and observation error drawn from  $\text{Normal}(0, 0.2^2)$  but ignored, and (4) 50 time steps with observation error in which the quantity of observation error was assumed known. Within each scenario the dots represent stochastic draws from the true population distributions combined with model fits. Underlaid boxplots show the median, interquartile range, and 1.5 times the interquartile range.

Example Stan code for a heavy-tailed Gompertz model with AR<sub>1</sub> correlated residuals and a specified level of observation error. The specific code for used for the various models in our analysis is available at <https://github.com/seananderson/heavy-tails>.

```

data {
  int<lower=3> N;           // number of observations
  vector[N] y;            // vector to hold ln abundance observations
  real<lower=0> nu_rate;    // rate parameter for nu exponential prior
}
parameters {
  real lambda;            // Gompertz growth rate parameter
  real<lower=-1, upper=2> b; // Gompertz density dependence parameter
  real<lower=0> sigma_proc; // process noise scale parameter
  real<lower=2> nu;       // t-distribution degrees of freedom
  real<lower=-1, upper=1> phi; // AR1 parameter
  vector[N] U;           // unobserved states
  real<lower=0> sigma_obs; // specified observation error SD
}
transformed parameters {
  vector[N] epsilon;      // error terms
  epsilon[1] <- 0;
  for (i in 2:N) {
    epsilon[i] <- U[i] - (lambda + b * U[i - 1])
                  - (phi * epsilon[i - 1]);
  }
}
model {
  // priors:
  nu ~ exponential(nu_rate);
  lambda ~ normal(0, 10);
  sigma_proc ~ cauchy(0, 2.5);
  phi ~ normal(0, 1);
  // data model:
  for (i in 2:N) {
    U[i] ~ student_t(nu,
                    lambda + b * U[i - 1]
                    + phi * epsilon[i - 1],
                    sigma_proc);
  }
  y ~ normal(U, sigma_obs);
}

```

Stan code for the multilevel beta regression:

```
// Beta regression with group-level intercepts for
// taxonomic class, order, and species
// Uncertainty specified around the predictors x1, x2, x3
data {
  int<lower=0> N; // rows of data
  int<lower=0> n_class; // number of classes
  int<lower=0> n_order; // number of orders
  int<lower=0> n_sp; // number of species
  int<lower=1,upper=n_class> class_id[N];
  int<lower=1,upper=n_order> order_id[N];
  int<lower=1,upper=n_sp> sp_id[N];
  vector[N] x1; // predictor
  vector[N] x2; // predictor
  vector[N] x3; // predictor
  vector[N] x4; // predictor
  vector[N] x5; // predictor
  real<lower=0,upper=1> y[N]; // response
  vector<lower=0>[N] x1_sigma; // sd around predictor
  vector<lower=0>[N] x2_sigma; // sd around predictor
  vector<lower=0>[N] x3_sigma; // sd around predictor
}
parameters {
  vector[n_class] a_class; // class-level deviates
  vector[n_order] a_order; // order-level deviates
  vector[n_sp] a_sp; // species-level deviates
  real b1; // coefficients
  real b2;
  real b3;
  real b4;
  real b5;
  real mu_a; // global intercept
  real<lower=0> sigma_a_order; // group-level standard deviations
  real<lower=0> sigma_a_class;
  real<lower=0> sigma_a_sp;
  real<lower=0> phi; // dispersion parameter
  vector[N] x1_true; // unobserved true predictor values
  vector[N] x2_true;
  vector[N] x3_true;
}
transformed parameters {
```

```

vector[N] Xbeta; // linear predictor
vector<lower=0, upper=1>[N] mu; // transformed linear predictor
vector<lower=0>[N] A; // beta dist. parameter
vector<lower=0>[N] B; // beta dist. parameter
for (i in 1:N) {
  Xbeta[i] <- mu_a + a_class[class_id[i]]
    + a_order[order_id[i]]
    + a_sp[sp_id[i]]
    + b1 * x1_true[i]
    + b2 * x2_true[i]
    + b3 * x3_true[i]
    + b4 * x4[i]
    + b5 * x5[i];
  mu[i] <- inv_logit(Xbeta[i]);
}
A <- mu * phi;
B <- (1.0 - mu) * phi;
}
model {
  // group-level intercept distributions:
  a_class ~ normal(0, sigma_a_class);
  a_order ~ normal(0, sigma_a_order);
  a_sp ~ normal(0, sigma_a_sp);
  // measurement error:
  x1 ~ normal(x1_true, x1_sigma);
  x2 ~ normal(x2_true, x2_sigma);
  x3 ~ normal(x3_true, x3_sigma);
  // priors:
  mu_a ~ cauchy(0, 10);
  phi ~ cauchy(0, 10);
  b1 ~ cauchy(0, 2.5);
  b2 ~ cauchy(0, 2.5);
  b3 ~ cauchy(0, 2.5);
  b4 ~ cauchy(0, 2.5);
  b5 ~ cauchy(0, 2.5);
  sigma_a_class ~ cauchy(0, 2.5);
  sigma_a_order ~ cauchy(0, 2.5);
  sigma_a_sp ~ cauchy(0, 2.5);
  // likelihood:
  y ~ beta(A, B);
}

```

The GPDD IDs used in our analysis.

1 3 4 5 6 7 8 9 10 11 12 13 14 15 16 17 18 44 45 46 47 58 61 64 1149 1150 1153 1157 1159 1160 1162 1163  
 1165 1166 1168 1169 1170 1173 1174 1177 1179 1184 1185 1188 1189 1190 1195 1196 1197 1199 1200 1201 1202  
 1203 1204 1205 1206 1217 1227 1228 1229 1233 1234 1235 1237 1238 1239 1240 1243 1244 1247 1342 1377 1522  
 1523 1524 1525 1534 1602 1613 1618 1633 1660 1663 1664 1667 1669 1670 1671 1674 1682 1683 1792 1826 1829  
 1830 1831 1865 1866 1868 1869 1870 1875 1876 1880 1881 1883 1885 1886 1887 1888 1893 1894 1927 1964 1965  
 1966 1968 1970 1971 1973 1974 1976 1981 1982 1983 1986 1987 1991 1992 1993 1994 1998 1999 2003 2004 2005  
 2006 2007 2012 2013 2015 2016 2017 2018 2019 2020 2024 2025 2026 2027 2028 2031 2032 2033 2034 2066 2721  
 2722 2726 2732 2735 2736 2757 2758 2759 2770 2771 2772 2774 2775 2777 2778 2781 2829 2844 2857 2867 2869  
 2887 2903 2915 2974 2976 2991 3001 3003 3017 3051 3056 3059 3068 3214 3216 3218 3233 3249 3251 3253 3260  
 3265 3283 3356 3358 3360 3378 3442 3466 3468 3470 3477 3482 3508 3521 3625 3627 3639 3664 3673 3676 3678  
 3680 3706 3708 3716 3774 3776 3784 3795 3799 3811 3827 3829 3838 3840 3853 3866 3882 5019 5020 5032 5034  
 5035 5039 6057 6144 6527 6528 6529 6530 6532 6533 6534 6535 6536 6537 6539 6541 6542 6547 6548 6549 6550  
 6553 6554 6555 6556 6558 6560 6561 6562 6564 6565 6567 6568 6569 6570 6581 6582 6583 6633 6673 6674 6675  
 6676 6677 6678 6681 6683 6684 6685 6686 6687 6688 6770 6865 6867 6868 6869 6870 6876 6882 6885 6889 6890  
 6902 6904 6917 6920 6921 6922 6939 6940 6973 7048 7052 7053 7054 7060 7061 7067 7088 7089 7091 7092 7093  
 7094 7098 7099 7101 7102 7115 7116 9191 9192 9194 9195 9196 9200 9211 9215 9216 9217 9218 9219 9220 9221  
 9222 9223 9224 9225 9232 9308 9309 9330 9331 9381 9382 9393 9436 9437 9438 9439 9440 9441 9442 9443 9444  
 9445 9446 9468 9469 9470 9472 9477 9486 9488 9489 9490 9491 9492 9500 9501 9502 9503 9506 9515 9517 9518  
 9519 9586 9587 9606 9611 9612 9639 9641 9642 9644 9646 9647 9648 9650 9652 9654 9655 9656 9657 9658 9659  
 9661 9662 9663 9665 9667 9668 9669 9672 9673 9674 9675 9676 9677 9678 9679 9680 9681 9682 9688 9689 9690  
 9691 9793 9794 9795 9796 9797 9835 9836 9893 9894 9895 9896 9897 9898 9899 9900 9901 9902 9903 9904 9905  
 9907 9919 9921 9932 9933 9934 9936 9938 9948 9949 9950 9951 9953 9990 9991 9993 9994 9995 9997 9998 9999  
 10000 10001 10002 10005 10006 10007 10008 10009 10010 10011 10012 10013 10029 10030 10031 10036 10039  
 10040 10041 10042 10044 10045 10046 10047 10048 10049 10050 10051 10053 10054 10055 10060 10061 10063  
 10065 10070 10071 10085 10088 10089 10090 10092 10093 10094 10096 10097 10098 10099 10100 10101 10110  
 10111 10112 10113 10114 10117 10118 10120 10121 10122 10123 10124 10125 10127 10128 10131 10134 10136  
 10137 10140 10141 10142 10143 10144 10145 10149 10153 10156 10158 10159 10160 10161 10162 10163 10164  
 10165 20527 20530 20532 20534 20535 20536 20537 20539 20540 20541 20542 20543 20544 20546 20547 20548  
 20549 20550 20551 20552 20553 20555 20577 20578 20579 20580 20581 20582 20583 20587 20626 20628 20634  
 20635 20636 20639 20649 20650 20651 20652 20653 20654 20655 20656 20657 20658 20659 20660 20662 20663

## Chapter 5

# General discussion

The study of diversity and stability in population ecology has a long history (MacArthur 1955; May 1973; McCann 2000; Loreau 2010); linking financial concepts with ecology presents new ways to approach some of the issues in this field (Figge 2004). My second chapter links theoretical development of the ecological portfolio effect with empirical data and derives practical recommendations for measuring portfolio effects. My third chapter explores how we can apply portfolio optimization concepts to inform decisions about conservation prioritization. My fourth chapter rigorously assesses the evidence for extreme events in population ecology. Together, my thesis further develops the expanding field of ecological portfolios and in doing so contributes to our understanding of variance, covariance, and extreme events in ecological systems. In this general discussion, I summarize theoretical and methodological advances made by this thesis. I conclude by considering future applied ecology and conservation challenges and questions for the field to address.

My thesis makes a number of theoretical and methodological contributions to the study of variance and extremeness in ecology. I extend a classic feature of ecology—Taylor’s power law—into an empirical tool. We can use this approach to ask questions about the stability of metapopulation (and possibly community) dynamics while accounting for mean–variance scaling relationships and uneven population sizes. The approach has since been used by Mellin et al. (2014) to show that mean–variance portfolio effects increase with spatial dissimilarity in reef fish community structure and by Siple (2014) to show that spawning subpopulation structure stabilizes Pacific herring populations in the Salish Sea. My third chapter contributes to our theoretical understanding of how the full portfolio management concept can translate to conservation priority setting for salmon metapopulations. This invites new applications of the



portfolio concept in which different parties might be considered the managers and investors and other attributes might be considered assets and value. My fourth chapter illustrates and tests a heavy-tailed phenomenological population dynamics model that can easily be applied to commonly available abundance time series.

My thesis also makes a number of software contributions. R packages and associated vignettes accompany my second and third chapters. The *ecofolio* R package has already been used by the above-mentioned Mellin et al. (2014) and Siple (2014). The *metafolio* R package is available on CRAN (Comprehensive R Archive Network), is flexible in the ecological system it can represent, and, being written in C++, can be used to rapidly explore efficient frontiers of conservation prioritization through Monte Carlo simulation. My fourth chapter is one of the first examples, to my knowledge, of the application of the Bayesian statistical software Stan to an ecological problem (<http://mc-stan.org/citations.html>). Estimating the degrees of freedom parameter in a *t* distribution is a challenging exercise (Gelman et al. 2014), particularly when fit as a state space model; Stan allowed for efficient sampling from these probability models. The source code for the *ecofolio* R package is available at <https://github.com/seananderson/ecofolio> and the code to recreate all the analyses in my third and fourth chapters is available at <https://github.com/seananderson/metafolio> and <https://github.com/seananderson/heavy-tails>.

## 5.1 Challenges

As we continue to apply portfolio optimization concepts to ecological decision making, there are a number of likely future challenges. One key challenge will be that ecological problems are often multidimensional (e.g. Keeney 1982), whereas financial portfolio optimization concentrates on a one-dimensional variable (monetary value). As a simple example, an ecological manager needs to balance resources available for hunting or fishing while leaving sufficient resources for ecosystem stability and function. Therefore, at first glance portfolio optimization might appear to be only applicable to a narrow range of ecological decision making. However, existing approaches developed for other decision-making tools may allow portfolio theory to be applied to multidimensional objectives. For instance, whereas the roots of decision analysis—a formal method for evaluating complex decision problems—deal with decision making for one-dimensional objectives, decision analysis is commonly extended to multiple objectives (e.g. Keeney and Raiffa 1976; Kiker et al. 2005; Sethi 2010). Separate objectives can be maintained, allowing decision makers to explicitly see trade-offs, or objectives can be condensed into a

single dimension through multiattribute utility theory, among other approaches (Keeney and Raiffa 1976). A similar approach may be applicable to ecological portfolio optimization.

Ecological and financial data differ in many fundamental ways that will affect how financial portfolio theory can be applied to ecological systems (Table 5.1). For example, ecological data are often of short duration, recorded at low frequency (e.g. each year), and sometimes contain missing values. Financial data, on the other hand, are often available at extremely high frequency (e.g. by the second), recorded on long time scales (e.g. decades), and rarely if ever contain missing values. Econometric techniques built to manage high-frequency regularly spaced financial data (e.g. Hautsch 2012) may not apply to many of today's ecological data. However, these techniques may become increasingly useful as similar types of ecological data become more common (e.g. the Ocean Tracking Network, Cooke et al. 2011). Another difference between financial and ecological data is that ecological data often include considerable measurement error that adds uncertainty around the true value of ecological assets. Financial stock returns, however, reflect the trading value of a stock by definition. Therefore, to accurately apply financial portfolio optimization to ecological portfolios, we may need to adopt methods that can incorporate measurement error. Solutions may include Bayesian methods, Monte Carlo simulation, and state space modelling (Morgan and Henrion 1990).

While there are still problems to solve before we can fully explore the application of portfolio concepts to ecological systems, the availability of appropriate data and relevant statistical methods continues to improve. Higher frequency, longer duration, and spatially explicit ecological data that we can apply portfolio concepts to will continue to accrue. My thesis has benefited from a number of large datasets, many of which were not available a decade ago. Likewise, statistical tools for propagating uncertainty and fitting complex spatio-temporal models are improving rapidly, e.g., TMB: Kristensen (2014), R-INLA: Rue et al. (2014), Stan: Stan Development Team (2014). For these reasons, among others, the application of quantitative portfolio concepts to ecology is likely to expand.

## 5.2 Outlook

How can we move ecological portfolios beyond an academic exercise to using their principles in applied management? The application of portfolio concepts to ecological systems is still a young discipline and there exist many important future questions to address. I outline three groups of these questions below.

Table 5.1: Attributes of financial and ecological data and their implications for ecological portfolios.

Data attributes	Financial portfolios	Ecological portfolios	What this means for ecological portfolios
Interdependence	A diverse portfolio is unlikely to have strong dependence between assets	Populations may be affected by changes in other populations of the same species (e.g. competition or migration) or other species (e.g. predation)	Interactions may need to be accounted for; greater uncertainty in ecological portfolios
Measurement error	There is no measurement error	There is often substantial measurement error	Uncertainty needs to be propagated through analyses
Frequency and duration	High frequency, regular recording intervals, missing values are rare, long durations	Lower frequency, often irregular recording intervals, missing values common, often short durations	Greater uncertainty in optimal solutions; time-series methods require unique approach (e.g. missing values may need to be imputed, autocorrelation different)
Mean-variance scaling	Variance scales directly with investment	Variance may scale indirectly with investment	The mean-variance relationship may need to be accounted for (Anderson et al. 2013)
Number of assets	Typically unlimited; generally high	Typically limited; generally low	Potentially less opportunity for portfolio diversification

First, how can the portfolio effect and portfolio optimization inform management and conservation and in what other contexts can it be applied? For instance, how might portfolio optimization inform the debate about the advantages of forming single large or several small reserves (SLOSS)? Several small reserves provide the basis for a portfolio structure, but stability would depend on the rate at which the correlation of environmental correlations decays with distance or on the degree of localized population adaption to environmental conditions. Fitting or simulating models from a portfolio perspective could inform these kinds of ecological decision making. As another example, what can portfolio optimization tell us about managing the recovery of populations? Portfolio selection emphasizes a risk–return trade-off and society’s preference for a particular position on an efficient frontier may shift for endangered species management compared to managing populations at a healthy abundance.

Second, recent work has shown clear theoretical advantages to ecological conservation

that applies portfolio theory (Crowe and Parker 2008; Halpern et al. 2011; Ando and Mallory 2012; Anderson et al. 2014), although, to my knowledge, portfolio theory has yet to be formally integrated into real-world conservation planning. On the other hand, the general lessons of portfolio theory are already used in many cases of resource management. For example, managers can allow resource users to integrate across space and species (Kasperski and Holland 2013), resource users can choose to pool profits (Sethi et al. 2012), and managers can make decisions that maintain a diversity of life-history characteristics and local adaptations (Hilborn et al. 2003). The general principles of maintaining representation, resilience, and redundancy can be integrated into conservation decision making without any formal quantitative application of portfolio theory (Haak and Williams 2012).

Third, will shifting climate isotherms (Burrows et al. 2011; Pinsky et al. 2013) combined with increases in the frequency and magnitude of climate extremes (Easterling et al. 2000; IPCC 2012) translate to a greater probability of population dynamic black swans (Jentsch et al. 2007; Thompson et al. 2013)? Can we develop predictive models of population catastrophes in space and time? And what conservation approaches make some populations more robust to extremes and some populations more likely to recover from them? Addressing these types of questions may be vital to effective ecological management in the coming decades.

The study of variance and covariance in ecology has helped make great strides towards effective ecological decision making. However, decision makers ultimately tend to care about risk—probability combined with magnitude of loss—and therefore extremeness. My fourth chapter deals with the reality of extreme events in population ecology whereas the previous two chapters explore mechanisms and approaches that can cope with these. Ultimately, diverse natural portfolios of populations, species, and habitats are a critical component to maintaining stability and buffering against ecological catastrophes and resource-use collapses in an increasingly stressful world.

# Bibliography

- Allee, W. C. (1931). *Animal Aggregations: A Study in General Sociology*. The University of Chicago Press for The American Society of Naturalists, Chicago.
- Allen, A., Li, B.-L., and Charnov, E. (2001). Population fluctuations, power laws and mixtures of lognormal distributions. *Ecol. Lett.*, 4(1):1–3.
- Allendorf, F. W., Bayles, D., Bottom, D. L., Currens, K. P., Frissell, C. A., Hankin, D., Lichatowich, J. A., Nehlsen, W., Trotter, P. C., and Williams, T. H. (1997). Prioritizing Pacific salmon stocks for conservation. *Conserv. Biol.*, 11(1):140–152.
- Alvarez, L. W., Alvarez, W., Asaro, F., and Michel, H. V. (1980). Extraterrestrial cause for the Cretaceous-Tertiary extinction. *Science*, 208(4448):1095–1108.
- Anderson, R. M., Gordon, D. M., Crawley, M. J., and Hassell, M. P. (1982). Variability in the abundance of animal and plant species. *Nature*, 296(5854):245–248.
- Anderson, S. C. (2014). *metafolio: Salmon metapopulation simulations for conservation planning through portfolio optimization*. R package version 0.1.0. <http://cran.r-project.org/package=metafolio>.
- Anderson, S. C., Cooper, A. B., and Dulvy, N. K. (2013). Ecological prophets: quantifying meta-population portfolio effects. *Methods Ecol. Evol.*, 4(10):971–981.
- Anderson, S. C., Moore, J. W., McClure, M. M., Dulvy, N. K., and Cooper, A. B. (2014). Portfolio conservation of metapopulations under climate change. *Ecol. Appl.*, In press. DOI: 10.1890/14-0266.1.
- Ando, A. W. and Hannah, L. (2011). Lessons from finance for new land-conservation strategies given climate-change uncertainty. *Conserv. Biol.*, 25(2):412–414.
- Ando, A. W. and Mallory, M. L. (2012). Optimal portfolio design to reduce climate-related conservation uncertainty in the Prairie Pothole Region. *Proc. Natl. Acad. Sci. U.S.A.*, 109(17):6484–6489.
- Baldursson, F. and Magnússon, G. (1997). Portfolio fishing. *Scand. J. Econ.*, 99(3):389–403.
- Ballantyne IV, F. (2005). The upper limit for the exponent of Taylor’s power law is a consequence of deterministic population growth. *Evol. Ecol. Res.*, 7:1213–1220.

- Balvanera, P., Pfisterer, A. B., Buchmann, N., He, J.-S., Nakashizuka, T., Raffaelli, D., and Schmid, B. (2006). Quantifying the evidence for biodiversity effects on ecosystem functioning and services. *Ecol. Lett.*, 9(10):1146–1156.
- Barnes, R. F. W. and Tapper, S. C. (1986). Consequences of the myxomatosis epidemic in Britain's rabbit (*Oryctolagus cuniculus* L.) population on the numbers of brown hares (*Lepus europaeus* Pallas). *Mammal. Rev.*, 16(3-4):111–116.
- Barnosky, A. D., Matzke, N., Tomiya, S., Wogan, G. O. U., Swartz, B., Quental, T. B., Marshall, C., McGuire, J. L., Lindsey, E. L., Maguire, K. C., Mersey, B., and Ferrer, E. A. (2011). Has the Earth's sixth mass extinction already arrived? *Nature*, 471(7336):51.
- Bartoń, K. (2012). MuMIn: multi-model inference. R package version 1.7.7.
- Battin, J., Wiley, M. W., Ruckelshaus, M. H., Palmer, R. N., Korb, E., Bartz, K. K., and Imaki, H. (2007). Projected impacts of climate change on salmon habitat restoration. *Proc. Natl. Acad. Sci. U.S.A.*, 104(16):6720–6725.
- Beechie, T., Imaki, H., Greene, J., Wade, A., Wu, H., Pess, G., Roni, P., Kimball, J., Stanford, J., Kiffney, P., and Mantua, N. (2013). Restoring salmon habitat for a changing climate. *River Res. Applic.*, 29(8):939–960.
- Brett, J. R. (1952). Temperature tolerance in young pacific salmon, genus *Oncorhynchus*. *J. Fish. Res. Bd. Can.*, 9(6):265–323.
- Broekhuizen, N., Evans, H. F., and Hassell, M. P. (1993). Site characteristics and the population dynamics of the pine looper moth. *J. Anim. Ecol.*, 62(3):511–518.
- Brook, B. W. and Bradshaw, C. J. A. (2006). Strength of evidence for density dependence in abundance time series of 1198 species. *Ecology*, 87(6):1445–1451.
- Brook, B. W., Traill, L. W., and Bradshaw, C. J. A. (2006). Minimum viable population sizes and global extinction risk are unrelated. *Ecol. Lett.*, 9(4):375–382.
- Brown, T. L. (2003). *Making Truth: Metaphor in Science*. University of Illinois Press.
- Bumpus, H. C. (1899). The elimination of the unfit as illustrated by the introduced sparrow, *Passer domesticus*. *Biol. Lect. Mar. Biol. Woods Hole*, 11:209–226.
- Burnham, K. P. and Anderson, D. R. (2002). *Model Selection and Multimodel Inference: A Practical Information-Theoretic Approach, Second Edition*. Springer, New York.
- Burrows, M. T., Schoeman, D. S., Buckley, L. B., Moore, P., Poloczanska, E. S., Brander, K. M., Brown, C., Bruno, J. F., Duarte, C. M., Halpern, B. S., Holding, J., Kappel, C. V., Kiessling, W., O'Connor, M. I., Pandolfi, J. M., Parmesan, C., Schwing, F. B., Sydeman, W. J., and Richardson, A. J. (2011). The pace of shifting climate in marine and terrestrial ecosystems. *Science*, 334(6056):652–655.

- Caddy, J. F. and McGarvey, R. (1996). Targets or limits for management of fisheries? *N. Am. J. Fish. Manage.*, 16(3):479–487.
- Canty, A. and Ripley, B. (2012). boot: Bootstrap R (S-Plus) functions. R package version 1.3-7.
- Cardinale, B. J., Duffy, J. E., Gonzalez, A., Hooper, D. U., Perrings, C., Venail, P., Narwani, A., Mace, G. M., Tilman, D., Wardle, D. A., Kinzig, A. P., Daily, G. C., Loreau, M., Grace, J. B., Larigauderie, A., Srivastava, D. S., and Naeem, S. (2012). Biodiversity loss and its impact on humanity. *Nature*, 486(7401):59–67.
- Carlson, S. M. and Satterthwaite, W. H. (2011). Weakened portfolio effect in a collapsed salmon population complex. *Can. J. Fish. Aquat. Sci.*, 68:1579–1589.
- Clark, F., Brook, B. W., Delean, S., Reşit Akçakaya, H., and Bradshaw, C. J. A. (2010). The theta-logistic is unreliable for modelling most census data. *Methods Ecol. Evol.*, 1(3):253–262.
- Clarke, W. E. and Backhouse, J. (1885). An autumn ramble in Eastern Iceland, with some notes from the Faröes. *Ibis*, 27(4):364–380.
- Colebrook, J. M. (1978). Continuous plankton records-zooplankton and environment, northeast Atlantic and North-Sea, 1948-1975. *Oceanologica Acta*, 1(1):9–23.
- Connors, B. M., Cooper, A. B., Peterman, R. M., and Dulvy, N. K. (2014). The false classification of extinction risk in noisy environments. *Proc. R. Soc. Lond. B*, 281(1787).
- Conrad, K., Woiwod, I., Parsons, M., Fox, R., and Warren, M. (2004). Long-term population trends in widespread British moths. *J. Insect Cons.*, 8(2):119–136.
- Cooke, S. J., Iverson, S. J., Stokesbury, M. J. W., Hinch, S. G., Fisk, A. T., VanderZwaag, D. L., Apostle, R., and Whoriskey, F. (2011). Ocean Tracking Network Canada: A network approach to addressing critical issues in fisheries and resource management with implications for ocean governance. *Fisheries*, 36(12):583–592.
- Cooper, A. B. and Mangel, M. (1999). The dangers of ignoring metapopulation structure for the conservation of salmonids. *Fish. Bull.*, 97(2):213–226.
- Costanza, R., Daly, M., Folke, C., Hawken, P., Holling, C. S., McMichael, A. J., Pimentel, D., and Rapport, D. (2000). Managing our environmental portfolio. *BioScience*, 50(2):149–155.
- Cottingham, K. L., Brown, B. L., and Lennon, J. T. (2001). Biodiversity may regulate the temporal variability of ecological systems. *Ecol. Lett.*, 4(1):72–85.
- Crowe, K. A. and Parker, W. H. (2008). Using portfolio theory to guide reforestation and restoration under climate change scenarios. *Climatic Change*, 89(3-4):355–370.
- Crozier, L. G., Hendry, A. P., Lawson, P. W., Quinn, T., Mantua, N. J., Battin, J., Shaw, R. G., and Huey, R. B. (2008). Potential responses to climate change in organisms with complex life histories: evolution and plasticity in Pacific salmon. *Evol. Appl.*, 1(2):252–270.

- D'Ancona, U. (1954). *The Struggle for Existence*. E.J. Brill.
- de Mazancourt, C., Isbell, F., Larocque, A., Berendse, F., De Luca, E., Grace, J. B., Haegeman, B., Wayne Polley, H., Roscher, C., Schmid, B., Tilman, D., van Ruijven, J., Weigelt, A., Wilsey, B. J., and Loreau, M. (2013). Predicting ecosystem stability from community composition and biodiversity. *Ecol. Lett.*, 16(5):617–625.
- de Valpine, P. and Hastings, A. (2002). Fitting population models incorporating process noise and observation error. *Ecol. Monograph.*, 72(1):57–76.
- DeClerck, F. A. J., Barbour, M. G., and Sawyer, J. O. (2006). Species richness and stand stability in conifer forests of the Sierra Nevada. *Ecology*, 87(11):2787–2799.
- Dennis, B. and Ponciano, J. M. (2014). Density-dependent state-space model for population-abundance data with unequal time intervals. *Ecology*, 95(8):2069–2076.
- Dennis, B., Ponciano, J. M., Lele, S. R., Taper, M. L., and Staples, D. F. (2006). Estimating density dependence, process noise, and observation error. *Ecol. Monograph.*, 76(3):323–341.
- Denny, M. W., Hunt, L. J. H., Miller, L. P., and Harley, C. D. G. (2009). On the prediction of extreme ecological events. *Ecol. Monograph.*, 79(3):397–421.
- DFO (2005). Canada's policy for conservation of wild Pacific salmon. Technical report, Fisheries and Oceans Canada, Vancouver, BC.
- Doak, D. F., Bigger, D., Harding, E. K., Marvier, M. A., O'Malley, R. E., and Thomson, D. (1998). The statistical inevitability of stability-diversity relationships in community ecology. *Amer. Nat.*, 151(3):264–276.
- Doak, D. F., Estes, J. A., Halpern, B. S., Jacob, U., Lindberg, D. R., Lovvorn, J., Monson, D. H., Tinker, M. T., Williams, T. M., Wootton, J. T., Carroll, I., Emmerson, M., Micheli, F., and Novak, M. (2008). Understanding and predicting ecological dynamics: are major surprises inevitable? *Ecology*, 89(4):952–961.
- Dobson, A. and Hudson, P. (1995). The interaction between the parasites and predators of red grouse *Lagopus lagopus scoticus*. *Ibis*, 137:S87–S96.
- Dorner, B., Peterman, R. M., and Haeseke, S. L. (2008). Historical trends in productivity of 120 Pacific pink, chum, and sockeye salmon stocks reconstructed by using a Kalman filter. *Can. J. Fish. Aquat. Sci.*, 65:1842–1866.
- Drake, J. M. (2014). Tail probabilities of extinction time in a large number of experimental populations. *Ecology*, 95:1119–1126.
- Easterling, D. R., Meehl, G. A., Parmesan, C., Changnon, S. A., Karl, T. R., and Mearns, L. O. (2000). Climate extremes: observations, modeling, and impacts. *Science*, 289(5487):2068–2074.
- Edwards, S. (2004). Portfolio management of wild fish stocks. *Ecol. Econom.*, 49(3):317–329.



- Ehrlich, P. R. and Pringle, R. M. (2008). Where does biodiversity go from here? A grim business-as-usual forecast and a hopeful portfolio of partial solutions. *Proc. Natl. Acad. Sci. USA*, 105(S1):11579–11586.
- Eliason, E. J., Clark, T. D., Hague, M. J., Hanson, L. M., Gallagher, Z. S., Jeffries, K. M., Gale, M. K., Patterson, D. A., Hinch, S. G., and Farrell, A. P. (2011). Differences in thermal tolerance among sockeye salmon populations. *Science*, 332(6025):109–112.
- Elmqvist, T., Folke, C., Nyström, M., Peterson, G., Bengtsson, J., Walker, B., and Norberg, J. (2003). Response diversity, ecosystem change, and resilience. *Front. Ecol. Environ.*, 1(9):488–494.
- Fa, J. E. (1984). Structure and dynamics of the Barbary macaque population in Gibraltar. In Fa, J. E., editor, *The Barbary Macaque*, pages 263–306. Springer-Verlag US.
- Fair, L. F., Willette, T. M., Erickson, J. W., Yanusz, R. J., and McKinley, T. R. (2011). Review of salmon escapement goals in Upper Cook Inlet, Alaska, 2011. Fishery Manuscript Series 10–06, Alaska Department of Fish and Game.
- Fernandez, C. and Steel, M. F. J. (1998). On Bayesian modeling of fat tails and skewness. *J. Am. Stat. Assoc.*, 93(441):359–371.
- Ferrari, S. and Cribari-Neto, F. (2004). Beta regression for modelling rates and proportions. *J. Appl. Stat.*, 31(7):799–815.
- Figge, F. (2004). Bio-folio: applying portfolio theory to biodiversity. *Biodivers. Conserv.*, 13(4):827–849.
- Fraser, D. J., Weir, L. K., Bernatchez, L., Hansen, M. M., and Taylor, E. B. (2011). Extent and scale of local adaptation in salmonid fishes: review and meta-analysis. *Heredity*, 106(3):404–420.
- Fronczak, A. and Fronczak, P. (2010). Origins of Taylor’s power law for fluctuation scaling in complex systems. *Phys. Rev. E*, 81:066112.
- Gaines, S. D. and Denny, M. W. (1993). The largest, smallest, highest, lowest, longest, and shortest: Extremes in ecology. *Ecology*, 74(6):1677–1692.
- Gaston, K. J. (1988). Patterns in the local and regional dynamics of moth populations. *Oikos*, 53(1):49–57.
- Gelman, A. (2006). Prior distributions on variance parameters in hierarchical models. *Bayesian Analysis*, 1(3):515–533.
- Gelman, A. (2008). Scaling regression inputs by dividing by two standard deviations. *Statist. Med.*, 27:2865–2873.
- Gelman, A. (2013). How to model distributions that have outliers in one direction. URL <http://andrewgelman.com/2013/12/09/model-distributions-outliers-one-direction/>.

- Gelman, A., Carlin, J. B., Stern, H. S., Dunson, D. B., Vehtari, A., and Rubin, D. B. (2014). *Bayesian Data Analysis*. Chapman & Hall, Boca Raton, FL.
- Gelman, A. and Hill, J. (2006). *Data Analysis Using Regression and Multilevel/Hierarchical Models*. Cambridge University Press, Cambridge, UK.
- Gelman, A., Jakulin, A., Pittau, M. G., and Su, Y.-S. (2008). A weakly informative default prior distribution for logistic and other regression models. *Ann. Appl. Stat.*, 2(4):1360–1383.
- Gerber, L. R. and Hilborn, R. (2001). Catastrophic events and recovery from low densities in populations of otariids: implications for risk of extinction. *Mammal. Rev.*, 31(2):131–150.
- Greene, C. M., Hall, J. E., Guilbault, K. R., and Quinn, T. P. (2010). Improved viability of populations with diverse life-history portfolios. *Biol. Lett.*, 6(3):382–386.
- Gross, K., Cardinale, B. J., Fox, J. W., Gonzalez, A., Loreau, M., Polley, H. W., Reich, P. B., and Ruijven, J. v. (2013). Species richness and the temporal stability of biomass production: A new analysis of recent biodiversity experiments. *Amer. Nat.*, In press.
- Gustafson, R. G., Waples, R. S., Myers, J. M., Weitkamp, L. A., Bryant, G. J., Johnson, O. W., and Hard, J. J. (2007). Pacific salmon extinctions: quantifying lost and remaining diversity. *Conserv. Biol.*, 21(4):1009–1020.
- Haak, A. L. and Williams, J. E. (2012). Spreading the risk: native trout management in a warmer and less-certain future. *N. Am. J. Fish. Manage.*, 32(2):387–401.
- Halford, A. R. and Thompson, A. A. (1994). Long-term monitoring of the great barrier reef. Technical Report Standard Operational Procedure Number 3, Australian Institute of Marine Science, Townsville, Australia.
- Halley, J. and Inchausti, P. (2002). Lognormality in ecological time series. *Oikos*, 99(3):518–530.
- Halpern, B. S., White, C., Lester, S. E., Costello, C., and Gaines, S. D. (2011). Using portfolio theory to assess tradeoffs between return from natural capital and social equity across space. *Biol. Cons.*, 144(5):1499–1507.
- Hannah, L., Midgley, G. F., Lovejoy, T., Bond, W. J., Bush, M., Lovett, J. C., Scott, D., and Woodward, F. I. (2002). Conservation of biodiversity in a changing climate. *Conserv. Biol.*, 16(1):264–268.
- Hanski, I. and Woiwod, I. P. (1993). Spatial synchrony in the dynamics of moth and aphid populations. *J. Anim. Ecol.*, 62(4):656–668.
- Harnik, P. G., Lotze, H. K., Anderson, S. C., Finkel, Z. V., Finnegan, S., Lindberg, D. R., Liow, L. H., Lockwood, R., McClain, C. R., McGuire, J. L., O’Dea, A., Pandolfi, J. M., Simpson, C., and Tittensor, D. P. (2012). Extinctions in ancient and modern seas. *Trends Ecol. Evolut.*, 27(11):608–617.
- Hautsch, N. (2012). *Econometrics of Financial High-Frequency Data*. Springer, Berlin Heidelberg.

- Heessen, H. J. L. (1996). Time-series data for a selection of forty fish species caught during the International Bottom Trawl Survey. *ICES J. Mar. Sci.*, 53(6):1079–1084.
- Heller, N. E. and Zavaleta, E. S. (2009). Biodiversity management in the face of climate change: a review of 22 years of recommendations. *Biol. Cons.*, 142(1):14–32.
- Hilborn, R., Maguire, J.-J., Parma, A. M., and Rosenberg, A. A. (2001). The precautionary approach and risk management: can they increase the probability of successes in fishery management? *Can. J. Fish. Aquat. Sci.*, 58(1):99–107.
- Hilborn, R. W., Quinn, T., Schindler, D., and Rogers, D. (2003). Biocomplexity and fisheries sustainability. *Proc. Natl. Acad. Sci. U.S.A.*, 100(11):6564–6568.
- Hilborn, R. W. and Walters, C. (1992). *Quantitative Fisheries Stock Assessment: Choice, Dynamics, and Uncertainty*. Chapman and Hall, London.
- Hildebrandt, P. and Knoke, T. (2011). Investment decisions under uncertainty — A methodological review on forest science studies. *Forest Policy Econ.*, 13(1):1–15.
- Hoekstra, J. (2012). Improving biodiversity conservation through modern portfolio theory. *Proc. Natl. Acad. Sci. U.S.A.*, 109(17):6360–6361.
- Hoffman, M. D. and Gelman, A. (2014). The No-U-Turn Sampler: adaptively setting path lengths in Hamiltonian Monte Carlo. *J. Mach. Learn. Res.*, 15:1593–1623.
- Holling, C. S. (2001). Understanding the complexity of economic, ecological, and social systems. *Ecosystems*, 4(5):390–405.
- Hutchings, J. A. and Myers, R. A. (1993). The effect of age on the seasonality of maturation and spawning of Atlantic cod, *Gadus morhua*. *Can. J. Fish. Aquat. Sci.*, 50:2468–2474.
- Hyytiäinen, K. and Penttinen, M. (2008). Applying portfolio optimisation to the harvesting decisions of non-industrial private forest owners. *Forest Policy Econ.*, 10(3):151–160.
- IMCC (2011). Portfolio effect in fisheries. Symposium 25. In *2<sup>nd</sup> International Marine Conservation Congress*, Victoria, BC, Canada.
- Inchausti, P. and Halley, J. (2002). The long-term temporal variability and spectral colour of animal populations. *Evol. Ecol. Res.*, 4:1033–1048.
- IPCC (2012). Managing the risks of extreme events and disasters to advance climate change adaptation. In Field, C. B., Barros, V., Stocker, T., Qin, D., Dokken, D. J., Ebi, K. L., Mastrandrea, M. D., Mach, K. J., Plattner, G.-K., Allen, S. K., Tignor, M., and Midgley, P. M., editors, *A Special Report of Working Groups I and II of the Intergovernmental Panel on Climate Change*. Cambridge University Press, Cambridge, UK, and New York, NY, USA.
- Isaak, D. J. and Rieman, B. E. (2013). Stream isotherm shifts from climate change and implications for distributions of ectothermic organisms. *Global Change Biol.*, 19(3):742–751.

- Isaak, D. J., Thurow, R. F., Rieman, B. E., and Dunham, J. B. (2007). Chinook salmon use of spawning patches: relative roles of habitat quality, size, and connectivity. *Ecol. Appl.*, 17(2):352–364.
- Isaak, D. J., Wollrab, S., Horan, D., and Chandler, G. (2012). Climate change effects on stream and river temperatures across the northwest u.s. from 1980–2009 and implications for salmonid fishes. *Climatic Change*, 113(2):499–524.
- [IUCN] The World Conservation Union (2001). IUCN Red List categories and criteria. version 3.1. Technical report, IUCN Species Survival Commission, Gland (Switzerland) and Cambridge (UK).
- Ives, A. R. and Carpenter, S. R. (2007). Stability and diversity of ecosystems. *Science*, 317(5834):58–62.
- Ives, A. R., Dennis, B., Cottingham, K. L., and Carpenter, S. R. (2003). Estimating community stability and ecological interactions from time-series data. *Ecol. Monograph.*, 73(2):301–330.
- Janczura, J. and Weron, R. (2012). Black swans or dragon-kings? A simple test for deviations from the power law. *The European Physical Journal Special Topics*, 205(1):79–93.
- Jensen, A. J., Zubchenko, A. V., Heggberget, T. G., Hvidsten, N. A., Johnsen, B. O., Kuzmin, O., Loenko, A. A., Lund, R. A., Martynov, V. G., Næ sje, T. F., Sharov, A. F., and Økland, F. (1999). Cessation of the Norwegian drift net fishery: changes observed in Norwegian and Russian populations of Atlantic salmon. *ICES J. Mar. Sci.*, 56(1):84–95.
- Jentsch, A., Kreyling, J., and Beierkuhnlein, C. (2007). A new generation of climate-change experiments: events, not trends. *Front. Ecol. Environ.*, 5(7):365–374.
- Johnson, N., Zhao, G., Hunsader, E., Qi, H., Johnson, N., Meng, J., and Tivnan, B. (2013). Abrupt rise of new machine ecology beyond human response time. *Sci. Rep.*, 3.
- Johnson, S. P. and Schindler, D. E. (2013). Marine trophic diversity in an anadromous fish is linked to its life-history variation in fresh water. *Biol. Lett.*, 9(1):20120824.
- Karp, D. S., Ziv, G., Zook, J., Ehrlich, P. R., and Daily, G. C. (2011). Resilience and stability in bird guilds across tropical countryside. *Proc. Natl. Acad. Sci. USA*, 108(52):21134–21139.
- Kasperski, S. and Holland, D. S. (2013). Income diversification and risk for fishermen. *Proc. Natl. Acad. Sci. USA*, 110(6):2076–2081.
- Katz, R. W., Brush, G. S., and Parlange, M. B. (2005). Statistics of extremes: modelling ecological disturbances. *Ecology*, 86(5):1124–1134.
- Keeney, R. L. (1982). Decision analysis: an overview. *Operations Research*, 30(5):803–838.
- Keeney, R. L. and Raiffa, H. (1976). *Decisions with multiple objectives*. John Wiley & Sons, Inc.
- Keith, L. B. (1963). *Wildlife's ten-year cycle*. University of Wisconsin Press, Madison, WI.

- Keitt, T. H. and Stanley, H. E. (1998). Dynamics of North American breeding bird populations. *Nature*, 393(6682):257–260.
- Kendeigh, S. C. (1982). *Bird populations in east central Illinois: fluctuations, variations, and development over a half-century*. University of Illinois Press, Champaign, IL.
- Kiker, G. A., Bridges, T. S., Varghese, A., Seager, T. P., and Linkov, I. (2005). Application of multicriteria decision analysis in environmental decision making. *Integrated Environmental Assessment and Management*, 1(2):95–108.
- Kilpatrick, A. M. and Ives, A. R. (2003). Species interactions can explain Taylor’s power law for ecological time series. *Nature*, 422(6927):65–68.
- Kirby, R. R., Beaugrand, G., and Lindley, J. A. (2009). Synergistic effects of climate and fishing in a marine ecosystem. *Ecosystems*, 12(4):548–561.
- Knape, J. (2008). Estimability of density dependence in models of time series data. *Ecology*, 89(11):2994–3000.
- Knape, J. and de Valpine, P. (2012). Are patterns of density dependence in the Global Population Dynamics Database driven by uncertainty about population abundance? *Ecol. Lett.*, 15(1):17–23.
- Kocik, J. F. and Sheehan, T. F. (2006). Status of fishery resources off the northeastern US: Atlantic salmon. Technical report, NEFSC Resource Evaluation and Assessment Division.
- Koellner, T. and Schmitz, O. J. (2006). Biodiversity, ecosystem function, and investment risk. *BioScience*, 56(12):977–985.
- Kristensen, K. (2014). *TMB: General random effect model builder tool inspired by ADMB*. R package version 1.1. <https://github.com/kaskr/adcomp>.
- Krkošek, M., Connors, B. M., Morton, A., Lewis, M. A., Dill, L. M., and Hilborn, R. (2011). Effects of parasites from salmon farms on productivity of wild salmon. *Proc. Natl. Acad. Sci. U.S.A.*, 108(35):14700–14704.
- Lack, D. (1969). Population changes in the land birds of a small island. *J. Anim. Ecol.*, 38(1):211–218.
- Lackey, R. T. (2003). Pacific Northwest salmon: Forecasting their status in 2100. *Rev. Fish. Sci.*, 11(1):35–88.
- Larson, B. (2011). *Metaphors for Environmental Sustainability: Redefining our Relationship with Nature*. Yale University Press.
- Lavergne, S., Mouquet, N., Thuiller, W., and Ronce, O. (2010). Biodiversity and climate change: Integrating evolutionary and ecological responses of species and communities. *Annu. Rev. Ecol. Syst.*, 41(1):321–350.

- Lee, T. M. and Jetz, W. (2008). Future battlegrounds for conservation under global change. *Proc. R. Soc. Lond. B*, 275(1640):1261–1270.
- Lehman, C. L. and Tilman, D. (2000). Biodiversity, stability, and productivity in competitive communities. *Amer. Nat.*, 156(5):534–552.
- Lepš, J. (1993). Taylor's power law and the measurement of variation in the size of populations in space and time. *Oikos*, 68(2):349–356.
- Levins, R. (1969). Some demographic and genetic consequences of environmental heterogeneity for biological control. *Bull. Entomol. Soc. Am.*, 15:237–240.
- Lindenmayer, D. B., Likens, G. E., Krebs, C. J., and Hobbs, R. J. (2010). Improved probability of detection of ecological "surprises". *Proc. Natl. Acad. Sci. U.S.A.*, 107(51):21957–21962.
- Lindström, E. R., Andrén, H., Angelstam, P., Cederlund, G., Hörnfeldt, B., Jäderberg, L., Lemnell, P.-A., Martinsson, B., Sköld, K., and Swenson, J. E. (1994). Disease reveals the predator: sarcoptic mange, red fox predation, and prey populations. *Ecology*, 75(4):1042–1049.
- Lindström, J., Ranta, E., Kaitala, V., and Lindén, H. (1995). The clockwork of Finnish tetraonid population dynamics. *Oikos*, 74(2):185–194.
- Loreau, M. (2010). *From Populations to Ecosystems: Theoretical Foundations for a New Ecological Synthesis*. Princeton University Press, Princeton, NJ.
- Loreau, M. and de Mazancourt, C. (2008). Species synchrony and its drivers: Neutral and nonneutral community dynamics in fluctuating environments. *Amer. Nat.*, 172(2):E48–E66.
- Luce, C. H., Abatzoglou, J. T., and Holden, Z. A. (2013). The missing mountain water: Slower westerlies decrease orographic enhancement in the Pacific Northwest USA. *Science*, 342(6164):1360–1364.
- Luce, C. H. and Holden, Z. A. (2009). Declining annual streamflow distributions in the Pacific Northwest United States, 1948–2006. *Geophys. Res. Lett.*, 36(16).
- MacArthur, R. (1955). Fluctuations of animal populations and a measure of community stability. *Ecology*, 36(3):533–536.
- Mace, G. M. (2005). Biodiversity: An index of intactness. *Nature*, 434:32–33.
- Mackenzie, J. M. D. (1952). Fluctuations in the numbers of British tetraonids. *J. Anim. Ecol.*, 21(1):128–153.
- Mangel, M. and Tier, C. (1994). Four facts every conservation biologist should know about persistence. *Ecology*, 75(3):607–614.
- Mantua, N., Tohver, I., and Hamlet, A. (2010). Climate change impacts on streamflow extremes and summertime stream temperature and their possible consequences for freshwater salmon habitat in Washington State. *Climatic Change*, 102(1-2):187–223.

- Margules, C. R. and Pressey, R. L. (2000). Systematic conservation planning. *Nature*, 405(6783):243–253.
- Markkula, M. (1965). Pests of cultivated plants in Finland 1965. *Maatal Ja Koetoim*, 20(185–195).
- Markowitz, H. (1952). Portfolio selection. *J. Finance*, 7(1):77–91.
- Markowitz, H. M. (1959). *Portfolio Selection: Efficient Diversification of Investments*. Wiley & Sons, New York.
- May, R. M. (1973). *Stability and Complexity in Model Ecosystems*. Princeton University Press, New Jersey.
- May, R. M., Levin, S. A., and Sugihara, G. (2008). Complex systems: ecology for bankers. *Nature*, 451(7181):893–895.
- McArdle, B. H., Gaston, K. J., and Lawton, J. H. (1990). Variation in the size of animal populations: Patterns, problems and artefacts. *J. Anim. Ecol.*, 59(2):439–454.
- McCann, K. S. (2000). The diversity-stability debate. *Nature*, 405(6783):228–233.
- McClure, M. M., Carlson, S. M., Beechie, T. J., Pess, G. R., Jorgensen, J. C., Sogard, S. M., Sultan, S. E., Holzer, D. M., Travis, J., Sanderson, B. L., Power, M. E., and Carmichael, R. W. (2008a). Evolutionary consequences of habitat loss for Pacific anadromous salmonids. *Evol. Appl.*, 1(2):300–318.
- McClure, M. M., Utter, F. M., Baldwin, C., Carmichael, R. W., Hassemer, P. F., Howell, P. J., Spruell, P., Cooney, T. D., Schaller, H. A., and Petrosky, C. E. (2008b). Evolutionary effects of alternative artificial propagation programs: implications for viability of endangered anadromous salmonids. *Evol. Appl.*, 1(2):356–375.
- McCullough, D. A. (1999). A review and synthesis of effects of alterations to the water temperature regime on freshwater life stages of salmonids, with special reference to Chinook salmon. EPA 910-R-99-010, US Environmental Protection Agency.
- McElhany, P., Ruckelshaus, M. H., Ford, M. J., Wainwright, T. C., and Bjorkstedt, E. P. (2000). Viable Salmonid Populations and the recovery of Evolutionarily Significant Units. Technical Report NOAA Tech. Memo. NMFS-NWFSC-42, U.S. Department of Commerce.
- Meehl, G. A. and Tebaldi, C. (2004). More intense, more frequent, and longer lasting heat waves in the 21st century. *Science*, 305(5686):994–997.
- Mellin, C., Bradshaw, C. J. A., Fordham, D. A., and Caley, M. J. (2014). Strong but opposing  $\beta$ -diversity-stability relationships in coral reef fish communities. *Proc. R. Soc. Lond. B*, 281(1777):20131993.
- Mellin, C., Huchery, C., Caley, M. J., Meekan, M. G., and Bradshaw, C. J. A. (2010). Reef size and isolation determine the temporal stability of coral reef fish populations. *Ecology*, 91(11):3138–3145.

- Millennium Ecosystem Assessment (2005). Ecosystems and human well-being: biodiversity synthesis. Technical report, World Resources Institute, Washington, DC.
- Minot, E. O. and Perrins, C. M. (1986). Interspecific interference competition—nest sites for blue and great tits. *J. Anim. Ecol.*, 55(1):331–350.
- Minto, C., Myers, R. A., and Blanchard, W. (2008). Survival variability and population density in fish populations. *Nature*, 452(7185):344–347.
- Moloney, P. D., Hearne, J. W., Gordon, I. J., and Mcleod, S. R. (2011). Portfolio optimization techniques for a mixed-grazing scenario for Australia’s rangelands. *Nat. Res. Mod.*, 24(1):102–116.
- Moore, J. W., McClure, M., Rogers, L. A., and Schindler, D. E. (2010). Synchronization and portfolio performance of threatened salmon. *Conserv. Lett.*, 3(5):340–348.
- Morgan, M. G. and Henrion, M. (1990). *Uncertainty: A Guide to Dealing with Uncertainty in Quantitative Risk and Policy Analysis*. Cambridge University Press.
- Mori, A. S., Furukawa, T., and Sasaki, T. (2013). Response diversity determines the resilience of ecosystems to environmental change. *Biol. Rev.*, 88(2):349–364.
- Muirhead-Thomson, R. C. (1991). *Trap Responses of Flying Insects*. Academic Press, London.
- NERC Centre for Population Biology, Imperial College (2010). *The Global Population Dynamics Database Version 2*.
- Newton, I., Rothery, P., and Dale, L. C. (1998). Density-dependence in the bird populations of an oak wood over 22 years. *Ibis*, 140(1):131–136.
- Núñez, M. A. and Logares, R. (2012). Black Swans in ecology and evolution: the importance of improbable but highly influential events. *Ideas in Ecology and Evolution*, 5:16–21.
- Odum, E. P. (1959). *Fundamentals of ecology*. Saunders, Philadelphia, 2nd edition.
- Patterson, D. A., Skibo, K. M., Barnes, D. P., Hills, J. A., and Macdonald, J. S. (2007). The influence of water temperature on time to surface for adult sockeye salmon carcasses and the limitations in estimating salmon carcasses in the Fraser River, British Columbia. *N. Am. J. Fish. Manage.*, 27(3):878–884.
- Perry, J. N. (1981). Taylor’s power law for dependence of variance on mean in animal populations. *J. Roy. Statist. Soc.*, 30(3):254–263.
- Perry, J. N. (1994). Chaotic dynamics can generate Taylor’s power law. *Proc. R. Soc. Lond. B*, 257(1350):221–226.
- Perry, J. N. and Woiwod, I. P. (1992). Fitting Taylor’s power law. *Oikos*, 65(3):538–542.



- Pestes, L. R., Peterman, R. M., Bradford, M. J., and Wood, C. C. (2008). Bayesian decision analysis for evaluating management options to promote recovery of a depleted salmon population. *Conserv. Biol.*, 22(2):351–361.
- Pine III, W. E., Martell, S. J. D., Walters, C. J., and Kitchell, J. F. (2009). Counterintuitive responses of fish populations to management actions: some common causes and implications for predictions based on ecosystem modeling. *Fisheries*, 34(4):165–180.
- Pinsky, M. L., Worm, B., Fogarty, M. J., Sarmiento, J. L., and Levin, S. A. (2013). Marine taxa track local climate velocities. *Science*, 341(6151):1239–1242.
- Policansky, D. and Magnuson, J. J. (1998). Genetics, metapopulations, and ecosystem management of fisheries. *Ecol. Appl.*, 8:S119–S123.
- Potts, G. R., Coulson, J. C., and Deans, I. R. (1980). Population dynamics and breeding success of the shag, *Phalacrocorax aristotelis*, on the Farne Islands, Northumberland. *J. Anim. Ecol.*, 49(2):465–484.
- Potts, G. R., Tapper, S. C., and Hudson, P. J. (1984). Population fluctuations in red grouse: analysis of bag records and a simulation model. *J. Anim. Ecol.*, 53(1):21–36.
- Pressey, R. L., Cabeza, M., Watts, M. E., Cowling, R. M., and Wilson, K. A. (2007). Conservation planning in a changing world. *Trends Ecol. Evolut.*, 22(11):583–592.
- Quinn, T. P. (2005). *The Behaviour and Ecology of Pacific Salmon and Trout*. American Fisheries Society, Bethesda, Maryland.
- R Core Team (2013). *R: A language and environment for statistical computing*. R Foundation for Statistical Computing, Vienna, Austria.
- R Core Team (2014). *R: A Language and Environment for Statistical Computing*. R Foundation for Statistical Computing, Vienna, Austria. Version 3.1.2.
- Rachev, S. R., Stoyanov, S. V., and Fabozzi, F. J. (2008). *Advanced Stochastic Models, Risk Assessment, and Portfolio Optimization*. John Wiley & Sons, Inc., New Jersey.
- Raymundo, L. J., Halford, A. R., Maypa, A. P., and Kerr, A. M. (2009). Functionally diverse reef-fish communities ameliorate coral disease. *Proc. Natl. Acad. Sci. USA*, 106(40):17067–17070.
- Reckhow, K. H. (1994). Importance of scientific uncertainty in decision making. *Environ. Manage.*, 18(2):161–166.
- Redfearn, A. and Pimm, S. L. (1988). Population variability and polyphagy in herbivorous insect communities. *Ecol. Monograph.*, 58(1):39–55.
- Robertson, G. and Gales, R., editors (1998). *Albatross biology and conservation*. Surrey Beatty & Sons, Chipping Norton, NSW, Australia.

- Rogers, L. A. and Schindler, D. E. (2008). Asynchrony in population dynamics of sockeye salmon in southwest Alaska. *Oikos*, 117(10):1578–1586.
- Rogers, L. A., Schindler, D. E., Lisi, P. J., Holtgrieve, G. W., Leavitt, P. R., Bunting, L., Finney, B. P., Selbie, D. T., Chen, G., Gregory-Eaves, I., Lisac, M. J., and Walsh, P. B. (2013). Centennial-scale fluctuations and regional complexity characterize Pacific salmon population dynamics over the past five centuries. *Proc. Natl. Acad. Sci. U.S.A.*, 110(5):1750–1755.
- Routledge, R. D. and Swartz, T. B. (1991). Taylor's power law re-examined. *Oikos*, 60(1):107–112.
- Ruckelshaus, M. H., Levin, P., Johnson, J. B., and Kareiva, P. M. (2002). The Pacific salmon wars: what science brings to the challenge of recovering species. *Annu. Rev. Ecol. Syst.*, 33(1):665–706.
- Rue, H., Martino, S., Lindgren, F., Simpson, D., Riebler, A., and Krainski, E. T. (2014). *INLA: Functions which allow to perform full Bayesian analysis of latent Gaussian models using Integrated Nested Laplace Approximation*. R package version 0.0-14. <http://www.r-inla.org>.
- Sanchirico, J. N., Smith, M. D., and Lipton, D. W. (2008). An empirical approach to ecosystem-based fishery management. *Ecol. Econom.*, 64(3):586–596.
- Saucy, F. (1994). Density dependence in time series of the fossorial form of the water vole, *Arvicola terrestris*. *Oikos*, 71(3):381–392.
- Scheuerell, M. D., Hilborn, R., Ruckelshaus, M. H., Bartz, K. K., Lagueux, K. M., Haas, A. D., and Rawson, K. (2006). The Shiraz model: a tool for incorporating anthropogenic effects and fish-habitat relationships in conservation planning. *Can. J. Fish. Aquat. Sci.*, 63(7):1596–1607.
- Schindler, D. E., Augerot, X., Fleishman, E., Mantua, N. J., Riddell, B., Ruckelshaus, M., Seeb, J., and Webster, M. (2008). Climate change, ecosystem impacts, and management for Pacific salmon. *Fisheries*, 33(10):502–506.
- Schindler, D. E., Hilborn, R., Chasco, B., Boatright, C. P., Quinn, T. P., Rogers, L. A., and Webster, M. S. (2010). Population diversity and the portfolio effect in an exploited species. *Nature*, 465(7298):609–612.
- Schtickzelle, N. and Quinn, T. P. (2007). A metapopulation perspective for salmon and other anadromous fish. *Fish Fish.*, 8:297–314.
- Secor, D. H., Kerr, L. A., and Cadrin, S. X. (2009). Connectivity effects on productivity, stability, and persistence in a herring metapopulation model. *ICES J. Mar. Sci.*, 66:1726–1732.
- Segura, A. M., Calliari, D., Fort, H., and Lan, B. L. (2013). Fat tails in marine microbial population fluctuations. *Oikos*, 122(12):1739–1745.
- Sethi, S. A. (2010). Risk management for fisheries. *Fish Fish.*, 11(4):341–365.
- Sethi, S. A., Dalton, M., and Hilborn, R. (2012). Managing harvest risk with catch-pooling cooperatives. *ICES J. Mar. Sci.*, 69(6):1038–1044.

- Shaughnessy, P. D. (1982). The status of seals in South Africa and Namibia. In *Mammals in the Seas. Volume IV. Small Cetaceans, Seals, Sirenians and Otters*, pages 383–410. Food and Agriculture Organization of the United Nations, Rome, Italy.
- Sibly, R. M., Barker, D., Denham, M. C., Hone, J., and Pagel, M. (2005). On the regulation of populations of mammals, birds, fish, and insects. *Science*, 309(5734):607–610.
- Siple, M. (2014). Biocomplexity in Pacific herring (*Clupea pallasii*) of the Salish Sea. In *144<sup>th</sup> Annual meeting of the American Fisheries Society*. <https://afs.confex.com/afs/2014/webprogram/Paper16198.html>.
- Sornette, D. (2009). Dragon-kings, black swans and the prediction of crises. *International Journal of Terraspace Science and Engineering*, 2(1):1–18.
- Stafford, J. (1971). The heron population of England and Wales. *Bird Study*, 18(4):218–221.
- Stan Development Team (2014). *Stan Modeling Language Users Guide and Reference Manual, Version 2.4.0*.
- Stockwell, C., Hendry, A., and Kinnison, M. (2003). Contemporary evolution meets conservation biology. *Trends. Ecol. Evol.*, 18:94–101.
- StreamNet (2011). Adult return-estimates of spawning population for Chinook salmon. URL <http://www.streamnet.org>.
- Sugihara, G. and May, R. M. (1990). Applications of fractals in ecology. *Trends Ecol. Evolut.*, 5(3):79–86.
- Sweatman, H., Cheal, A., Coleman, G., Emslie, M., Johns, K., Jonker, M., Miller, I., and Osborne, K. (2008). Long-term monitoring of the Great Barrier Reef. Technical Report Status Report Number 8, Australian Institute of Marine Science, Townsville, Australia.
- Taleb, N. N. (2007). *The Black Swan: The Impact of the Highly Improbable*. Random House.
- Taylor, L. R. (1986). Synoptic Dynamics, Migration and the Rothamsted Insect Survey: Presidential Address to the British Ecological Society, December 1984. *Journal of Animal Ecology*, 55(1):1–38.
- Taylor, L. R. and French, R. A. (1974). Effects of light-trap design and illumination on samples of moths in an English woodland. *Bulletin of Entomological Research*, 63(04):583–594.
- Taylor, L. R. and Taylor, R. A. J. (1977). Aggregation, migration and population mechanics. *Nature*, 265(5593):415–421.
- Taylor, L. R. and Woiwod, I. P. (1982). Comparative synoptic dynamics. I. Relationships between inter- and intra-specific spatial and temporal variance/mean population parameters. *J. Anim. Ecol.*, 51(3):879–906.

- Taylor, L. R., Woiwod, I. P., and Perry, J. N. (1980). Variance and the large scale spatial stability of aphids, moths and birds. *J. Anim. Ecol.*, 49(3):831–854.
- Thibaut, L., Connolly, S. R., and Sweatman, H. P. A. (2012). Diversity and stability of herbivorous fishes on coral reefs. *Ecology*, 93(4):891–901.
- Thibaut, L. M. and Connolly, S. R. (2013). Understanding diversity-stability relationships: towards a unified model of portfolio effects. *Ecol. Lett.*, 16(1):140–150.
- Thomas, C. D. (2010). Climate, climate change and range boundaries. *Divers. Distrib.*, 16(3):488–495.
- Thomas, C. D., Cameron, A., Green, R. E., Bakkenes, M., Beaumont, L. J., Collingham, Y. C., Erasmus, B. F. N., de Siqueira, M. F., Grainger, A., Hannah, L., Hughes, L., Huntley, B., van Jaarsveld, A. S., Midgley, G. F., Miles, L., Ortega-Huerta, M. A., Townsend Peterson, A., Phillips, O. L., and Williams, S. E. (2004). Extinction risk from climate change. *Nature*, 427(6970):145–148.
- Thompson, R. M., Beardall, J., Beringer, J., Grace, M., and Sardina, P. (2013). Means and extremes: building variability into community-level climate change experiments. *Ecol. Lett.*, 16(6):799–806.
- Thorson, J. T., Jensen, O. P., and Zipkin, E. F. (2014a). How variable is recruitment for exploited marine fishes? a hierarchical model for testing life history theory. *Can. J. Fish. Aquat. Sci.*, 71(7):973–983.
- Thorson, J. T., Ono, K., and Munch, S. B. (2014b). A Bayesian approach to identifying and compensating for model misspecification in population models. *Ecology*, 95(2):329–341.
- Thorson, J. T., Scheuerell, M. D., Buhle, E. R., and Copeland, T. (2014c). Spatial variation buffers temporal fluctuations in early juvenile survival for an endangered Pacific salmon. *J. Anim. Ecol.*, 83(1):157–167.
- Tilman, D. (1999). The ecological consequences of changes in biodiversity: a search for general principles. *Ecology*, 80(5):1455–1474.
- Tilman, D., Lehman, C. L., and Bristow, C. E. (1998). Diversity-stability relationships: Statistical inevitability or ecological consequence? *Amer. Nat.*, 151(3):277–282.
- Valone, T. J. and Hoffman, C. D. (2003). Population stability is higher in more diverse annual plant communities. *Ecol. Lett.*, 6(2):90–95.
- Walther, G.-R., Post, E., Convey, P., Menzel, A., Parmesan, C., Beebee, T. J. C., Fromentin, J.-M., Hoegh-Guldberg, O., and Bairlein, F. (2002). Ecological responses to recent climate change. *Nature*, 416(6879):389–395.
- Waples, R., Beechie, T., and Pess, G. R. (2009). Evolutionary history, habitat disturbance regimes, and anthropogenic changes: what do these mean for resilience of Pacific salmon populations? *Ecol. Soc.*, 14(1):3.

- Ward, E. J., Hilborn, R., Towell, R. G., and Gerber, L. (2007). A state–space mixture approach for estimating catastrophic events in time series data. *Can. J. Fish. Aquat. Sci.*, 64(6):899–910.
- West, F. W. and Fair, L. F. (2006). Abundance, age, sex, and size statistics for Pacific salmon in Bristol Bay, 2003. Fishery Data Series 06–47, Alaska Department of Fish and Game.
- Williams, C. B. (1948). The Rothamsted light trap. *Proceedings of the Royal Entomological Society of London. Series A, General Entomology*, 23(7-9):80–85.
- Williams, G. R. (1954). Population fluctuations in some Northern Hemisphere game birds (Tetraonidae). *J. Anim. Ecol.*, 23(1):1–34.
- Winfree, R. and Kremen, C. (2009). Are ecosystem services stabilized by differences among species? A test using crop pollination. *Proc. R. Soc. Lond. B*, 276(1655):229–237.
- Woiwod, I. P. and Hanski, I. (1992). Patterns of density dependence in moths and aphids. *J. Anim. Ecol.*, 61(3):619–629.
- Yeakel, J. D., Moore, J. W., Guimarães, P. R., and de Aguiar, M. A. M. (2014). Synchronisation and stability in river metapopulation networks. *Ecol. Lett.*, 17(3):272–283.
- Ziebarth, N. L., Abbott, K. C., and Ives, A. R. (2010). Weak population regulation in ecological time series. *Ecol. Lett.*, 13(1):21–31.